DOE/BC/10508-37
(DE86000299)

BACTERIA TRANSPORT THROUGH POROUS MEDIA

Annual Report for the Period Ending December 31, 1984

By
T. F. Yen

September 1986

Performed Under Contract No. AS19-81BC10508

University of Southern California
Los Angeles, California

Bartlesville Project Office
U. S. DEPARTMENT OF ENERGY
Bartlesville, Oklahoma

DISCLAIMER

Printed in the United States of America. Available from:
National Technical Information Service
U.S. Department of Commerce
5285 Port Royal Road
Springfield, VA 22161

NTIS price codes
Paper copy: **A08**
Microfiche copy: **A01**

DOE/BC/10508-37
Distribution Category UC-92a

BACTERIA TRANSPORT THROUGH POROUS MEDIA

Annual Report
December 31, 1984

By
T. F. Yen

DOE/BC/10508--37

DE86 000299

September 1986

Work Performed Under Contract No. AS19-81BC10508

Prepared for
U.S. Department of Energy
Assistant Secretary for Fossil Energy

James W. Chism, Project Manager
Bartlesville Project Office
P.O. Box 1398
Bartlesville, Oklahoma 74005

Prepared by
University of Southern California
Los Angeles, California 90017

OBJECTIVE

This research effort has the following objectives:

a) Examination of the interaction between bacteria and geological porous media containing oil and brine:

b) Study of transport phenomena of bacteria through porous media under applied pressure; and

c) Facilitation of bacteria transport through geological porous media under naturally-occurring reservoir conditions.

SCOPE OF WORK

In the third phase of the work we will improve the bacterial transport through derivatization of cellular surface functional groups and/or through modification of the rock surface. We also will investigate the influence of different nutrients on the surface properties of bacteria and hence on the transport in the geological core. Models will be set up for the simulation of the actual penetration of bacteria in an actual reservoir.

PERSONNEL INVOLVED

Principal Investigator:	T.F. Yen
Research Associate:	John Findley
	Long-Kuan Jang
Graduate Students:	Dawood Momeni
	You-Im Chang
	Phil Chang
	Jih-Fen Kuo
	Mukul Sharma

Table of Contents

Page

List of Tables

List of Figures

1. Introduction

Currently a variety of enhanced oil recovery (EOR) processes are under various stages of development. Microbial enhanced oil recovery (MEOR) is perhaps the youngest of these processes and has only recently gained acceptance as being a technically viable alternative to the other EOR processes. With a large percentage of oil (~70%) being unrecoverable by conventional means a great deal of effort has gone into the development of EOR processes. The DOE-sponsored university research programs in MEOR which began in 1979 have been the focal point of many of the developments that have launched MEOR from its infancy to its current status as an acceptable and viable alternative process. The initial studies conducted here and at other universities have been very promising and demonstrate the great potential MEOR has for the future.

At present, however, numerous problems need to be resolved before MEOR can be successfully applied on a commercial scale. It is advisable to focus attention on a few of these problems and resolve them so that some of the basic questions in MEOR may be answered with some degree of certainty. Transport of bacteria in reservoirs is one such problem that has been studied in our laboratories for the past few years. The problem of the transport of bacteria is linked closely with the success or failure of a bacterial injection process and its ability to enhance oil recovery. The injection and penetration of bacteria into a reservoir is the most

problematic and crucial of the steps in any MEOR process. Its study therefore is critically important to the implementation of any MEOR program.

During the first three years, the following significant progress has been made from our study of bacterial transport in porous media:

1. Spores together with nutrients were found to penetrate deep into formations with rather low permeability [1].
2. Prediction of deposition rate based on known properties of rock and cells has been made [2,7,8].
3. Modification of the rock surface as well as the bacterial surface by chemical methods for facilitating transport was demonstrated [3].
4. Bacterial transport through Berea sandstone by chemotaxis alone was first shown (without external pressure) [4].
5. Preliminary experiments of MEOR in the laboratory were successful. About 40% based on residual oil was recovered (better than caustic flooding) [5].
6. Surfactant-producing aerobe Bacillus subtilis and acid- and solvent-producing anaerobe Clostridum acetobutylicum were found to effectively displace residual heavy crude remaining after secondary waterflooding [6].

In 1984, we continued the research effort in this field and gained more useful knowledge on bacterial transport in porous media. Since the adhesion of bacterial cells onto the

solid surfaces plays an important role in the MEOR processes, the detailed mechanism of the adhesion should be fully understood. A theoretical model of convective diffusion of motile and non-motile bacteria toward solid surfaces (Chapter 2) is part of our effort to model the deposition of bacteria in a hydrodynamic field. The approach of colloidal chemistry was adopted to predict the rate of cells suspended in a laminar flow. Surface charges of rock matrix in a candidate oil reservoir plays an important role in dertermining the extent of bacterial transport. Study on interfacial electrochemitry of oxide surfaces in oil bearing sands and sandstones was performed (Chapter 3), a simplistic statistical mechanical model was developed to independently estimate the surface charges. In addition to the theoretical approaches, experimental work has also been carried out to study the effect of molasses-pyrophosphate mixture on bacterial transport and oil recovery efficiency (Chapter 4). It was found that sodium pyrophosphate greatly enhances bacterial transport and increases oil recovery. Experiments were also being conducted to investigate the bacteria-phage-rock interaction for the lytic control of bacteria in MEOR processes (Chapter 5). The results of these experiments indicated that the inhibition of bacterial establishment within a rock matrix is possible via lytic interaction. Various modes of processes have been proposed for MEOR field applications. No systematic approaches have been done to compare the proposed processes. Chapter 6 presents a bench-scale investigation of bacterial transport in sandpack columns and sandstone cores and its relationship with

oil recovery efficiency. Various oil recovery processes have been attempted and compared. Detailed discussions for the above-mentioned work are given in the following chapters.

1.1 Literature Cited

1. L. K. Jang and T. F. Yen, "Screening Tests for Bacterial EOR: A Study of Bacterial Transport", 183rd ACS National Meeting, March 1982, Las Vegas, NE.
2. L. K. Jang and T. F. Yen, "The role of Surface Interactions in the Adsorption of Microbial Cells onto Rock", 185th National ACS Meeting, Seatle, WA, April 1983.
3. L. K. Jang, J. E. Findley, and T. F. Yen, "Preliminary Investigation on the Transport Problems of Microorganisms in Porous Media", in Microbial Enhanced Oil Recovery (J. E. Zajic, D. G. Cooper, T. R. Jack, and N. Korsaric, eds.) Pennwell Books, Chap.7, 1983, pp. 45-49.
4. T.F. Yen, L.K. Jang, P.W. Chang, and J.E. Findley, "The Transport of Bacteria through Porous Media," Engineering Foundation Symposium on Microbial Enhancement of Oil Recovery, Afton, OK. May 1982.
5. Y.I. Chang, "Effects of Chemical Additives on Bacterial Transport through Porous Media & Their Application in Microbial Enhancement of Oil Recovery," Ph.D. Dissertation, USC, July 1984.

6. L.K. Jang, and T.F. Yen, "An Experimental Investigation on the Transport Problems of Microorganisms in Porous Media," ACS Petroleum Chem, Preprint, 28(2), 789-799, 1983.

7. L. K. Jang and T. F. Yen, "Role of Colloidal Forces in the Deposition of Bacterial Cells onto a Single Spherical Collector", 57th Colloid and Surface Science Symposium, Toronto, Ontario, Canada, June 1983.

8. L. K. Jang, "Modelling the Deposition of Bacteria in a Simple Hydrodynamic Field: Rate of Deposition onto a Spherical Collector", Ph. D. Dissertation USC, December 1983.

2. A THEORETICAL MODEL OF CONVECTIVE DIFFUSION OF MOTILE AND NON-MOTILE BACTERIA TOWARD SOLID SURFACES

2.1 Abstract

The rate of attachment of bacterial cells onto solid surfaces is influenced by many factors such as hydrodynamic field, the surface structures and physiological activities of cells, and the surface properties of solid surfaces. In this chapter, the approach of colloidal chemistry is adopted to predict the rate of attachment of cells suspended in a laminar flow. Two controversies in the theroy of colloidal stability are clarified. First, this paper shows that the convective diffusion of cells under various types of surface interaction ranging from strongly repulsive to strongly attractive can be modeled by apparent 1st-order surface reactions. Second, this paper indicates that the "motility" of cells should be rigorously interpreted as higher diffusivity (compared with the Brownian or thermal diffusivity of dead or non-motile cells or synthetic colloids) instead of a linear velocity of self-propulsion. The contribution from the motility of cells to the rate of deposition is analyzed theoretically. A statistical model of random-walk is used to estimate the diffusivity of motile cells resulting from flagella propulsion.

2.2 Introduction

Recent developments in the utilization of microbiological

technology indicate that bacteria may be beneficial in certain shallow, low-producting reservoirs which have undergone secondary or tertiary recovery processes. The well that produces less than 10 barrels per day is called a stripper well. It is very difficult or costly to recover the residual oil (which could be as high as 60-70% of the oil originally locked in place) by conventional methods especially in the case of heavy-oil reservoirs. Microbial enhanced oil recovery (MEOR), with ZoBell's pioneering work in 1940's (1) and with successful field tests demonstrated in the U.S.A. (2) and in Eastern Europe (2, 3), thus provides an alternative to tackle the problem.

An in-situ approach to recovering oil by microbial treatment is to inject potential bacterial species into the candidate stripper wells along with appropriate nutrients. The metabolites generated during the in-situ fermentation could release some more oil from the formation of the stripper reserviors. However, the microbial treatment on stripper wells does not always yield a significant increase in oil production. It has been established that high porosity and high permeability promise positive results (2, 3). For reservoirs with premeability around 0.1 darcy, the effect was found to be limited to the wellbore region (2). It was generally believed that one major reason for applying in-situ MEOR is that active metabolites are generated in-situ instead of being supplied ex-situ. Therefore, in considering the feasibility of MEOR, an exceedingly important parameter is the mobility of bacteria that have favorable oil displacement properties. The bacteria must be transported to locations deep within the reservoir.

Bacteria in a typical MEOR process are injected into the

reservoir formation followed by a period of static incubation. During the injection of bacteria along with nutrient, cells are gradually retained by the porous formation as they travel with the carrier medium. If the probability of retention by the porous formation is high, cells are less likely transported deep into the reservoir. According to the preliminary study done by the author and coworkers (4, 5), the injection of bacterial suspension into sandstone cores can be simulated by a deep bed filtration model. During the static incubation following the completion of injecting bacterial suspension, further spreading of cells is determined by the viability of cells, the amount of available nutrient, the effective diffusivity in the porous formation, and more importantly, by the absorption of cells onto rock grains. The stronger the cells tend to absorb onto rock grains, the slower the cells spread in the formation. The preliminary study indicated that various bacterial species also showed different mobilities through sandstone cores saturated with nutrient broth (4, 5). The above picture vividly reveals that the retention by porous rock is one of the key factors determining the transport of bacteria through the porous media. However, very little quantitative data are available in the literature.

Microbial cells of various species exhibit remarkable differences in physiological activity, nurtrient requirements, mode of multiplication, structure of interior and exterior organelles, response to stimulus, ability to migrate (e.g., gliding on solid surface, propelled by flagella, or non-motile), metabolic products, and favorable habitat. The environmental factors include wide variations of temperature, pressure, salinity, available nutrient, strength of water current, size of available passage, and pH.

Biological or chemical inhibitors can also exist in the bacterial habitat. In the case of petroleum reservoir, the oil and clays can also affect the activity of bacteria.

It is not intended in this chapter to cover all the above factors. In fact, each individual topic has been or is being extensively studied by scientists. The long-term effects (such as surface growth, corrosion, possible plugging of reservoir pores,...etc.) caused by the attached bacteria and their metabolic products will not be discussed either. Instead, the author will focus the discussion on the fundamentals concerning the rate of deposition of cells onto a solid substrate (called collector hereafter). From the engineering point of view, the rate of bacterial deposition determines the long-term effects as well as the penetration of bacteria in a reservoir and requires a more systematic investigation.

As a cell approaches the proximity of the solid surface by fluid convection, flagellar propulsion, Brownian motion, or by chemotaxis, body forces come into play. From a physical point of view, the cell with electric charges at the surface and nearly spherical shape in suspension resembles a lyophobic colloidal particle. The collector surface could also acquire electric charges through absorption of potential determining ions (p.d.i's). It is not surprising that the theory of lyophobic colloidal interactions, i.e., the DLVO theory (6, 7), with modification of the system geometry to account for the interaction between a tiny colloid and a large collector, has been applied to study the cell-collector interactions (8).

One could predict the theoretical transfer rate in the initial stage of deposition for cells suspended in a well-characterizated

flow field if all the physical parameters can be measured or determined. Those parameters could directly or indirectly reflect the physiological activity of cells (e.g., random-walk diffusivity, electrical charge density on cellular surface, and so forth) or could characterize the surface properties of the solid substrate. In order to investigate the combined effects of hydordynamics, cellular diffusivity, and body forces (called colloidal forces hereafter), the system of a single spherical collector placed in a horizontal flow of bacterial suspension is adopted (Fig. 2-1). The collector surface is assumed to be smooth and clean. It is also assumed that the "bacteria" modeled in this work are alive, motile or non-motile, smooth colloids showing no tendency of self-aggregation.

The relative importance of diffusion of cells to other mechanisms such as fluid convection and the colloidal forces depends on the location of the bacteria and the flow field around the collector. This can be depicted by the following transport equation:

$$\nabla \cdot \underset{\sim}{N} = 0 \tag{1}$$

$$\underset{\sim}{N} = \underset{\sim}{v}\, C - D\, \underset{\sim}{\nabla}\, C + \frac{\underset{\sim}{F}_{ex}}{f}\, C \tag{2}$$

where $\underset{\sim}{N}$ is the local flux of cells, $\underset{\sim}{v}$ is the velocity field of bacteria, D is the diffusivity of cells, F_{ex} is the colloidal force field, f is the hydrodynamic drag coefficient on a cell, and C is the concentration of cells. In the vicinity of the collector surface, the convective velocity field, $\underset{\sim}{v}$, of cells deviates from the undisturbed flow field, $\underset{\sim}{u}$, of the fluid creeping motion as a result of the hydrodynamic interaction. The diffusivity of cells is also retarded in the vicinity of the collector surface. This phenomenon is usually

called hydrodynamic retardation.

Furthermore, one should at this point distinguish clearly the random-walk motion of motile bacteria from the familiar phenomenon of Brownian motion as observed in synthetic colloids, non-motile bacteria, or dead bacteria. For non-motile bacteria, alive or dead, the cells acquire Brownian motion through the unbalanced bombardment by the surrounding liquid molecules. This usually results in a low diffusivity, $D_{T,\infty}$ of cells given by Stokes-Einstein law. For live, motile bacterial species, the cells move through the medium by flagellar propulsion. Periodically, they trash about or "tumble" for a moment before they again head randomly in a new direction. A much higher diffusivity $D_{M,\infty}$ (sometimes as high as one thousand fold of the Brownian diffusivity) could occur due to random-walk motion of motile bacteria. As the motile bacteria age or die, the flagella cease functioning and the diffusivity becomes identical to the Brownian diffusivity. Accordingly, the cellular motility and the physiological activity could influence the deposition of cells onto the collector. However, no vigorous analysis on the contribution from motility to the rate of deposition has been performed.

In this chapter, it is attempted to develop solutions for the covective diffusion equation (Eqs. 1 and 2) under the condition of slow creeping flow such that the diffusion boundary layer is thicker than the surface force boundary layer. Once the general solution is obtained, the rate of deposition can be predicted. Although in the past some efforts have been spent by colloidal scientists in finding theoretical solutions, some of the ambiguities remain to be resolved. First, most previous work claimed that only the deposition of colloidal particles under the influence of strongly repulsive surface

interaction (namely Type I surface interaction as shown later) can have an exact solution. (8, 9). Second, it was also claimed that the model of apparent lst-order surface reaction can only be used to simulate the rate of deposition under the influence of Type I surface interaction. In this chapter, the authors will show that the solution for the deposition of colloids and bacterial cells under the influence of all types of surface interaction ranging from strongly repulsive to strongly attractive can be obtained.

In the subsequent sections, the diffusion coefficients of non-motile bacteria and live, motile bacteria will be compared using a well-established model of random walk. Various types of surface interaction between a bacterium and a collector resulting from long-range van der Waals attraction and short-range electrostatic repulsion will be discussed. Finally, the solution to the transport equation will be developed using the technique of boundary-layer analysis. A general lst-order surface reaction model will also be revealed.

2.3 Diffusivity of Motile Bacteria

Small particles (micron or submicron in size) of non-living matter are known to exhibit Brownian motion in liquid. Due to the unbalanced bombardment by the surrounding liquid molecules, those particles move around in a haphazard manner. As predicted by the Stokes-Einstein theory, the particle which receives thermal energy KT through the bombardment by the surrounding molecules, has a diffusion coefficient $D_{T,\infty}$ in the unbounded liquid which is given by

$$D_{T,\infty} = \frac{K\,T}{f_\infty} = \frac{K\,T}{6\,\pi\,\mu\,a_p} \qquad (3)$$

where K is the Boltzmann constant, T is temperature, is the viscosity of liquid, and a_p is the radius of the particle.

Many motile bacterial species are capable of swimming through water by flagella propulsion. Motile bacteria can have different arrangements of flagella such as monotrichous, lophotrichous, peritrichous, or polar arrangements (10). Cell movement requires coordination in the motion of all flagella of a cell. It has been established that in cells with multiple flagella, all the flagella rotating counterclockwise can form a single bundle and act as a coordinated unit. Cells are propelled forward in this manner for a short distance (ranging from a few to 100 m) before the flagella reverse their direction of rotation. The bundle of flagella than flies apart and all coordination between individual flagella is lost. The cells trash about or tumble for a moment and again head randomly for a new direction (11). The resultant random-walk motion consists of a traveling phase (also called "run" in Ref. 12) and a hunting phase (also called "twiddle" in Ref. 12) (13). The traveling phase is characterized by a speed, direction time duration, and a path length. A typical pattern is shown in Fig. 2-2. It has been established that in the absence of chemical attractants (repellents), the angle between successive traveling line paths has a random distribution (11-15).

It is apparent that the random-walk motion of live, viably growing motile bacteria is much more active than the Brownian motion of non-living particles and non-motile or dead cells. When the motile

bacteria age or die, the cells could loose their flagella or the flagella could cease functioning. Accordingly, the dead cells of motile bacterial species exhibit only weak Brownian motion with a diffusivity given by Eq. 3.

If one can record the motion of a live, motile cell in a stagnant medium (Fig. 2-2), the motile diffusion coefficient of that species can be calculated as (11, 13-15)

$$D_{M,\infty} = \frac{v_M^2 \tau}{3 (1 - \alpha)} \qquad (4)$$

where V_M is the linear swimming speed, τ is the mean duration of a traveling path between two turns, and is the mean cosine of angle of turn. In Eq. 4, it was assumed that the species under investigation is non-chemotatic.

In Table 4-1, the diffusivities of motile species are compared with the diffusicities of non-living colloidal particles of the same size. It is found that the motile diffusivity $D_{M,}$ can be as high as 10^3 fold of Brownian diffusivity $D_{T,\infty}$ of non-motile or dead cell or synthetic colloids. The contribution from the motility to the overall deposition rate will be revealed later in the subsequent sections.

2.4 Colloidal Force Between a Bacterium and a Collector

In Eq. 2, the colloidal force F_{ex} exerting on a bacterium as it approaches the collector surface can also be expressed as the gradient of interaction potential energy V_I:

$$\underset{\sim}{F}_{ex} = - \underset{\sim}{\nabla} V_I \qquad (5)$$

The various surface interactions acting in different ranges can contribute to the overall interaction potential energy, V_I. According to DLVO theory, V_I mainly comprises a long-range London-van der Waals dispersion energy, V_A, and a short-range electrostatic like-charge repulsion energy or opposite-charge attraction energy, V_R:

$$V_I = V_A + V_R \qquad (6)$$

$$V_A = A \left[\frac{1}{6} \ln\left(\frac{h + 2a_p}{h}\right) - \frac{a_p (h + a_p)}{3 h(h + 2a_p)} \right] \qquad (7)$$

$$V_R = \frac{\pi \varepsilon_o \varepsilon_r a_p a_c}{a_p + a_c} \left\{ 2 \psi_1 \psi_{2,\infty} \left(\frac{\pi}{2} - \tan^{-1} \sinh \kappa h \right) \right. \qquad (8)$$

$$\left. - (\psi_{2,\infty}^2 - \psi_1^2) \ln \left[1 + \exp(-2 \kappa h) \right] \right\}$$

where a_p is the radius of the bacterium. The Hamaker constant A_{132} characterizing the electromagnetic interaction between the collector (denoted as 1) and the bacterium (2) separated by a third material of water (3) can be estimated from the known Hamaker constant A_{ii} (i=1,2,3) of the individual materials or A_{ij} (i,j=1,2,3) of the interaction between materials i and j in a vacuum (16, 17):

$$\begin{aligned} A_{132} &\simeq 1.6 \left(\sqrt{A_{11}} - \sqrt{A_{33}}\right)\left(\sqrt{A_{22}} - \sqrt{A_{33}}\right) \\ &\simeq 1.6 \sqrt{A_{131}} \sqrt{A_{232}} \\ &\sim 0.1\text{-}1.9 \times 10^{-20} \text{ J} \end{aligned} \qquad (9)$$

In Eq. 8, Ψ_1 , and $\Psi_{2,\infty}$ are the surface potential on the collector and the bacterium, respectively, h is the separation distance, ε_0 is the permittivity in a vacuum (= 8.854 X 10^{-12} $C^2J^{-1}M^{-1}$), ε_r is the dielectric constant of the aqueous solution (=78.5), and κ is the reciprocial Debye-Huckel parameter or double layer reciprocal screening length.

In the expression for electrostatic repulsion (Eq. 8), it is assumed that the surface potential on the collector remains constant while the surface charge density remains constant during the electrical double-layer interaction. Although the force between the collector surface (usually negatively charged on silica-water interface at neutral pH) and the bacterium surface (also negatively charged) due to electrostatic repulsion can not be easily and directly measured, the above assumption can be justified on the theoretical basis. It is known that bacterial cells at neutral pH are negatively charged due to the hydrolysis of carboxylic groups in materials constituting the surface, while the collector surface (assuming mainly to be silica) acquires surface charges through the absorption of p.d.i's. It is apparent that during the approach of two surfaces, the p.d.i's on the collector can easily diffuse toward or away from the surface to reach new equilibrium states, while the valency and the charge density on the cell reamined fixed. Therefore, the electrical potential of the collector remains constant while its electrical charge density varies as the surface of the collector is influenced by an external electrical double layer (say, by the one outside the bacterial surface). Since the charge density on the bacterial surface is fixed, the electrical potential remains constant during interaction.

Research in the past indicated that the charge characteristics on bacterial surface is dependent upon the materials composing the cell wall which in turn varies in composition with physiological activity and cellular age (18). We have determined the zeta potential of Bacillus subtilis, a spore-forming aerobe, and Pseudomonas putida (ATCC 12633), a non-spore forming aerobe, at various growth phases using Zeta Reader (Model ZP-12 by Komline-Sanderson, Peapack, New Jersey 07977, U.S.A.). The results are shown in Table 2-2. From the data, the zeta potential on Ps. putida does not vary too much with time. However, the zeta potential on B. subtilis increases significantly as cells age and develop spores. The higher zeta potential on spores (and presumably a higher repulsive force with the collector surface) may probably explain our experimental finding that spores are more easily pushed through the sandstone core as compared with vegatative cells (4, 5).

If one plots the overall interaction potential energy V_I (Eqs. 6-8) versus dimensionless separation distance H (= h/a_p) by varying respective physical parameters in their possible ranges, four types of surface interaction ranging from strongly repulsive (Type I, Fig. 2-3) to strongly attractive (Type IV, Fig. 2-6) can be obtained (Figs. 2-3 to 2-6).

2.5 Solution to the Convective Diffusion Equation For Non-Motile Bacteria

Since the relative intensity of the three transport mechanisms (i.e., convection, diffusion, and surface forces) varies with the separation distance, the technique of boundary-layer analysis can

yield different ranges over which one or two of the transport mechanisms dominate. Following a similar procedure of similarity transformation by Levich (19) and order of magnitude analysis and using a proper matching procedure, a composite solution describing the distribution of non-motile bacteria outside the collector surface can be obtained (16):

$$C^{c}_{CD,T}(X) = \left[1 + \frac{\int_0^X \exp(-\frac{4}{9}X'^3)dX' - 1.15}{1.15 + R_F - X_F}\right] + \left[\frac{\exp(-\frac{V_I}{K\,T})}{1.15 + R_F - X_F} \int_1^X \frac{\exp(\frac{V_I}{K\,T})}{F_1} dX'\right] - \left[\frac{R_F + X - X_F}{1.15 + R_F - X_F}\right] \qquad (10)$$

$$\Delta_D G_1$$

The term in the first bracket on the right-hand side of Eq. 10 is the solution for the (outer) diffusion boundary layer in which the contribution to the overall flux from hydrodynamic field and diffusivity of cells dominate over surface forces. The term in the second bracket is the solution for the (inner) surface force boundary layer in which the contribution from surface foces and diffusivity of cells are comparable while the influence of hydrodynamic field diminishes. Between the two layers, there lies a transition zone into which the extrapolations from the outer solution and the inner solution become a straight line, i.e., the term in the third bracket, and merge. Therefore, Eq. 10 provides a composite solution for all regions outside the collector surface.

In Eq. 10, X is the position of cellular center normalized with

the thickness of the diffusion boundary layer which increases with angular position (16), X_F is the position of cellular center as the cell approaches the edge of surface force boundary layer, and R_F is the integral

$$R_F = \int_{\frac{1}{\Delta_D G_1}}^{X_F} \frac{\exp\left(\frac{\bar{V}_I}{KT}\right)}{F_1} dX' \qquad (11)$$

where F_1 is the hydrodynamic retardation function

$$F_1 = \frac{H}{H + 1} \qquad (12)$$

and $\Delta_D G_1$, is the dimensionless thickness (relative to cellular radius) of diffusion boundary layer at angular position θ . The variation of G_1, with θ is plotted in Fig. 2-7.

It is apparent from Eqs. 10 and 11 that the resultant solution is strongly dependent upon the integral R_F which in turn is determined by the shape of interaction energy. Qualitatively speaking, the strong repulsion in the case of Type I surface interaction strongly retards the deposition of cells and, from the kinetic point of view, the further diffusion from the outer diffusion boundary layer would also be retarded.

A typical distribution of non-motile cells outside the collector under the influence of four types of surface interaction is plotted versus dimensionless separation distance according to Eq. 10 (Figs. 2-8 to 2-11). It is shown that although the range of surface interaction is very small compared with the dimension of the collector, the distribution of cells is strongly influenced by the

type of surface interaction. In Figs. 2-8 to 2-11, R is the ratio of collector size to bacterial size, Pe_T is the Peclet number defined as

$$Pe_T = \frac{2\, a_c\, U_\infty}{D_{T,\infty}} \qquad (13)$$

Once the distribution of cells outside the collector surface is obtained, the deposition rate, i.e., the bacterial flux, $N(\theta)$ at any angular position can be expressed as an apparent 1st-order surface reaction (16):

$$N(\theta) = - K_1\, C_{surf} \qquad (14)$$

where

$$k_1 = \left(\frac{D_{T,\infty}}{a_p}\right)\left(\int_{\sigma}^{\Delta_{F,2}} \frac{\exp\left(\frac{V_I}{K\,T}\right)}{F_1}\, dH \quad -1\right)^{-1} \qquad (15)$$

where $\Delta_{F,2} \sim 1.$

and C_{surf} = apparent surface concentration as the straight line portion of Eq. 10 is extrapolated to the surface of the collector.

Eq. 14 is obtained by extrapolating the straight line portion of Eq. 10, i.e., the term in the third bracket, to the collector surface. Since the straight line represents the solution for the transition zone in which diffusion is the dominant transport mechanism, the diffusive flux toward the collector surface must be subsequently balanced by a "reaction" occurring on the surface. In other words, the diffusive flux equals the rate of absorptive

"reaction" on the surface.

Research in the past claimed that this kind of model is only valid for the cases of the Type I and Type II surface interaction. For the cases of Type III and Type IV surface interaction, this model is not valid because a negative value of C_{surf} occurs which is "physically" impossible. The authors of the present chapter would like to point out that the apparent surface concentration is merely a result of extrapolation, not a "physical" concentration. One should interpret the negative apparent surface concentration in the latter two cases as a shift of the effective position of sink from the surface of the collector to the edge of surface force boundary layer as a result of strong attractive surface interaction (Fig. 2-12). Since the position of the effective sink is shifted outwards, the effective distance of diffusion is shortened and, therefore, the rate of depostion is enhanced compared to the pure diffusion (of molecules) in the absence of surface forces and hydrodynamic retardation.

Once the local deposition rate is obtained, the integration over the surface would give the overall depostion rate (denoted as I). If one plots the dimensionless deposition rate, the Sherwood Number Sh

$$Sh = \frac{I}{4 \pi a_c D_{T,\infty} C_\infty} \times 2 \qquad (16)$$

versus Hamaker constant A_{132} using the surface potentials and Peclet number as parameters (Fig. 2-13), one finds a significant variation of Sh with A_{132}. In lower A_{132} regions, the surface interaction belongs to Type I and the energy barrier hinders the

deposition. As A_{132} increases, the surface interaction gradually shifts from Type I to Type IV. In higher A_{132} regions, the deposition rate is close to that of pure diffusion (i.e., Levich's theory of molecular diffusion toward the collector (19).

2.6 Convective Diffusion of Motile Cells Toward Collector Surface

If one solves Eqs. 1 and 2 in which the motile diffusivity $D_{M,\infty}$ substitutes for D, a composite solution similar to Eq. 9 is obtained:

$$C^{c}_{CD,M}(X) = \left[1 + \frac{\int_0^X \exp(-\frac{4}{9}X'^3)dX' - 1.15}{1.15 + R_F' - X_F'}\right] + \left[\frac{\exp(-\lambda_{TM}\frac{V_I}{KT})}{1.15 + R_F' - X_F'} \int_{\frac{1}{\Delta_D' G_1}}^{X} \frac{\exp(\lambda_{TM}\frac{V_I}{KT})}{F_1} dX'\right] - \left[\frac{R_F' + X - X_F'}{1.15 + R_F' - X_F'}\right] \quad (17)$$

where the parameter λ_{TM} is the ratio of non-motile diffusivity (or Brownian diffusivity) $D_{T,\infty}$ to motile diffusivity $D_{M,\infty}$. Since λ_{TM} appearing in the exponential term is a small number, one would predict that in the cases of Type I and Type II surface interaction, the effective height of energy barrier (a positive value) will be much reduced and the deposition rate is greatly enhanced compared to that of non-motile bacteria. In other words, the energy of a motile cell derived from the vigorous flagella porposion can help to penetrate the energy barrier. For Type III and Type IV

surface interaction, introducing a small number λ_{TM} into the exponential term does not signigicantly alter the distribution of cells outside the collector surface. The deposition rate in the latter two cases is therefore higher than that of non-motile cells of the same size by a factor of $(\lambda_{TM})^{-1}$.

2.7 Discussion

As a suspension of cells is injected into an one-dimensional porous medium, the probability of cells being retained along the length of the medium was expressed by a phenomenological parameter, the deep bed filtration coefficient K_o (5). This coefficient can be related to the Sherwood number of deposition onto a single grain by

$$K_o = \frac{3(1-\phi)}{a_c} \cdot Sh \cdot Pe_T^{-1} \qquad (18)$$

Where ϕ = porosity of media

where the hydrodynamic field around a collector is modified to take into account the influence of neighboring collectors. We have compared the results of injecting cells into a Berea Sandstone core (5) to the present model and found a fair match between the two.

In the bio-"huff-and-puff" process of MEOR created by this research group, cells to grow and migrate through the oil-containing porous medium filled with nutrient broth with both ends sealed following the inoculation of bacteria (20, 21). Although experimental data on the linear rate of penetration are available (5), we need to further investigate the combined effects of cellular activity,

available nutrient, and the attachment of cells to the sand grains. A model is currently being developed in our research group.

The model developed in this work is aimed at simulating the deposition of cells onto a clean collector, or the deposition in the initial stage. The already deposited cells would certainly alter the apparent surface properties of the collector and, therefore, the rate of deposition can be affected.

The present model is focused on the nearly spherical, rigid cells. Cells of certain species can attach to the collector surface by the structures extrucling from the cell wall. Since the dimension of those structures can be longer than or comparable to the range of electrostatic interaction, the energy barrier of Types I and II surface interaction can be penetrated by them.

One of the most important conclusions drawn from this work is that the investigation on the surface properties and the surface interaction is essential in the research of transport of bacteria in the porous media. Our results indicate that modifying the surface charges on both surfaces can theoretically prevent the attachment of cells to collector surfaces by increasing the short-range electrostatic repulsive force. Furthermore, the extent of modification (i.e., the zeta potential) needed to achieve this purpose can be estimated by our model. We have already successfully attempted several methods including adding certain chemicals to the suspending solutuion or chemically modifying functionaly groups on cellular surface. However, more work remain to be done. The long-range van der Waals force between cells and collector surface can also be modified such that the value of A_{132} can be greatly decreased or becomes negative. As far as the surface interaction is

concerned, we have modified the conventional DLVO theory of colloidal stability by using a condition of constant charge density of cells and considering the possible variation of zeta potential among species and with growth phase. In practice, the curve of Sh versus A_{132} may not be so sensitive as that plotted in Fig. 2-13. If one uses the retarded form of van der Waals interactive energy instead of the unretarded form (Eq. 7), and, the expression for the electrostatic repulsion can be modified by taking into account the existence of an associated layer of ions on surfaces, a better model of surface interaction can be obtained.

2.8 Nonmenclature

A_{ii}	Hamaker constant for individual material i	
A_{ij}	Hamaker constant for the interaction between i and j	(J)
A_{ijk}	Hamaker constant for the interaction between i and k with fluid j embeded in the gap	(J)
a_c	radius of a spherical collector	(m)
a_p	radius of a spherical cell or a colloid	(m)
C	dimensionless concentration of cellular center (general)	
C_∞	dimensionless conc. of cells in the free stream (=1)	
$C^c_{CD,\ T}$	composite solution for the convective diffusion of non-motile bacteria subject to hydrodynamic retardation and surface forces at $R^3 Pe^{-1}_T > 1$	
C_{surf}	the apparent concentration of cells on the	

$C^{c}_{CD,\,M}$	composite solution for the convective diffusion of motile bacteria at $R^{3}Pe^{-1}_{M}>1$	
D	diffusion coefficient	(m^2/sec)
$D_{T,\infty}$	values of D_T and D_M in the free stream	(m^2/sec)
F_{ex}	overall colloidal force exerted on a spherical colloid (or cell) resulting from interaction with a much larger collector	(N)
F_i	hydrodynamic retardation functions (i=1,2,3,Chap.2)	
	hydrodynamic drag coefficient on a colloid (or a cell) near the collector	(Kg/sec)
G_1	a function used in normalizing the diffusion boundary-layer coordinate	
H	dimensionless separation distance (h/a_p)	
h	separation distance between a cell (or colloid) and the collector	(m)
K	Boltzmann constant (=1.38x10^{-23} J/^{O}K)	
k_1	rate constant of the apparent lst-order surface reaction in surface force boundary layer analysis	(sec^{-1})
N	local bacterial flux	($m^{-2}sec^{-1}$)
Pe_T	Peclet number with respect to Brownian thermal diffusivity (=$2a_c U_\infty / D_{T,\infty}$)	
Sh	Sherwood number (=2I/4 $a_c D_\infty C_\infty$)	
T	Temperature	(^{O}K)
U_∞	free stream velocity	(m/sec)
$\underset{\sim}{u}$	undisturbed creeping flow field	(m/sec)
$\underset{\sim}{v}$	velocity field of a cell in the vicinity of the collector	(m/sec)
v_M	linear swimming velocity of a motile bacteria	(m/sec)

V_A	London-van der Waals dispersion energy between a cell and the collector	(J)
V_R	electrostatic repulsion energy between a cell and the collector	(J)
V_I	overall interaction energy between a cell and the collector ($=V_A + V_R$)	(J)
X_F	The thickness of surface force boundary layer normalized with respect to diffusion boundary layer	
X_o	the effective position of the sink as the London force dominates	
α	mean cosine of the angle of turn of motile bacteria	
ε_o	permittivity in vacuo ($=8.854 \times 10^{-12}$ C^2 J^{-1} m^{-1})	
ε_r	dielectric constant of water ($=78.5$ at 298^oK)	
κ	reciprocal Debye-Huckel parameter or double-layer thickness	
λ_{TM}	ratio of the thermal diffusivity to the ranom-walk diffusivity of motile bacteria	
μ	viscosity of an aqueous solution	(Kg/m sec)
τ	mean duration of a traveling path of bacterial random walk	
Ψ_1	zeta potential on collector surface	
$\Psi_{2,\infty}$	zeta potential on bacterial surface	(V)

2.9 Literature Cited

1. C. E. ZoBell, "Bacterial Release of Oil-Bearing Materials," World Oil, Part I in Vol. 126, No. 13, pp. 36-47 (1947), part II in Vol. 127, No. 1, 35-41 (1947).
2. B. Bubela, "Role of Geomicrobiology in Enhanced Recovery of Oil:

Statue Quo," APEA J., pp. 161-166 (1978).

3. K. Karaskiewics, "Recovery of Crude Oil from Reservoir by Use of Bacteria," translated from Nafta (Polish), Vol. 24, No. 7, 198-202. (1968).
4. L.-K. Jang, M. M. Sharma, J. E. Findley, P. W. Chang, and T. F. Yen, "An Investigation of the Transport of Bacteria through Porous Media," in E. C. Donaldson and J. B. Clark (eds.), International Symposium on Microbial Enhancement of Oil Recovery, Proceedings, held May 16-21, 1982, Shangri-La, Afton, Oklahoma, CONF-8205140, the U.S. Dept. of Energy, 1982, pp. 60-70.
5. L.-K. Jang, P. W. Chang, J. E. Findley, and T. F. Yen, "Selection of Bacteria with Favorable Transport Properties through Porous Media for the Application of Microbial Enhanced Oil Recovery," Appl. Environ. Microbiol., V.46, No.5, 1066-1072 (1983).
6. B. V. Derjagin and L. D. Landau "Theory of the Stability of Strongly Charged Lyophobic Sols and of the Adhesion of Strongly Charged Particles in Solutions of Electrolytes," Acta pysicochimica USSR, Vol. 14, 633-662 (1941).
7. E. J. W. Verway and J. Th. G. Overbeek, Theory of the stability of Lyophobic Colloids, Elsevier Co., Amsterdam, Holland, 1948.
8. L. A. Spielman and S. K. Friedlander, "Role of Electrical Double Layer in Particle Depostion by Convective Diffusion," J. Colloid and Interface Sci., Vol. 46, No. 1, 22-31 (1974).
9. Z. Adamczyk and T. Dabros, "On the Convective Diffusion of Particles under Electrical Double-Layer Forces," J. Colloid and Interface Force Sci., Vol. 64, No. 3, 580-583 (1978).
10. T. D. Brock, Biology of Microorganisms, Prentice-Hall, Inc., Englewood Cliffs, New Jersey, 1974, pp. 49-57.

11. N. K. H. Slater, N. S. Powell, and P. Johnson, "The Relevance of Bacterial Motility of Fermeter Contaminations: An Experimental Study for Bacillus cereus," Trans IChemE. Vol. 59, 170-176 (1981).

12. G. H. Weiss, "Random Walks and Their Applications," American Scientists, Vol. 71, No. 1, 65-71 (1983).

13. H. C. Berg and D. A. Brown, "Chemotaxis in Escherichia coli analyzed by Three-dimensional tracking," Nature, Vol. 239, 500-504 (1972).

14. R. J. Nossal and G. H. Weiss, "A Generalized Pearson Random Walk Allowing for Bias," J. Stat. Phys. Vol. 10, No. 3, 245-253 (1974).

15. P. S. Lovely, "Statistical Measures of Bacterial Motility and Chemotaxis," J. Theor. Biol., Vol. 50, 477-496 (1975).

16. L.-K., Jang, Modeling the Depostion of Bacteria in a Simple Hydrodynamic Field: Rate of Depostion onto a Spherical Collector, PhD Dissertation, Chemical Engineering, University of Southern California, Los Angeles, CA 90089, Dec. 1983.

17. J. Visser, "On Hamaker Constant: A Comparison between Hamaker Constants and Lifshitz-van der Waals Constants," Advan. Colloid Interface Sci., Vol. 3, 331-363 (1972).

18. M. R. J. Salton, "The Anatomy of the Bacterial Surface," Bacteriological Review, Vol. 25, No. 2, 77-99 (1961).

19. V. G. Levich, Physicochemical Hydrodynamics, Prectice-Hall, Inc., Englewood Cliffs, NJ., 1962, PP. 81-87.

20. L.-K. Jang, M. M. Sharma, and T. F. Yen, "The Transport of Bacteria in Porous Media and Its Significance in Microbial Enhanced Oil Recovery," SPE Paper No. 12770, Presented at the 1984 California Regional Meeting Held in Long Beach, CA, April

11-13, 1984, Proceedings, PP. 387-393. SPE Paper No. 12770.

21. L -K. Jang and T. F. Yen, "An Experimental Investigation on the Role of Bacterial Growth and Bacterial Transport in MEOR Processes," ACS, Div. Petroleum Chem. Vol. 28, No. 2 789-799 (1983).

Table 2-1 Diffusion Coefficients of various bacteria [11]

Species	Motile diffusivity	Brownian diffusivity
Salmonella	1.3×10^{-9} m^2/sec	4.3×10^{-13} m^2/sec
typhimurium	$0.4\text{-}1.6 \times 10^{-9}$	
	4.4×10^{-9}	
	5.6×10^{-9}	
Escherichia coli	7.0×10^{-9}	5.0×10^{-13}
	8.7×10^{-11}	
Bacillus cereus	$3.6(\pm 0.3) \times 10^{-10}$	$4.6(\pm 0.2) \times 10^{-13}$

Table 2 - 2 Zeta potential of *Bacillus subtilis* and *Pseudomonas putida*(ATCC 12633) as determined from the electrophoretic mobility measurements

Species	Cultural Age	Suspending Medium	Zeta Potential(mV)
Bacillus subtilis a spore-forming Gram positive aerobe	18 hr	el*	33.6
	18 hr	A**	27.1
	18 hr	B***	37.8
	3 days	A	47.0
	3 days	G****	51.8
	3 days	B	63.28
Pseudomonas putida, a non-sporeforming Gram negative aerobe	12 hr	el	53.9
	12 hr	B	52.4
	15 hr	G	58.3
	15 hr	A	58.7
	3 days	A	56.9

* Electrolyte solution containing 1,000 ppm NaCl

** Buffer solution containing 0.0663 M KH_2PO_4 and 0.0267 M NaOH, pH = 7.0

*** Buffer solution containing 0.0127 M KH_2PO_4 and 0.0054 M NaOH, pH = 7.0

**** Cells remained in growth medium without further separation and resuspension in synthetic solutions

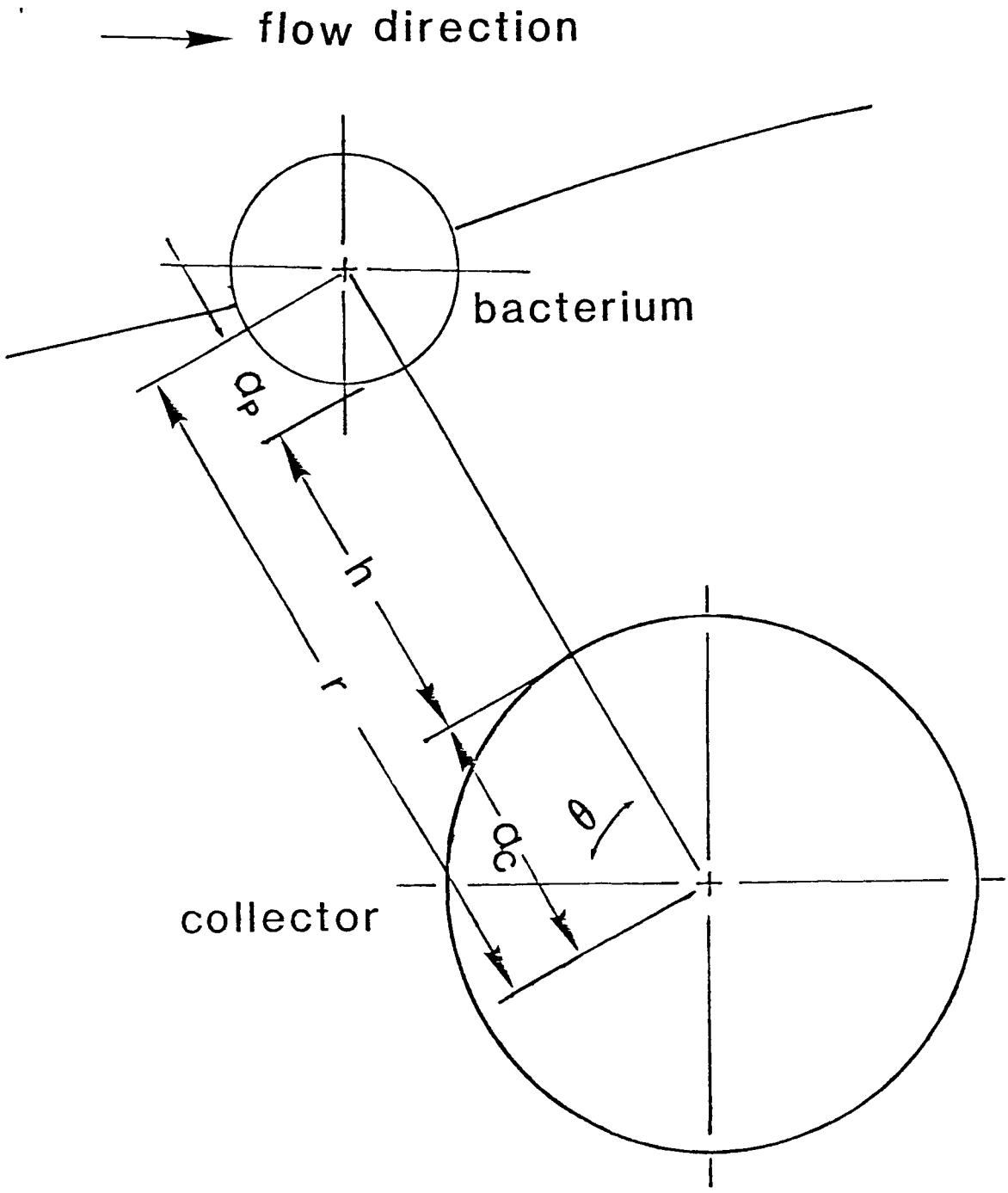

Fig. 2-1 The spherical coordinate system (r, θ, ϕ) locating the bacterial center near a much larger spherical collector. The cellular size is exagerated for illustration.

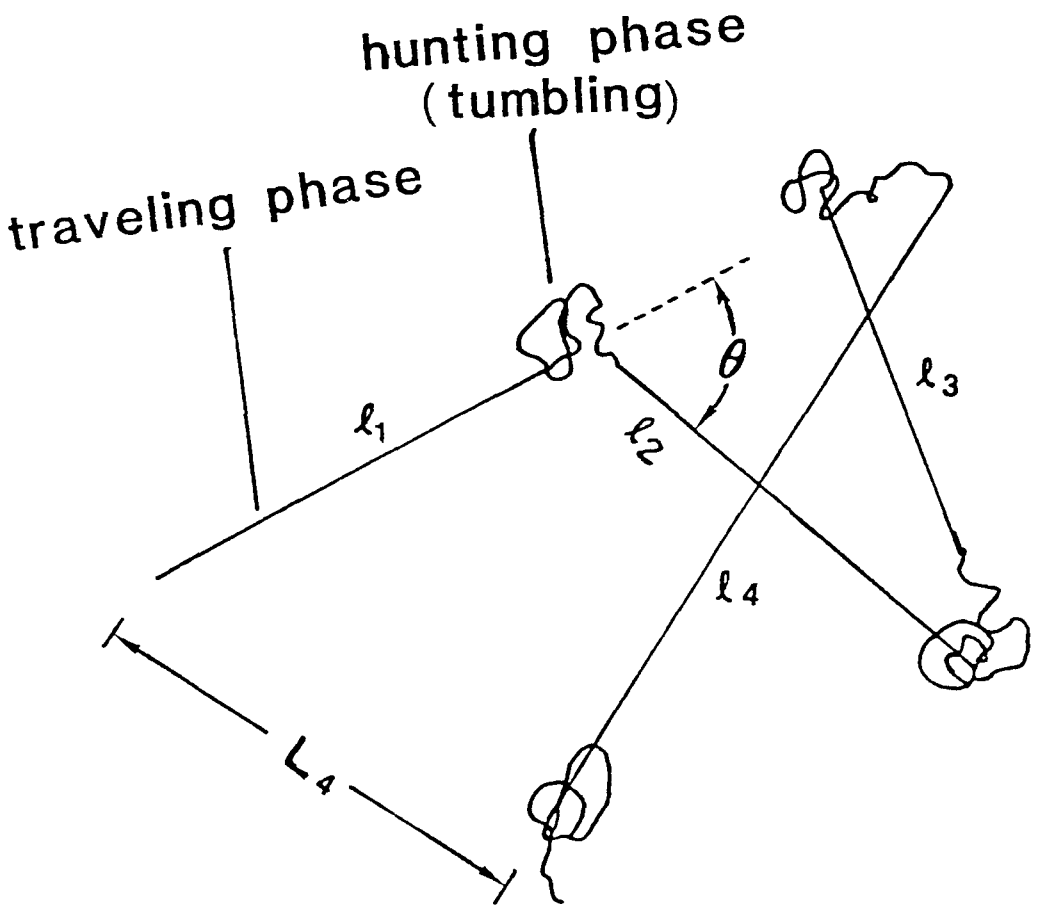

Fig. 2-2 The random-walk motion of a live, motile bacterium. It consists of a traveling phase and a hunting phase (tumbling). The angle between successive traveling lines has a random distribution at the absence of chemical attractants (or repellents).

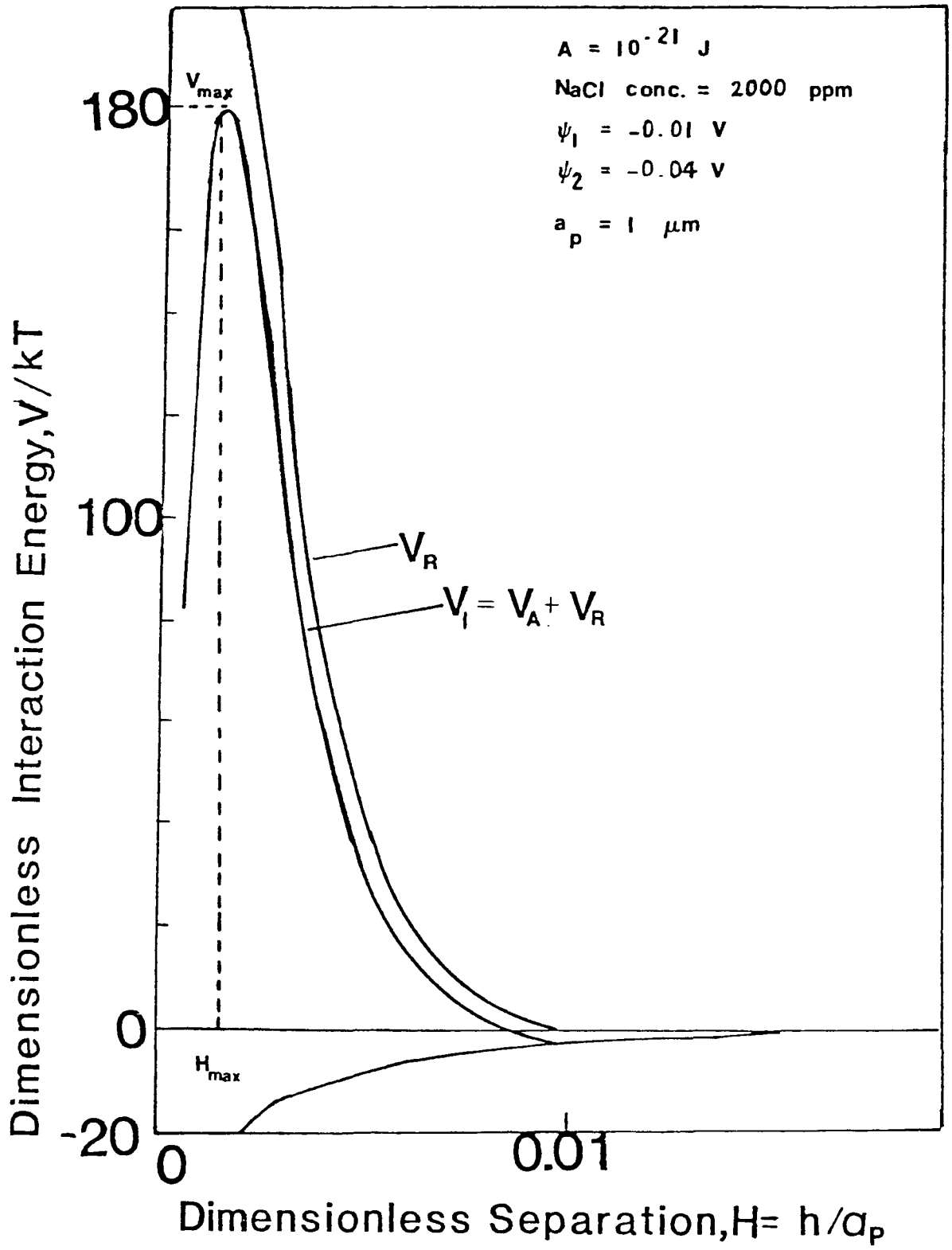

Fig. 2-3 Type I surface interaction.

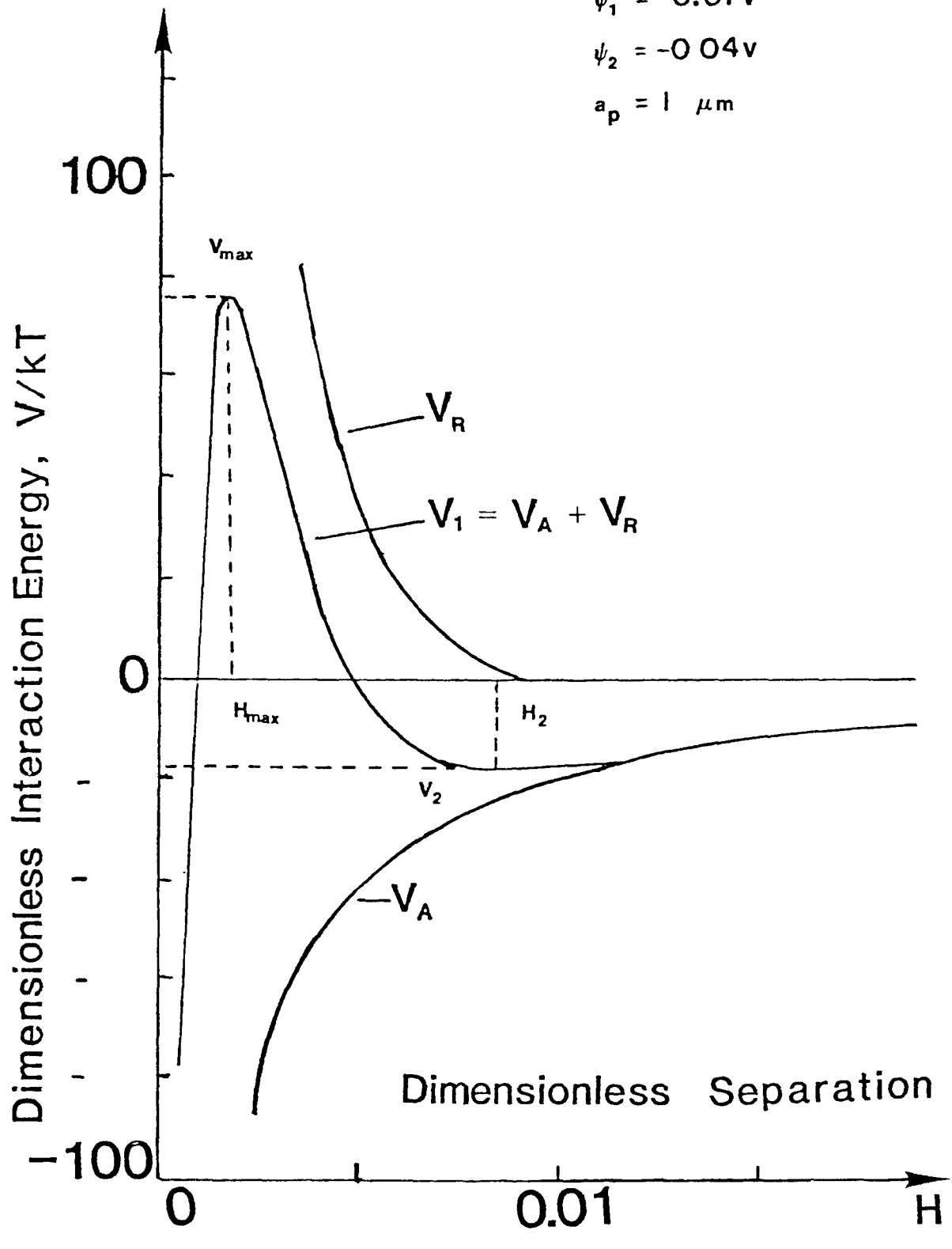

Fig. 2-4 Type II surface interaction.

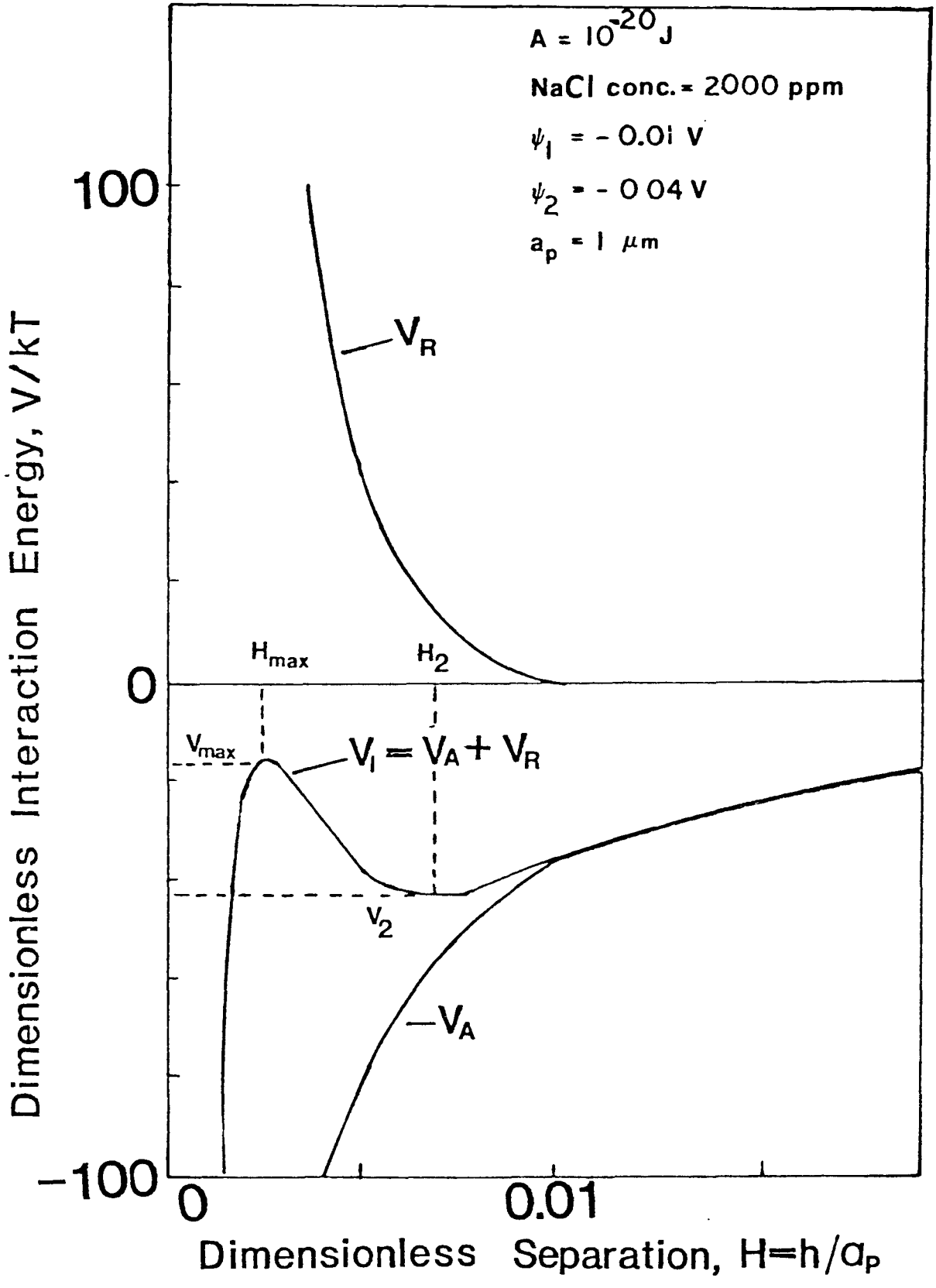

Fig. 2-5 Type III surface interaction.

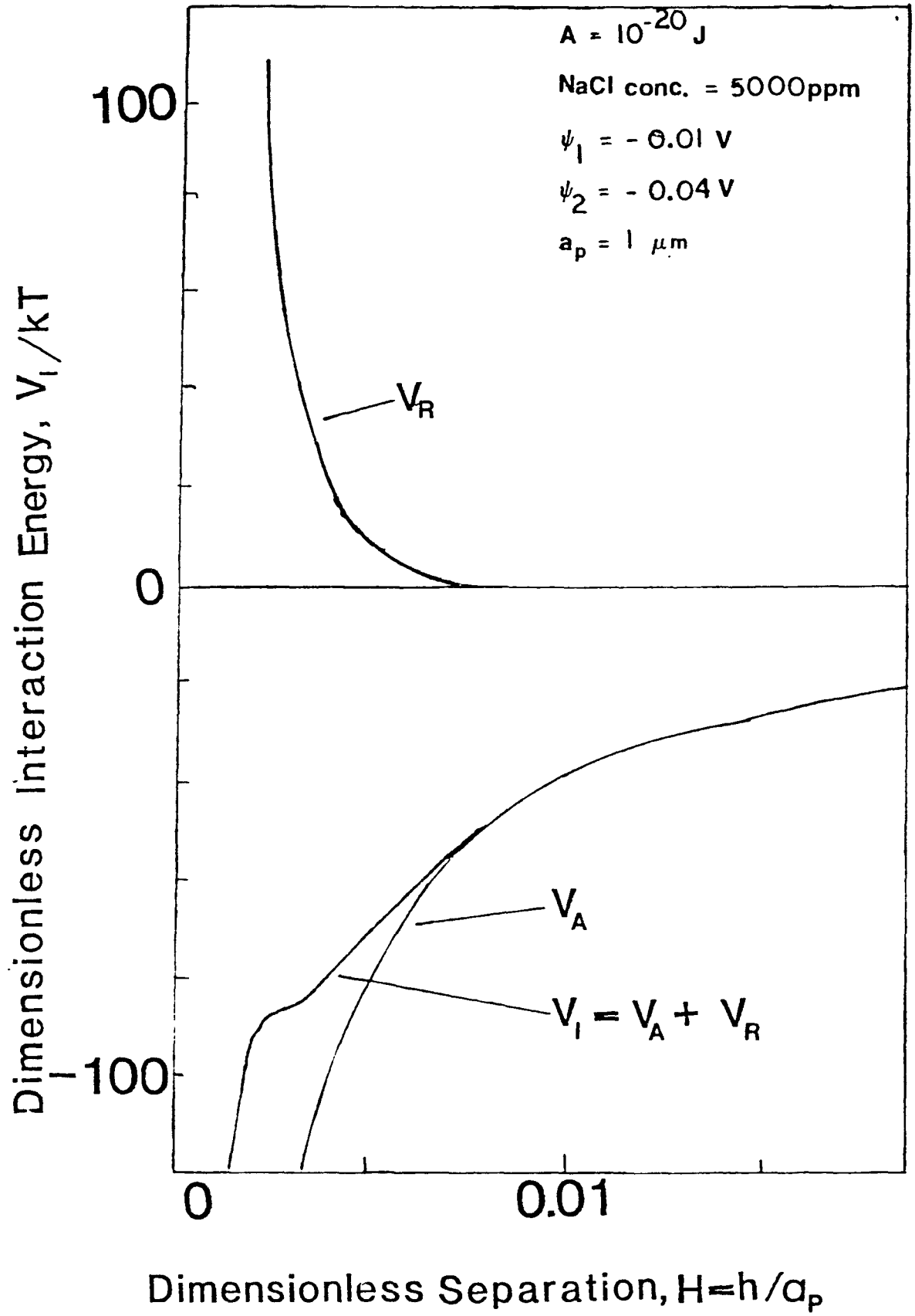

Fig. 2-6 Type IV surface interaction.

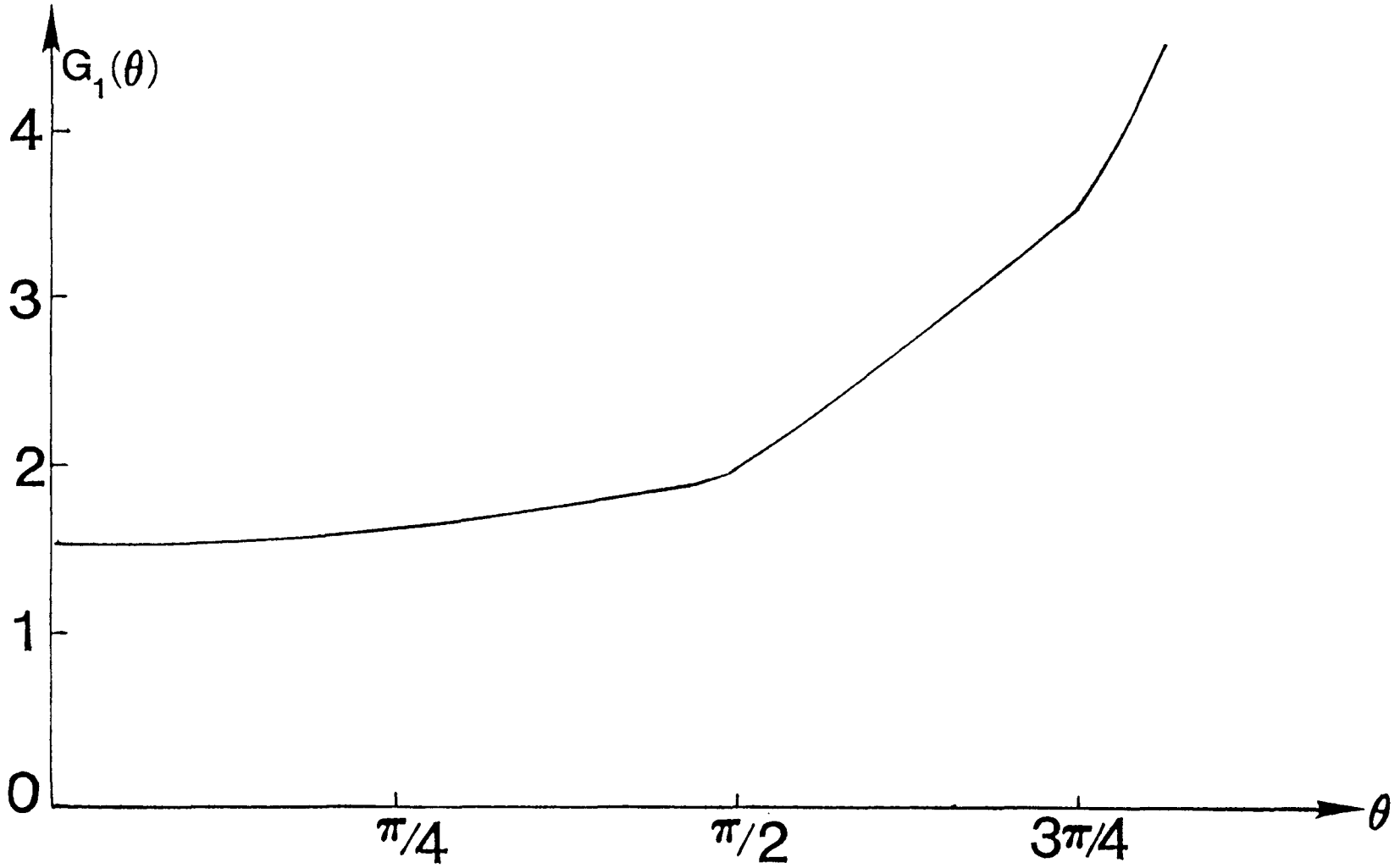

Fig. 2-7 The function G_1 vs. θ.

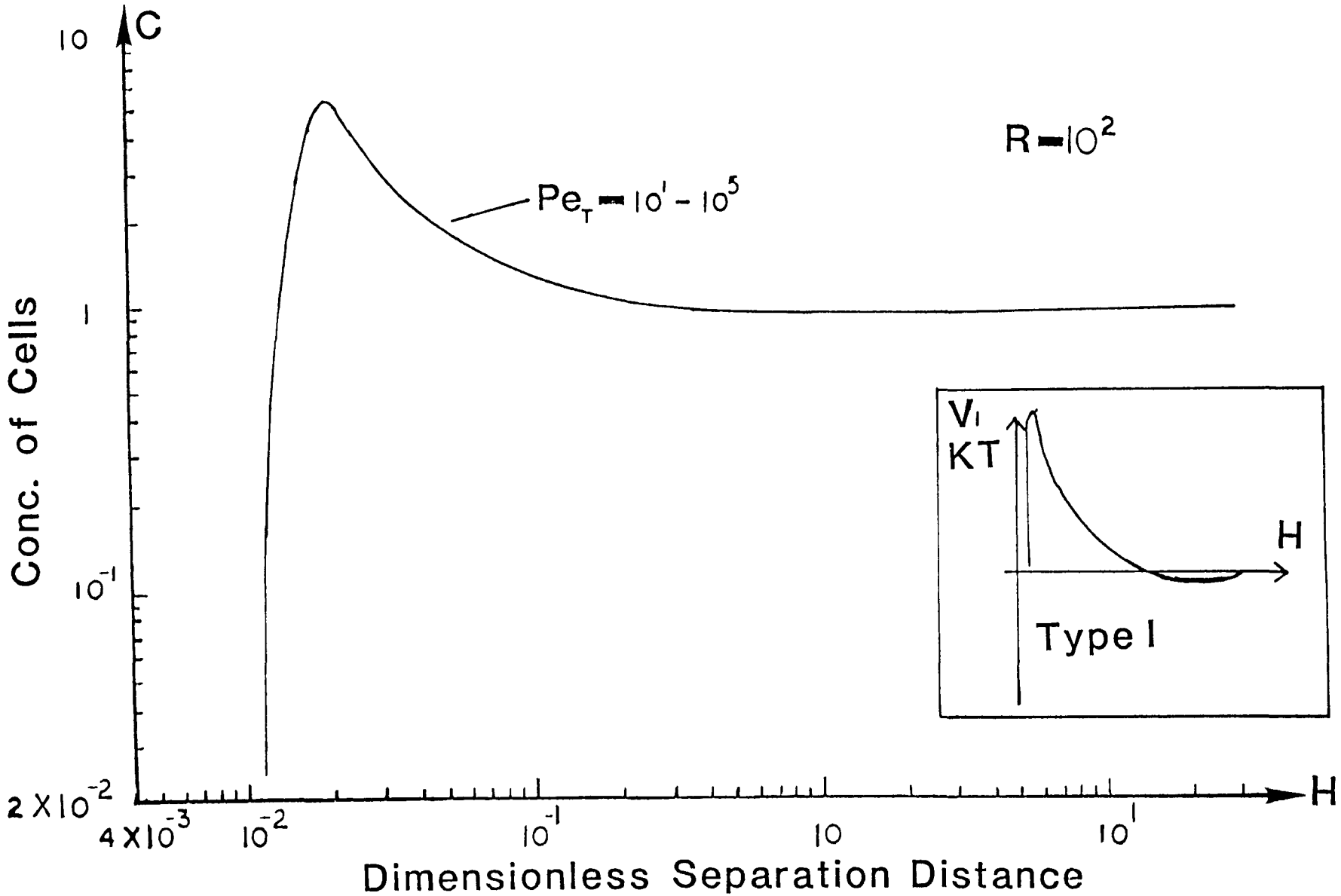

Fig. 2-8 A typical distribution of non-motile cells outside the collector surface under the influence of Type I surface interaction. The concentration of cells is expressed in a dimensionless unit normalized with respect to the free stream concentration.

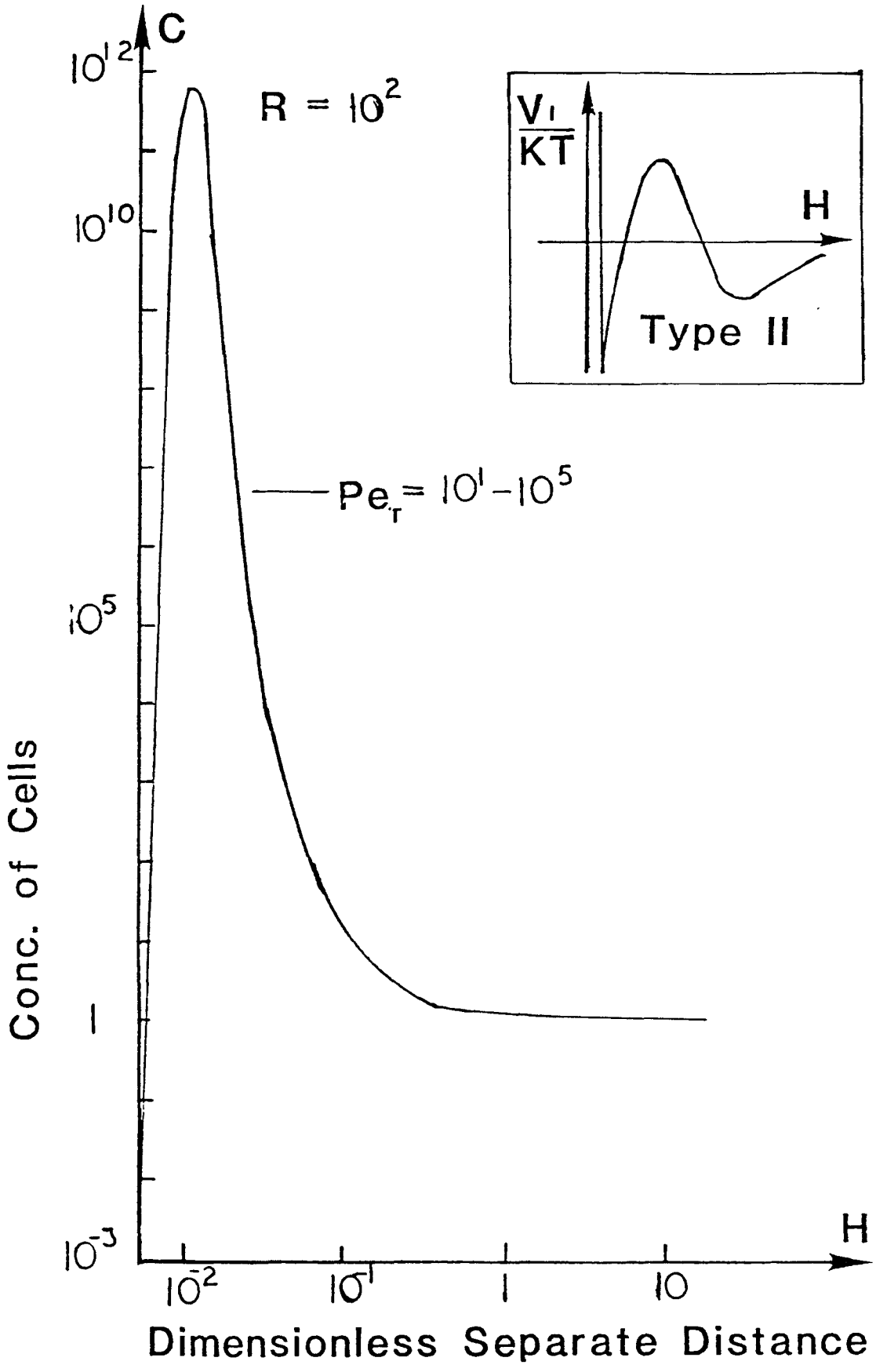

Fig. 2-9 A typical distribution of non-motile cells outside the collector surface under the influence of Type II surface interaction.

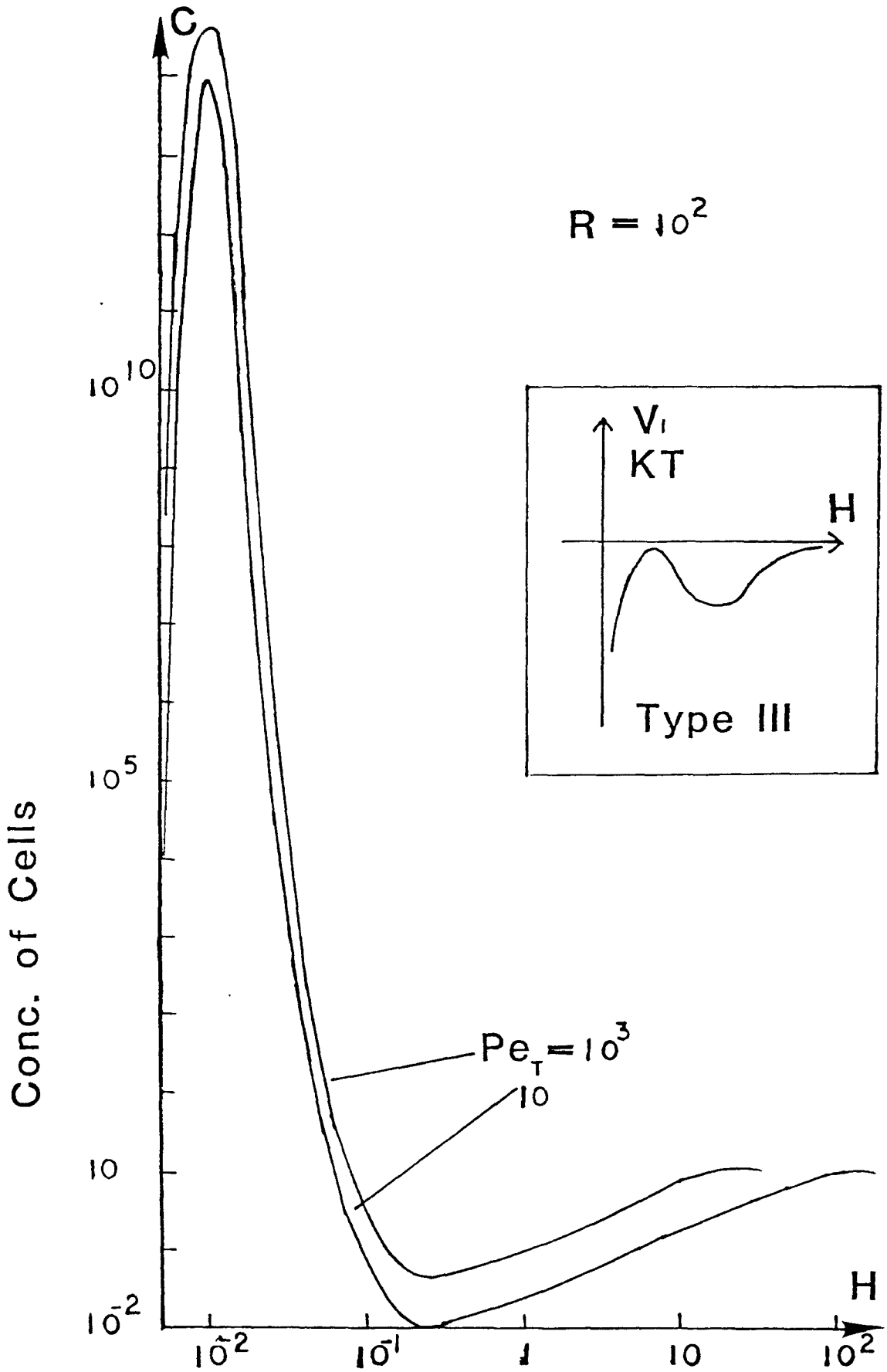

Fig. 2-10 A typical distribution of non-motile cells outside the front stagnation point of the collector under the influence of Type III surface interaction.

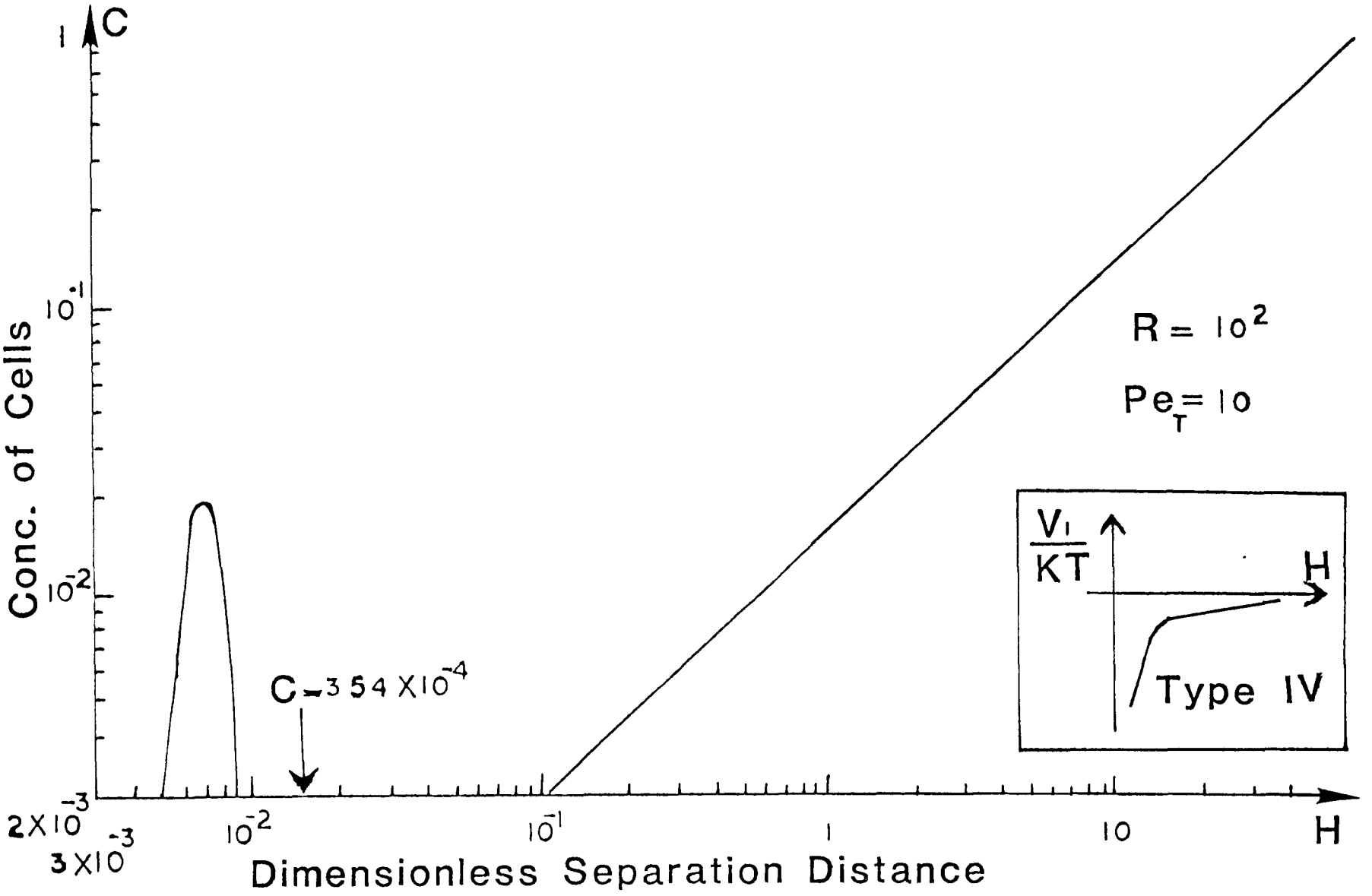

Fig. 2-11 A typical distribution of non-motile cells outside the front stagnation point of the collector under the influence of Type IV surface interation.

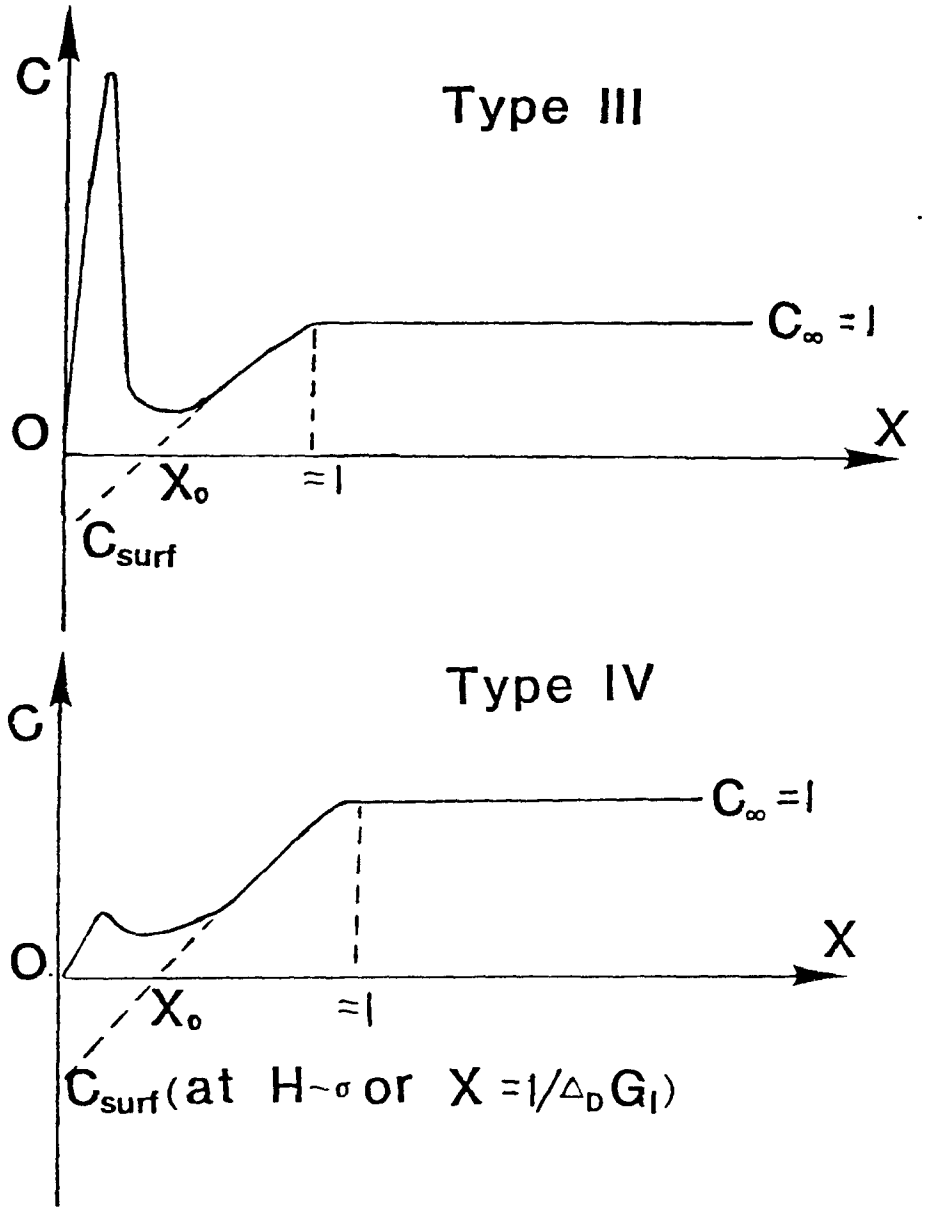

Fig. 2-12 Extrapolation of the intermediate solution to the surface of collector as the deposition is under the influence of Type III (top) or Type IV (bottom) surface interaction. X is the position of cellular center (= H + 1) normalized with the thickness of diffusion boundary layer ($\Delta_D G_1$). The extrapolated straight line intersect C = 0 at X_o, which can be taken as the effective position of the sink for the outer convective diffusion equation.

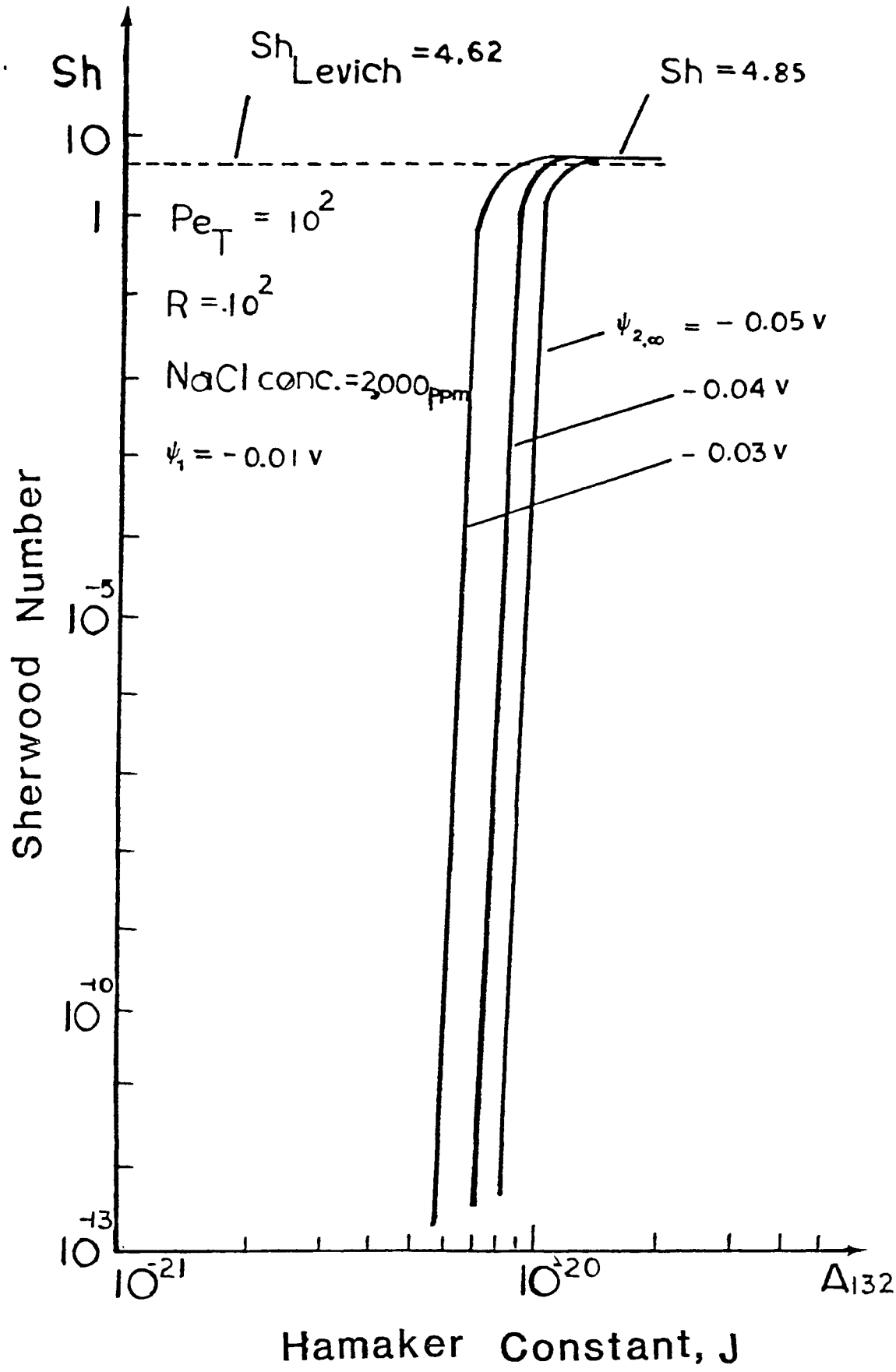

Fig. 2-13 A theoretical plot of Sherwood number for the deposition of non-motile bacteria. Pe_T is the Peclet number, R is the ratio of collector radius to bacterial radius, ψ_1 and $\psi_{2,\infty}$ are the zeta potentials on collector surface and bacterial surface, respectively.

3. INTERFACIAL ELECTROCHEMISTRY OF OXIDE SURFACES IN OIL-BEARING SANDS AND SANDSTONES

3.1 Abstract

It is shown that the detrital grains present in a consolidated sandstone formation and in unconsolidated sands behave as mixtures of oxides. Potentiometric titration results are presented for Ottawa sand, and unbaked and baked Berea sandstone samples. Generalized equations are presented for the site binding model of Davis et al. Such a model is used to estimate the adsorption equilibrium constants for the potential determining ions and the supporting electrolyte ions. Using these constants as input parameters the model equations are solved to yield the surface charge and surface potential distributions in the solution phase. A simplistic statistical mechanical model is developed to show that an independent estimation of the surface charges using the equilibrium constants determined from Davis' model yields values in good agreement with experiment. The potential applications of such a detailed electrochemical description of the sand and sandstone detrital grains are discussed.

3.2 Introduction

Crude oil is most often found in permeable sand and sandstone formations. The formation consists of a consolidated medium of large detrital grains made up of oxides of various metals like Si, Al, Fe, Ti etc., and of finer clays: kaolinite, illite and montmorillonite being a few common ones.

With the increasing use of enhanced oil recovery (EOR) agents, the surface charge properties of these surfaces is assuming great importance. A great number of studies have been done to study the surface charge behavior of clays, however, to our knowledge no such studies have been attempted with the large detrital grains, which constitute a large proportion of the sandstone formation by mass. It has long been recognized that whereas clays acquire their surface charge through isomorphous lattice substitutions, broken bonds at crystal faces and ends and leaching out of interlayer cations, the detrital grains, exposing oxide surfaces acquire their charge by other mechanisms as discussed later in this paper.

Much experimental and theoretical effort has been directed towards explaining the colloidal behavior of oxide-aqueous interfaces. It has been shown (1, 2) that for oxide surfaces, the potential drop across the double layer (ψ_0) changes by less than 59 mV per pH unit, as predicted by the Nernst equation. The high surface charge and the low electrokinetic potentials of oxide surfaces leads one to believe that the simple double layer models used to describe the colloidal properties of AgI-solution interfaces are not directly applicable to oxide systems. Lyklema (3), and Wright and Hunter (4) postulated a surface gel layer

that was permeable to counterions and was responsible for the high differential capacities of the Stern layer around oxide surfaces. Devanathan has discussed methods for estimating these capacities from charge-potential plots (18).

As has been rightly pointed out by Smit et al. (5), the nature of the counterion distribution in the solution phase depends largely on the microcrystalline structure of the oxide under study. In the case of silica one not only has to distinguish between precipitated, highly porous silica and pyrogenic silica, but also between the degree of hydration of the surface sites. In synthetically prepared oxide surfaces it is often possible to establish with some degree of certainty whether a particular surface is porous or impermeable to counter ion penetration. Such a conclusion could prove to be very useful in providing a suitable colloid-chemical model for the surface charge distribution. However in the case of naturally occurring oxide surfaces it is very often difficult to postulate either a pyrogenic nonporous silica model or a highly porous gel model. Indeed scanning electron micrographs in this paper indicate that such surfaces present both smooth, impermeable pyrogenic silica (2) type surfaces and highly porous surfaces. The degree of hydration of such surfaces is usually high, particularly in the case of permeable water/oil bearing geologic formations. The formation of hydrous oxides on the surface could take place in the following manner:

$$Al_2O_3 + H_2O \rightleftharpoons 2\,Al(OH)_3 \rightleftharpoons 2Al(OH)_n^{(3-n)+} + 2(3-n)OH^- \quad (1)$$

$$SiO_2 + 2H_2O \rightleftharpoons Si(OH)_4 \rightleftharpoons Si(OH)_n + (4-n)\,OH^- \quad (2)$$

It is generally believed that such oxides and hydrous oxides develop their surface charge by the adsorption of protons or hydroxyl groups

to certain surface sites, SOH , yielding discrete charged surface sites, SOH_2^+ or SO^-.

$$SOH_2^+ \underset{}{\overset{H^+}{\rightleftharpoons}} SOH \underset{}{\overset{OH^-}{\rightleftharpoons}} SO^- + H_2O \qquad (3)$$

The precise locations of these charged sites will depend on the surface morphology. For a porous surface this charge may by lodged within the porous structure and the counter-ion double layer may either begin within the pores or just outside depending on the relative sizes of the pores and the counter ions. Such models have been presented by Deryaguin et al (6,7).

Yates et al (8) developed a site binding model to describe the double layer at the oxide-water interface. This model assumes that the primary charging mechanism mentioned above, is correct and in addition accounts for complex formation between these charged surface sites and simple 1:1 electrolytes. In addition to forming complexes the counterions form a Gouy-Chapman diffuse double layer, to balance the remaining unneutralized charge. Davis, James and Leckie, in a series of papers (9, 10, 11) developed this concept further and showed that it could be used to interpret potentiometric titration data obtained by various authors to obtain a complete picture of the double layer at on oxide-water interface.

It is the aim of the present work to present data on the surface charge properties of detrital grains present in oil bearing sands and sandstones. Since such detrital grains are known to be mixtures of metal oxides, the site binding model, hitherto used only for pure oxide surfaces was applied. It was shown that such a model, describes the double layer around such particles quite well, but that no correlation exists between mineralogy and surface charge properties. Some useful

conclusions immediately obvious from such an analysis are discussed. An alternative treatment of the problem using a multicomponent Langmuir isotherm to describe the adsorption process is explored and then set aside as it does not as yet provide as good a description as the present model. The surface charge and surface potential variations in the electrolyte medium derived in this paper have been used in subsequent work to describe detrital grain-clay interactions, and the adsorption behavior of sandstone formations (12, 13).

3.3 Materials and Methods

The sandstone sample was obtained from Berea and is a standard sample used to represent sandstones in petroleum engineering experiments. The sample referred to as "baked" was heated in a furnace to a temperature of 700^{o}C for a period of two hours. This treatment is commonly done to immobilize the clays, and is used in experiments where the effect of clay migration is to be minimized. This however as is shown in this paper is a misconception, as not only the clays but also the oxide surfaces studied in this paper are altered by such a treatment. The sample of commercial grade Ottawa sand was used without purification. It is thought to be representative of unconsolidated sandy formations.

The detrital grains were separated from the clays in the sandstone by disaggregating the consolidated sandstone sample carefully, so that the detrital grains were not crushed. This powder was then shaken and sonicated in water, and the clay fraction removed by standard sedimentation procedures to effect the removal of the less than 2 μm particles. This "washing" was done 8 to 10 times to ensure that complete removal of clay was achieved. No surfactants or other agents were used.

All chemicals used were analytical grade reagents.

SEM and EDAX of Samples

EDAX scans of the three oxide samples were done using a Cambridge S4-10 scanning electron microscope with a Tracor Northern-NS-880 energy dispersive X-ray analyzer. Many different grains were scanned and the composition of the three typical types of surfaces observed are given in Table 3-1. Each scan was made over a 40 μm x 40 μm area of the sample. At 20 kV the depth of investigation was ∿ 2 μm. The SEM pictures Figs 3-1, 3-2 & 3-3 are meant to show the surface topography and its cleanliness.

Determination of σ_o vs. pH curves

Potentiometric titrations were carried out to determine the surface charge properties of the samples. The method used was essentially the same as that used by Huang (14). Two titration cells each containing 5g of the sample and 20ml of a potassium chloride solution of desired concentration were stirred in a nitrogen atmosphere by a teflon magnetic stirrer, for about 20 minutes. The solids were allowed to settle and the supernatent liquid in one of the cells was decanted into teflon centriguge tubes and centrifuged for 15 minutes at 12000 rpm. The clear supernantent was then pipetted back into a titration cell without any solid sample, to be used as a blank run. The titrations were performed by adding small equal aliquots of HCl or NaOH solutions to the sample cell and the blank and recording the pH after allowing for an equilibriation time of 5-6 minutes, during which time the mixture was continually stirred. The pH was measured by a Corning digital 110 expanded scale pH meter, using a glass-colomel electrode with an accuracy of $\pm$0.2 mV. Standardization was done using buffers (VWR Sci.) at pH 4, 7 and 10. All pH measurements were made in clear supernatent after the particles had settled. Corrections were made for nonidealities due to variations in ionic strength (5). A saturated KCl bridge reduced the effects of a liquid junction potential, even

TABLE 3-1

Composition of the Surfaces Exposed by the Three samples Ottawa Sand and Unbaked and Baked Berea Sandstones Obtained by Energy Dispersive X-Ray Analysis (EDAX).

	SiO_2	Al_2O_3	K_2O	TiO_2	Fe_2O_3	Na_2O	CaO
Sand #1	68.5	19.0	0.6	0.1	1.8	4.8	4.8
Sand #2	42.8	19.2	0.7	1.4	34.1	0.7	0.7
Unbaked #1	50.8	35.9	6.9	0.00	2.8	0.8	2.5
Unbaked #2	90.2	4.7	1.6	1.4	1.4	0.4	0.00
Baked #1	61.3	25.9	6.2	0.2	4.7	0.8	0.7
Baked #2	74.0	13.6	6.1	0.8	2.9	0.9	1.3
Berea Clay	58.2	36.7	3.3	0.00	0.5	0.6	0.3

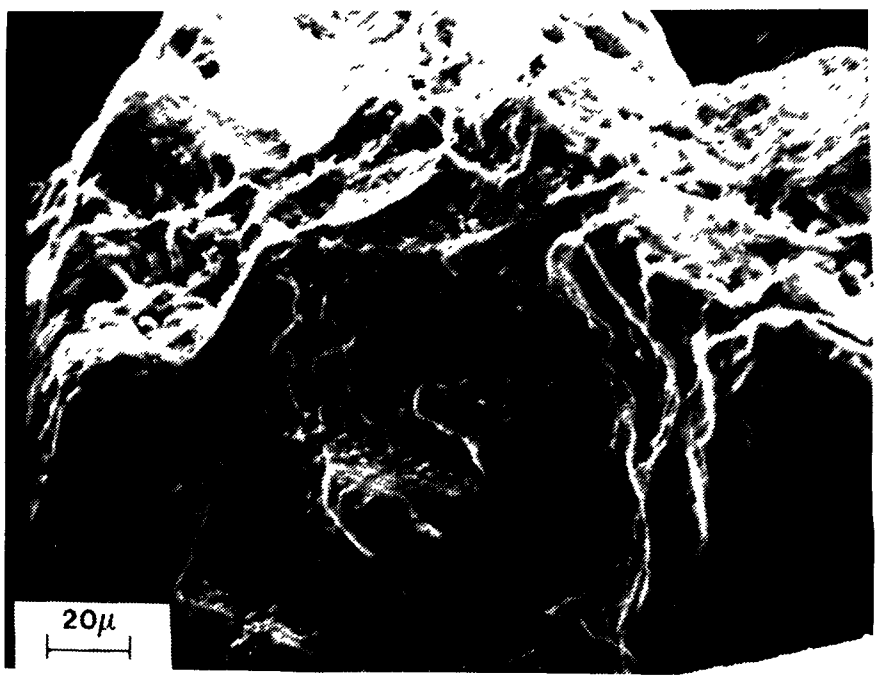

Fig. 3-1 - Scanning electron micrographs of the "washed" sand sample showing the smooth silicate surfaces and the uneven mixed oxide surfaces.

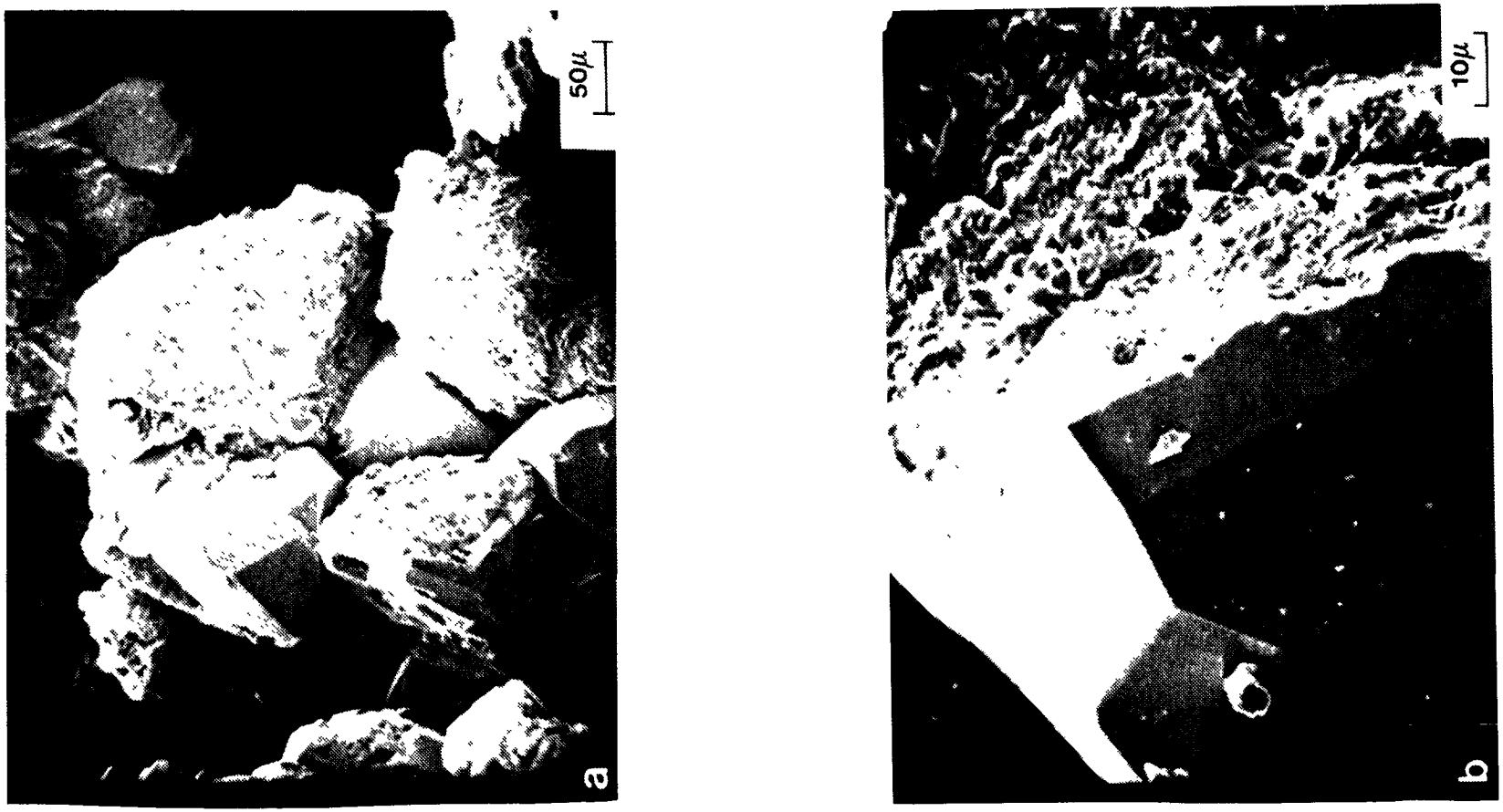

Fig. 3-2 - Scanning electron micrographs of the "washed" unbaked Berea sandstone, showing the perfectly smooth silicate surfaces, the rough mixed oxide surfaces, and traces of small clay particles still adhering to the surface.

Fig. 3-3 - Scanning electron micrographs of the "washed" baked Berea sandstone showing a different kind of oxide surface as compared to the unbaked sample. There is also evidence of traces of clay particles.

though it cannot be totally eliminated particularly for a suspension of charged particles.

The addition of acid was done sequentially on the acidic and basic sides. Fresh samples were used for each KCl concentration and for acidic and basic sides at each indifferent electrolyte concentration. No sample treatment such as leaching with a base was performed because of a fear of irreversible surface adsorption of the base. The equilibrium pH values measured for both the sample and the standard were recorded as a function of the amount of H+ or OH^- added. The concentration of the H^+ or OH^- ions present in the sample cell and the blank were calculated from the measured pH values. The amount of H^+ or OH^- adsorbed on the surface was taken as equal to the amount of HCl or NaOH added to the suspension minus the amount of acid or base required to bring the blank to the same pH.

The Electrical Double Layer Model

The double layer model originally proposed by Yates (8) and developed further by James, Davis and Leckie (9) has been used with essentially no conceptual changes. The equations have however been rewritten in more general form to account for more than one electrolyte and more than one set of potential determining ions. The additional assumptions required to make this generalization are clearly stated.

As has been discussed previously the mechanism of surface charge development is by the adsorption of potential determining ions (PDIs) which adsorb preferentially on the surface sites (SOH) to form charged sites. In addition to this other electrolyte ions do not adsorb on the surface sites but on the charged sites formed and form neutral complexes. The PDIs will be represented by X_i^+ and Y_j^- and the

complex forming ions by the symbols A_k^+ and B_l^- . The surface charge determining reactions may now be written as follows:

$$SOH + X_{is}^+ \underset{}{\overset{K_i^{cat}}{\rightleftharpoons}} SOHX_i^+ \qquad (i = 1, 2, 3 \ldots) \quad (4)$$

$$SOH + Y_{js}^- \underset{}{\overset{K_j^{an}}{\rightleftharpoons}} SOHY_j^- \qquad (j = 1, 2, 3 \ldots) \quad (5)$$

and the surface complexation reactions:

$$n_l SOHX_i^+ + B_{ls}^{n_l^-} \underset{}{\overset{K_{il}^{cat}}{\rightleftharpoons}} (SOHX_i)_{n_l} B_l (i,l = 1, 2, 3 \ldots) \quad (6)$$

$$m_k SOHY_j^- + A_{ks}^{m_k^+} \underset{}{\overset{K_{jk}^{an}}{\rightleftharpoons}} (SOHY_j)_{m_k} A_k (j,k = 1, 2, 3 \ldots) \quad (7)$$

The subscript s implies surface species. n_l and m_k are the valences of the supporting electrolyte ions A_k and B_l.

Examples of the PDI reactions would be,

$$SOH + H^+ \rightleftharpoons SOH_2^+ \quad (8)$$

$$SOH + OH^- \rightleftharpoons SO^- + H_2O \quad (9)$$

Examples of the surface complexation reactions would be

$$SO^- + Na^+ \rightleftharpoons SONa \quad (10)$$

$$SO^- + K^+ \rightleftharpoons SOK \quad (11)$$

$$2SO^- + Ca^{++} \rightleftharpoons (SO)_2Ca \quad (12)$$

$$2SOH_2^+ + SO_4^= \rightleftharpoons (SOH_2)_2SO_4 \quad (13)$$

The assumption here is that only monovalent ions of a size comparable to OH^- ions can be specifically adsorbed on the surface. All the other ions, mono and divalent may form complexes with these surface sites. It is entirely conceivable however that such a condition may be violated. For example,

$$SOH + HPO_4^{2-} \rightleftharpoons SOPO_3H^- + OH^- \quad (14)$$

or, as Hohl and Stumm (25) have observed, Pb^{++} forms complexes with

hydrous ν - Al_2O_3, and the reaction is quantified by the equilibria

$$AlOH + Pb^{2+} \rightleftharpoons AlOPb^{+} + H^{+} \qquad (15)$$

$$2AlOH + Pb^{2+} \rightleftharpoons (AlO)_2Pb + 2H^{+} \qquad (16)$$

Such cases are not considered in this generalization as it would make further development of the surface site model very complicated. Also ions as large as HPO_4^{2-} would probably be excluded from surface sites on porous surfaces due to steric effects.

The specifically adsorbed ions are present in an inner Stern layer and the surface complexes are formed outside this layer in an outer Stern layer. Beyond this we have the Gouy-Chapman layer. This is shown schematically in Fig. 3-7. If the distribution of ions in the electrical double layer is governed by Boltzmann's distribution, then the equilibrium relations may be written as:

$$\left[SOHX_i^{+}\right] = K_i^{cat}\left[SOH\right]\left[X_i^{+}\right]\exp\left(\frac{-e\psi_0}{kT}\right) \quad (i = 1, 2, \ldots) \qquad (17)$$

$$\left[SOHY_i^{-}\right] = K_j^{an}\left[SOH\right]\left[Y_j^{-}\right]\exp\left(\frac{+e\psi_0}{kT}\right) \quad (j = 1, 2, \ldots) \qquad (18)$$

$$\left[(SOHX_i)_{n_1}B_l\right] = K_{il}^{cat}\left[B_l^{n_l^-}\right]\left[SOHX_i^{+}\right]^{n_l}\exp\left(\frac{n_l e\psi_\beta}{kT}\right)(i,l = 1, 2, \ldots.) \qquad (19)$$

$$\left[(SOHY_j)_{m_k}A_k\right] = K_{jk}^{an}\left[A_k^{m_k^+}\right]\left[SOHY_j^{-}\right]^{m_k}\exp\left(\frac{-m_k e\psi_\beta}{kT}\right)(j,k = 1,2\ldots) \qquad (20)$$

The charge contained in the inner Stern layer located at the locus of the centers of the specifically adsorbed ions X_i and Y_j is given by,

$$\sigma_0 = F\left\{\sum_i\left[SOHX_i^{+}\right] - \sum_j\left[SOHY_j^{-}\right] - \sum_j\sum_k m_k\left[(SOHY_j)_{m_k}A_k\right] + \sum_i\sum_l n_l\left[(SOHX_i)_{n_l}B_l\right]\right\} \qquad (21)$$

where F is a conversion factor from sites/cm^2 to coulombs/cm^2

Similarly the charge in the outer Stern layer

$$\sigma_\beta = F\left\{\sum_k \sum_j m_k \left[(SOHY_j)_{m_k} A_k\right] - \sum_l \sum_i n_l \left[(SOHX_i)_{n_l} B_l\right]\right\} \qquad (22)$$

And the Gouy-Chapman layer charge for any general set of supporting electrolytes is obtained by integrating the Poisson equation for the boundary condition,

$$\psi_x \rightarrow \psi_\infty, \quad d\psi_x/dx \rightarrow 0 \quad \text{as } x \rightarrow \infty \qquad (23)$$

$$\sigma_d = \left\{2\varepsilon_r \varepsilon_o kT \left[\sum_k \left[A_k^{m_k+}\right] \exp\left(\frac{-m_k e \psi_d}{kT}\right) + \sum_l \left[B_l^{n_l-}\right] \exp\left(\frac{-n_l e \psi_d}{kT}\right)\right] - 1\right\}^{\frac{1}{2}} \qquad (24)$$

where $\left[A_k^{m_k+}\right]$ and $\left[B_l^{n_l-}\right]$ are bulk concentrations in ions/volume. For a single symmetric electrolyte, this equation will reduce to the familiar form,

$$\sigma = \left(8\left[A\right]\varepsilon_r \varepsilon_o kT\right)^{\frac{1}{2}} \sinh\left(\frac{Ze\,\psi_d}{2kT}\right) \qquad (25)$$

The entire interfacial region must of course remain electrostatically neutral, therefore,

$$\sigma_o + \sigma_\beta + \sigma_d = 0 \qquad (26)$$

Futher the inner and outer Stern layer capacitances will require that

$$\psi_o - \psi_\beta = \frac{\sigma_o}{C_1} \qquad (27)$$

and

$$\psi_\beta - \psi_d = \frac{\sigma_d}{C_2} \qquad (28)$$

Finally the total number of surface sites available for surface charge development (N_S sites/cm^2) is given by the sum of all possible sites.

$$N_S = \sum_i \left[SOHX_i^+\right] + \sum_j \left[SOHY_j^-\right] + \sum_l \sum_i \left[(SOHX_i^+)_{n_l} B_l^-\right] + \left[SOH\right] + \sum_k \sum_j \left[(SOHY_j^-)_{m_k} A_k^+\right] \qquad (29)$$

The Equations 17 to 22, 24 and 26 to 28 represent a set of $\left[i + j + (i * 1) + (j * k) + 7\right]$ equations. The unknowns in this system of

equations are N_s, C_1, C_2, K_i, K_j, K_{il}, K_{jk}, SOH , $SOHX_i^+$, $\left[SOHY_j^-\right]$, $\left[(SOHX_i^+)\,B_l^-\right]$, $\left[(SOHY_j^-)A_k^+\right]$, ψ_o, ψ_β, ψ_d , σ_o, σ_β, and σ_d assuming of course that m_k, n_l, $\left[X_i^+\right]$, $\left[Y_j^-\right]$, $\left[B_l\right]$, $\left[A_k\right]$ and T are known, which they will be in any defined system. In all we have $\left[10 + i + j + (i * l) + (j*k) + i + j + (i * l) + (k*j)\right]$ unknowns. Therefore, in order to solve this set of equations consistently, we must have a set of parameters that can be determined by experimentation

$$\text{\# of parameters} = \text{\# of unknowns} - \text{\# of equations}$$

$$= (i + j) + (i * l) + (j * k) + 3 \qquad (30)$$

These parameters are chosen to be K_i, K_j, K_{il}, K_{jk} and C_1, C_2 and N_S. If this set of parameters can be specified by some means the set of non linear algebraic equations can be solved self consistently to yield not only the various surface concentrations but also more importantly σ_o ,σ_β ,σ_d,ψ_o, ψ_β and ψ_d. This would describe completely the interfacial electrochemistry of such a system.

The Statistical Mechanical Approach

If the primary charging mechanism is assumed to be adsorption of potential determining ions the surface charge can be expressed by a multicomponent Langmuir type equation (16, 17).

$$\sigma_o = \sum_i \frac{z_i e N_{si} \gamma_i x_i K_i^{cat}}{1 + \sum_p \gamma_p x_p K_p^{cat}} + \sum_j \frac{z_j e N_{sj} \gamma_j x_j K_j^{an}}{1 + \sum_q \gamma_q x_q K_q^{an}} \qquad (31)$$

where $$K_i = \exp\left[\frac{-\Delta G_i}{kT}\right] \qquad (32)$$

ΔG_i = Free energy of adsorption of i.

$$= \phi_i + z_i e \psi_o \qquad (33)$$

ϕ = Free energy of specific adsorption of i due to non electrostatic forces.

x_i = mole fraction of component X_i.

γ_i = activity coefficient of X_i.

z_i = electronic charge of adsorbing species.

It is evident that the free energies of adsorption may be calculated from the equilibrium constants K_i and K_j estimated earlier.

$$\Delta G_i \text{ (per molecule)} = -kT \ln K_i \qquad (34)$$

$$K_i = \exp \frac{-\phi_i - z_i e \psi_0}{kT} = K_{io} \exp \left(\frac{-z_i e \psi_0}{kT} \right) \qquad (35)$$

K_{io} is the intrinsic equilibrium constant that does not depend upon the charged state of the surface, but only on non-electrostatic interactions.

3.4 Results and Discussion

SEM and EDAX results

The scanning electron micrographs of the three "clean" oxide samples shown in Figs. 3-1, 3-2 & 3-3 indicate that the Ottawa sand is very clean, but the baked and unbaked Berea sandstone samples show traces of clay like particles adhering to the large detrital oxide surfaces. These micrographs also show quite clearly the smooth non porous pyrogenic silica surfaces and the rough, uneven more porous surfaces.

It is clear that the samples are inhomogeneous and that different particles present surfaces of different composition. Although it is quite meaningless to talk of the composition of such an inhomogeneous mixture, certain noteworthy features may be used to characterize the samples better.

All three samples exhibit clean smooth crystalline surfaces and broken up and irregular surfaces. But where on the one hand Ottawa sand does not show any traces of clays, the other two samples do. EDAX scans show that all the smooth unbroken surfaces are 100% pure silica surfaces. However

the rough surfaces vary greatly in composition. The Ottawa sand sample has yellow grains that contain large amounts of Fe_2O_3 (see Sand 2 in Table 3-1). Substantial quantities of Al_2O_3 are also present on these rough surfaces. The unbaked and baked samples present 3 kinds of surfaces -(a) pure silica (b) broken and uneven surfaces of varying composition, and (c) clay covered surfaces. Surfaces Baked 1 and Unbaked 1 in Table 3-1 are examples of (c). Surfaces Baked 2 and Unbaked 2 are samples of (b). A clay sample EDAX is provided for comparison.

σ_0 vs pH curves

Figures 4, 5 and 6 show the σ_0 vs pH curves obtained for the three samples, by potentiometric titration experiments described earlier. The results show that KCl proves to be an indifferent electrolyte and the surfaces behave as oxide surfaces in that they exhibit the σ_0-pH curve typical of such amphoteric surfaces. The same point of zero charge (PZC) is obtained by conducting titrations at different indifferent electrolyte concentrations. The PZCs are indicated on the figures.

It is difficult to make any direct comparisons with previously reported data for pure oxide surfaces.

It would seem at first glance that the PZCs should be on the acidic side for samples that are predominantly silica. Yet this is only a conjecture as it would be very difficult to make any predictions for the PZC of such a complex mixture of oxides.

Evaluation of Equilibrium Constants For the Sand and Sandstone Oxide Surfaces

If, as has been frequently stated in the literature, H^+ and OH^- are the only potential determining ions for oxide surfaces, i = 1 and j = 1. Further if there is only one electrolyte in the solution then k = 1 and l = 1 and the set of equation reduces to that of Davis et al. (9).

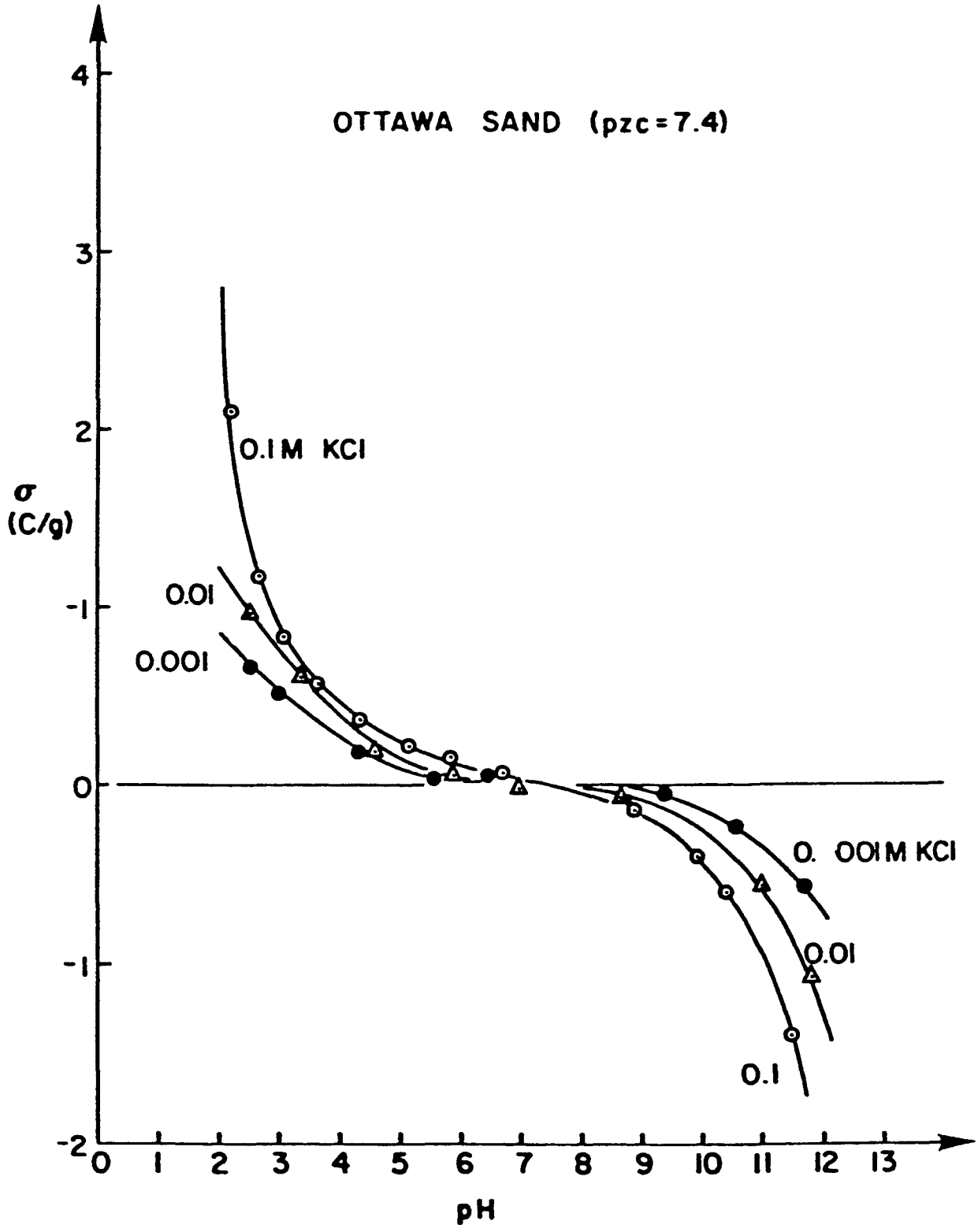

Fig. 3-4 - Surface charge (σ) vs pH plot for the Ottawa sand sample.

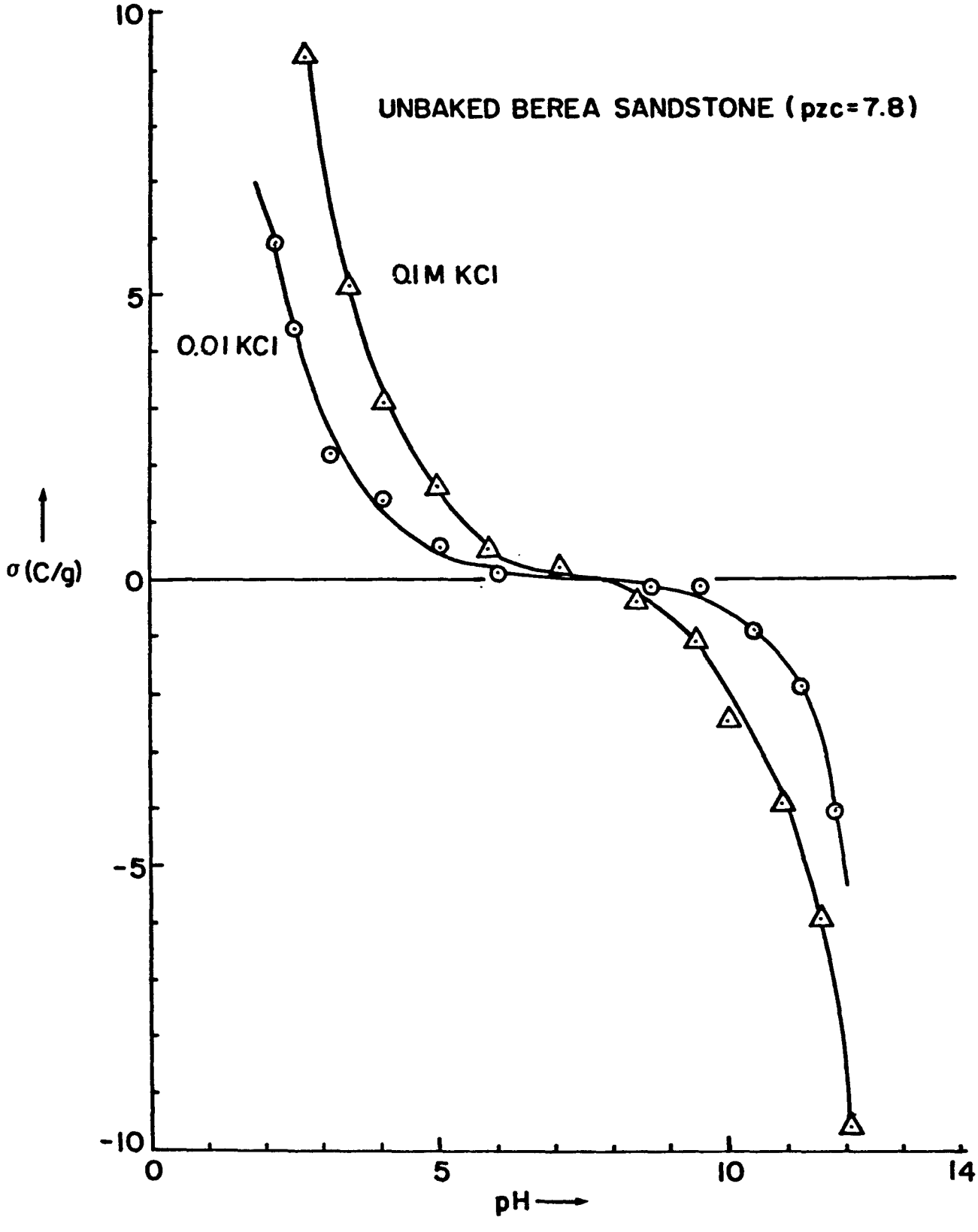

Fig. 3-5 - Surface charge vs. pH plot for the unbaked Bera sandstone sample.

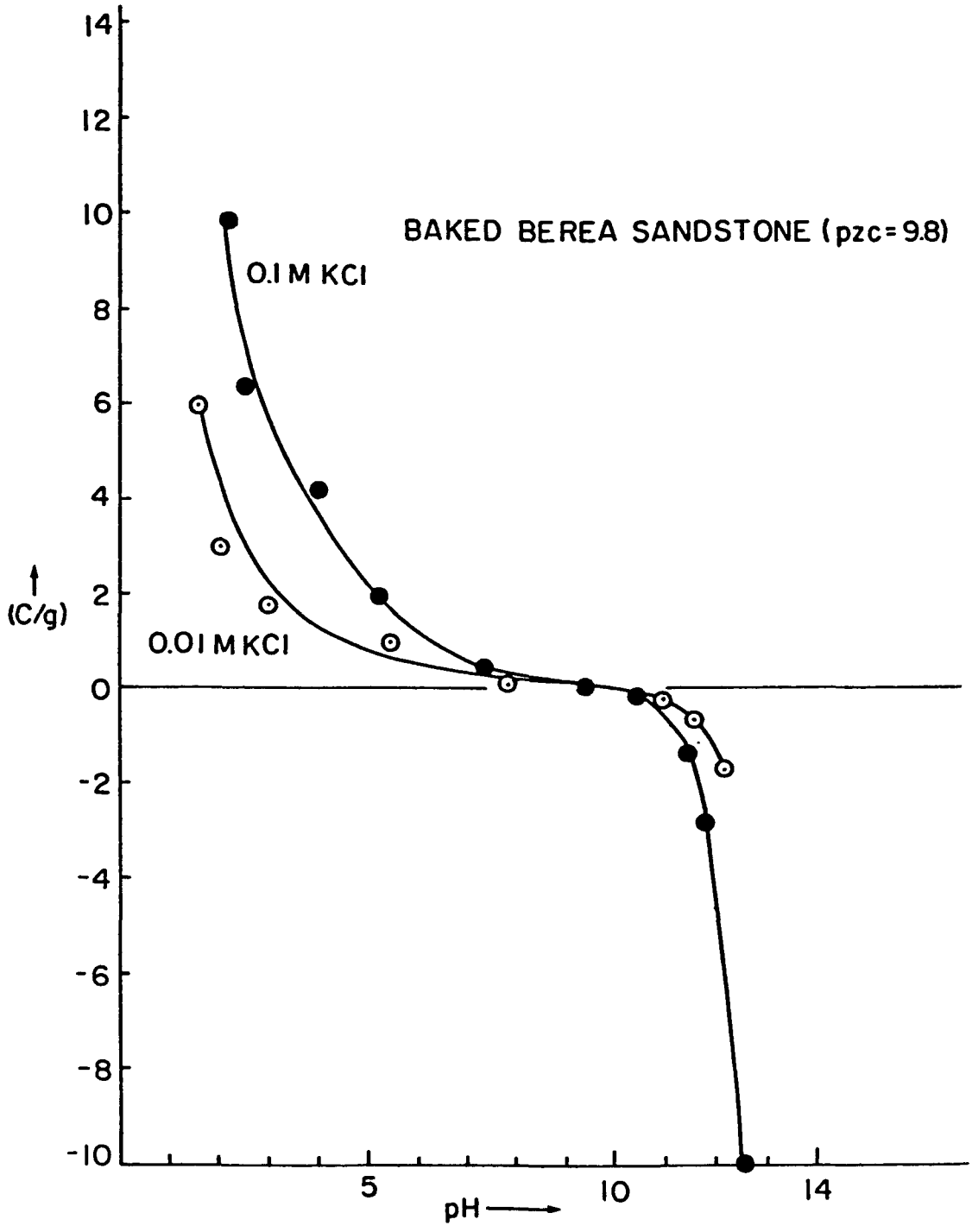

Fig. 3-6 - Surface charge vs. pH plot for the baked Berea sandstone sample.

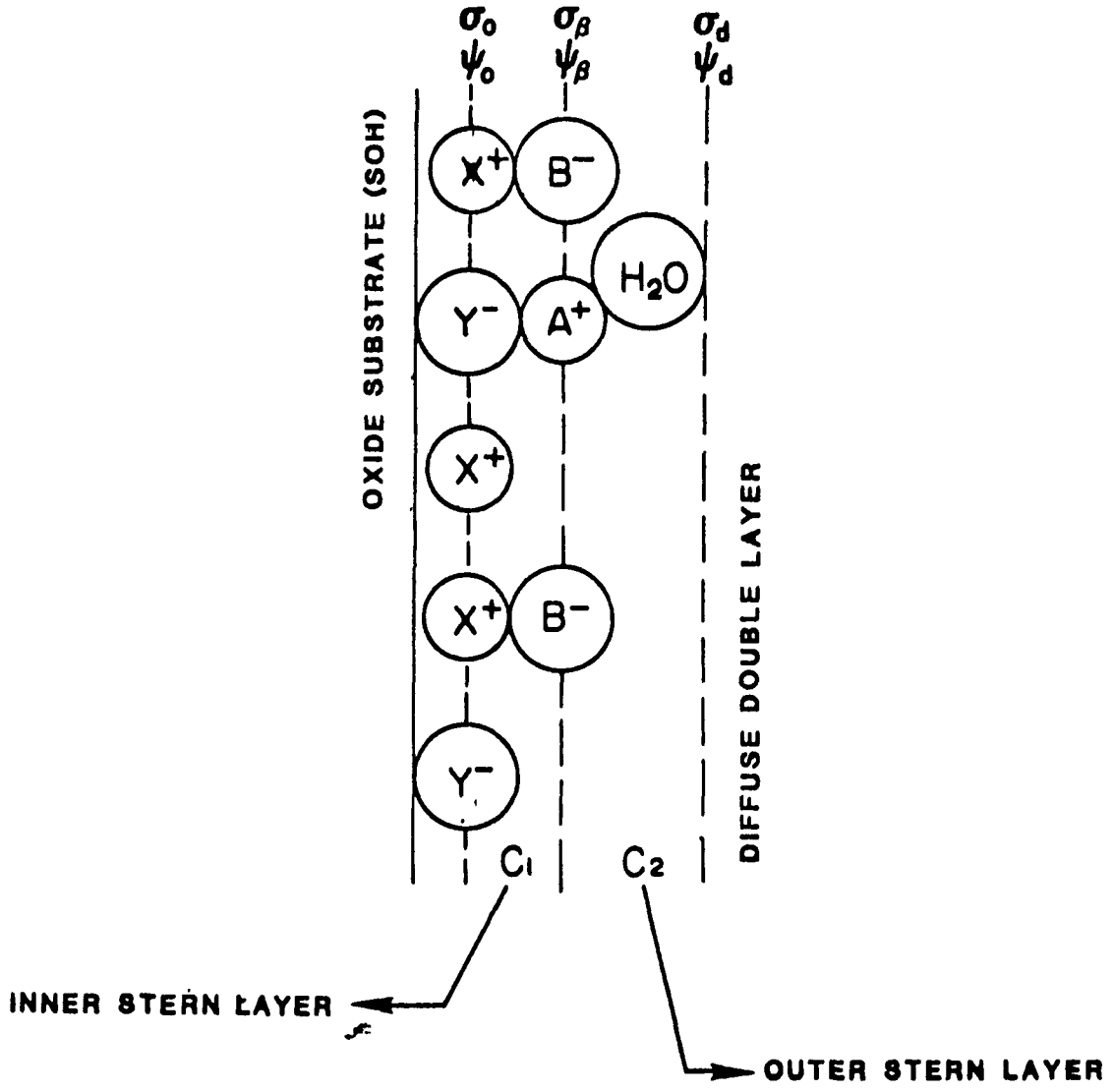

Fig. 3-7 – A schematic representation of the double layer model showing the position of the surface charges and potentials.

Such a simplification is essential if their method has to be used to estimate the K_i, K_j, K_{il} and K_{jk} values. For each electrolyte in solution a set of potentiometric titration curves must be experimentally determined and the K_{il} and K_{jk} values determined.

Davis' method (9) has been used here and it is shown that it can be applied, although only approximately, to complex mixtures of geologically occurring oxide surfaces.

As suggested by the above authors plots were constructed for pQ vs $\alpha_{\pm}$. As can be seen from Figs. 3-8, 3-9 and 3-10, for the 3 samples studied the points do not fall exactly on a straight line. The fit is not as good as that obtained by using data for pure oxide surfaces. However the trend is quite clearly indicated and a fairly good estimate of K_1^{cat}, K_1^{an}, K_{11}^{cat}, and K_{11}^{an}, can be made for each sample. The $K_{a_1}^{int}$, $K_{a_2}^{int}$, K_{cation}^{int} and K_{anion}^{int} (Ref. 9) are related to K_1^{cat}, K_1^{an}, K_{11}^{cat} and K_{11}^{an}, as follows,

$$K_1^{cat} = \frac{1}{K_{a_1}^{int}} \quad (36); \qquad K_1^{an} = K_{a_2}^{int} * 10^{14} \quad (37)$$

$$K_{11}^{cat} = K_{cation}^{int} \quad (38); \qquad K_{11}^{an} = K_{anion}^{int} \quad (39)$$

The K values are tabulated in Table 3-2.

The capacity for the inner and outer layers depends on a variety of parameters - the nature of the surface and the size and concentration of the counter-ions. Devanathan (18) has suggested a method for estimating differential capacities using potentiometric titration data for metal surfaces. Davis (9) has estimated C_1 and C_2 for various pure oxide systems seeking to match both the surface charge and zeta potential measurements. A value of 20 $\mu F\ cm^{-2}$ for C_1 and 100 to 140 $\mu F\ cm^{-2}$ for C_2 seems to be appropriate for most oxide-electrolyte systems.

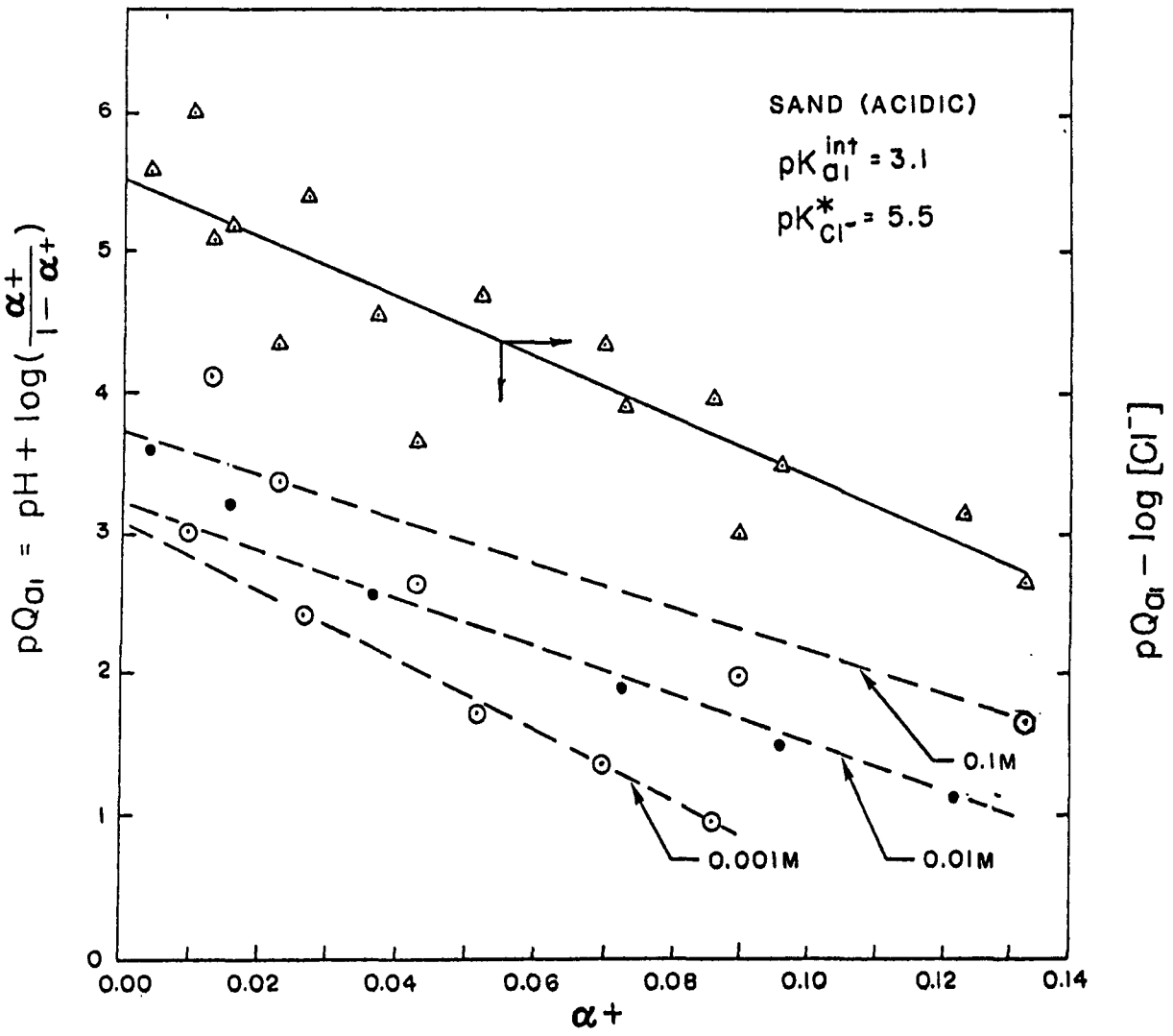

Fig. 3-8a - A plot of pQ_{a_1} and pQ_{a_1} - log (Cl^-) vs. α_+ to determine the equilibrium constants on the acidic side of the PZC., for Ottawa sand.

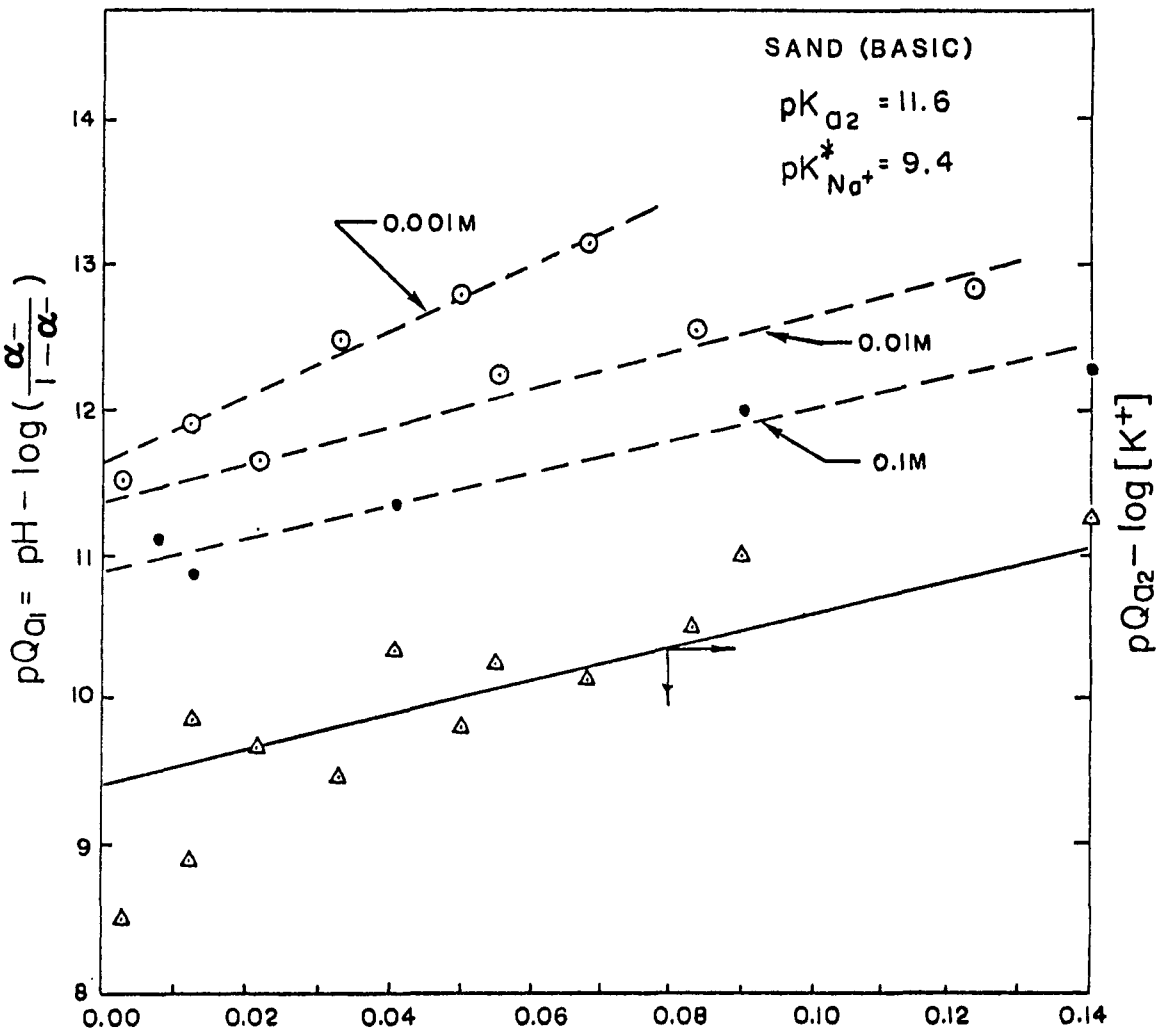

Fig. 3-8b - A plot of pQ_a and pQ_a - log (K^+) vs. _ on the basic side of the PZC. for Ottawa sand.

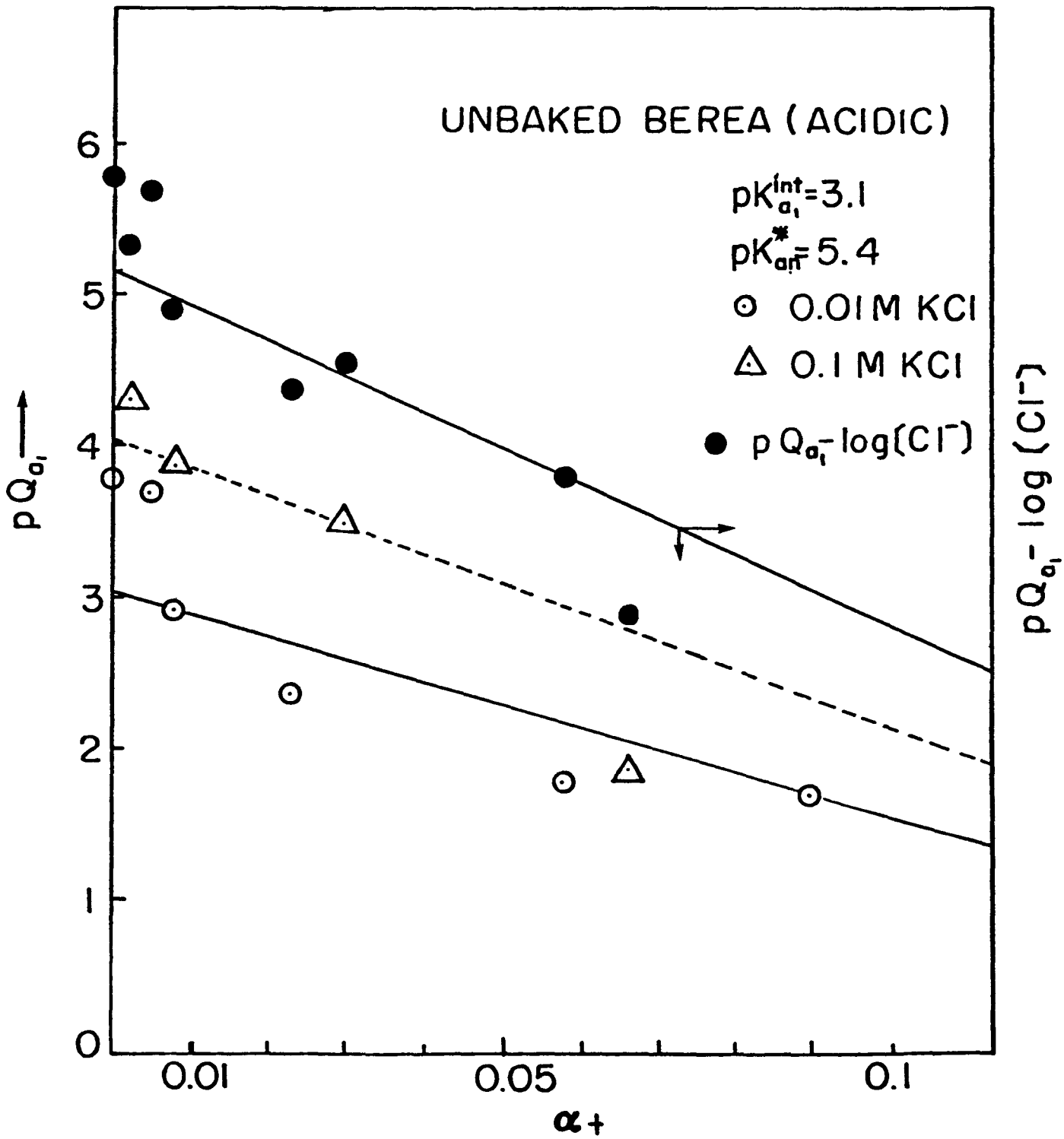

Fig. 3-9a - Plots similar to Fig 3- 8a for the unbaked Berea sample

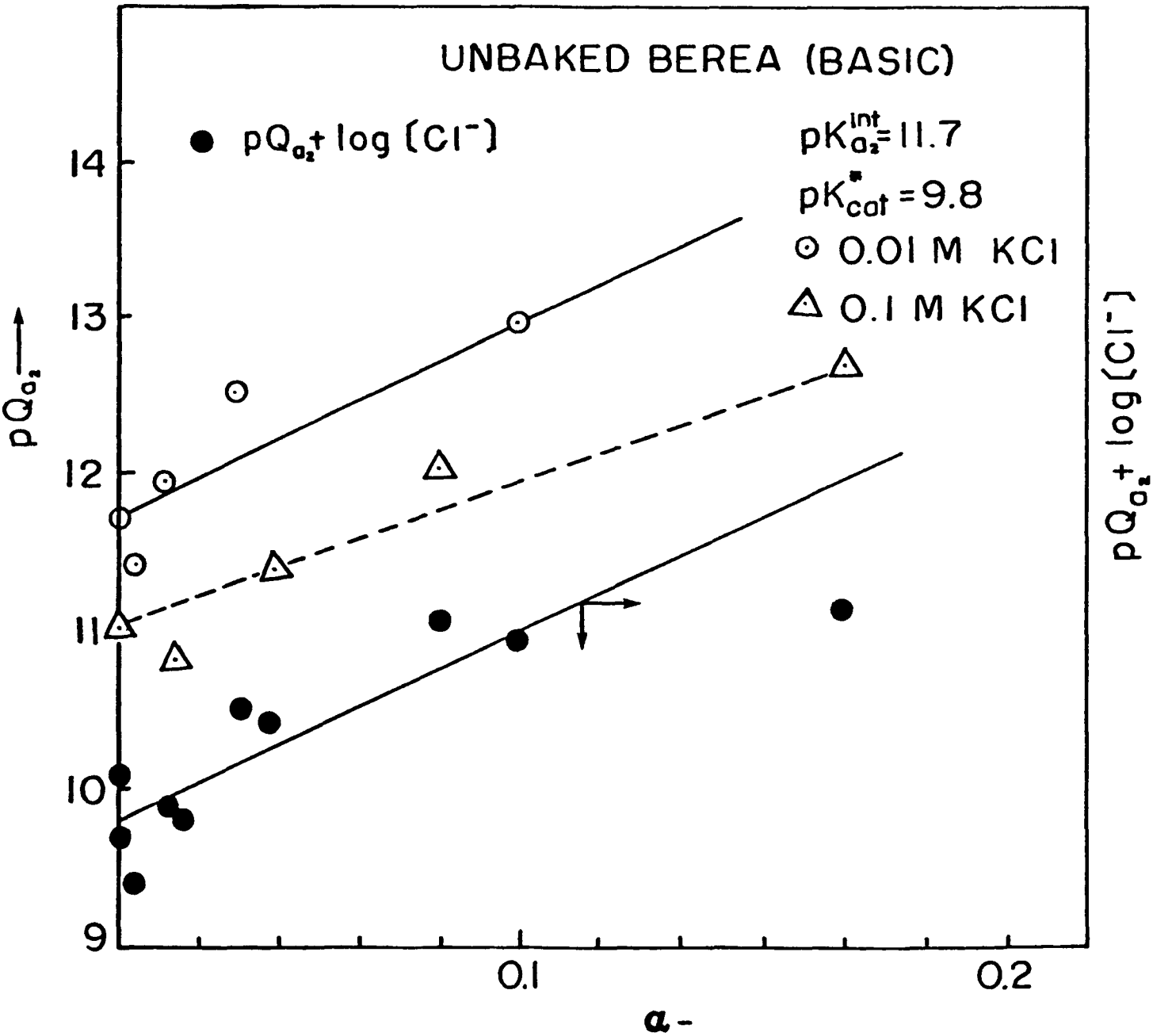

Fig. 3-9b - Plots similar to Fig 3- 8b for the unbaked Berea sample.

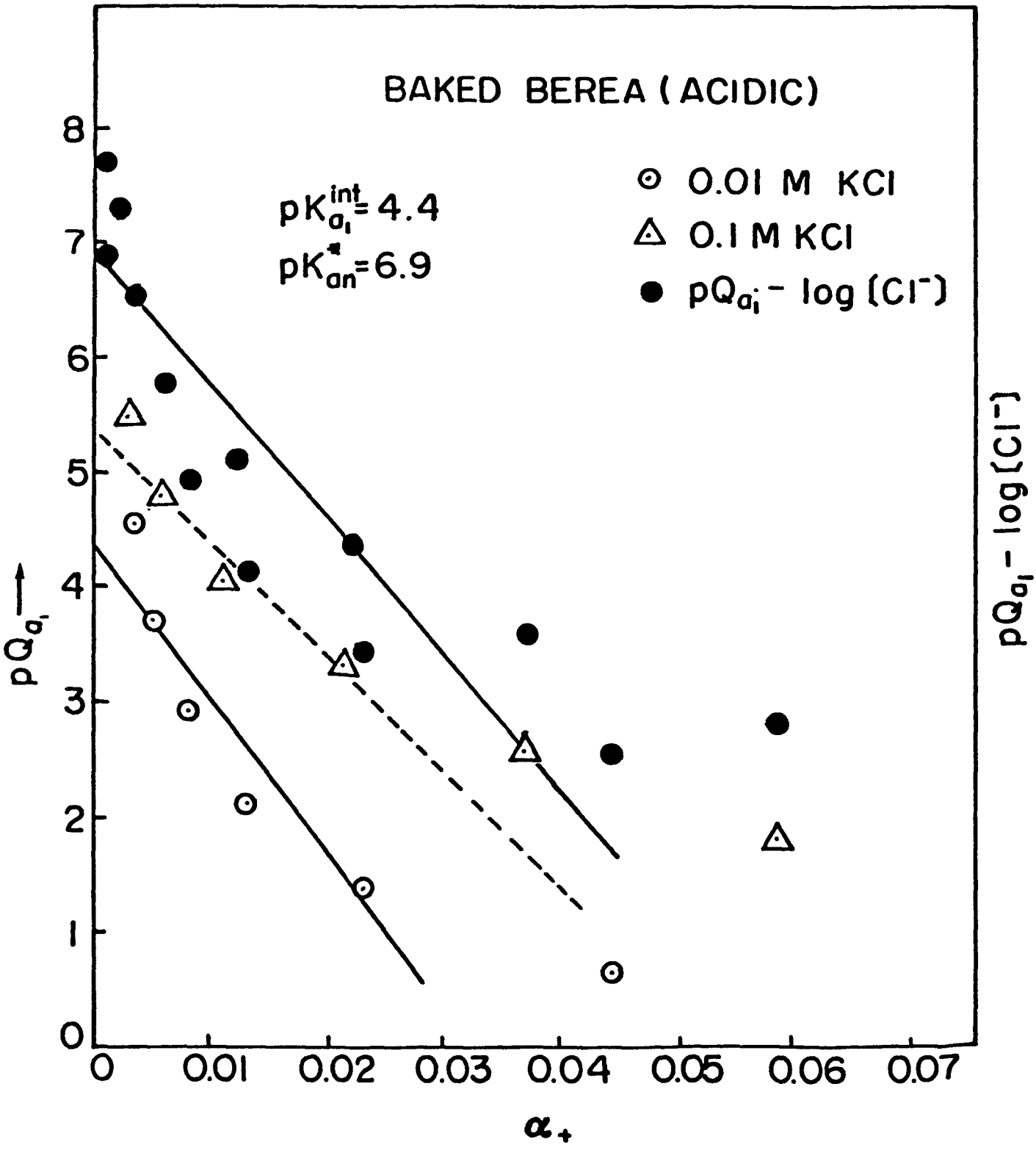

Fig. 3-10a - Plots similar to Fig 3 -8a for the baked Berea sample.

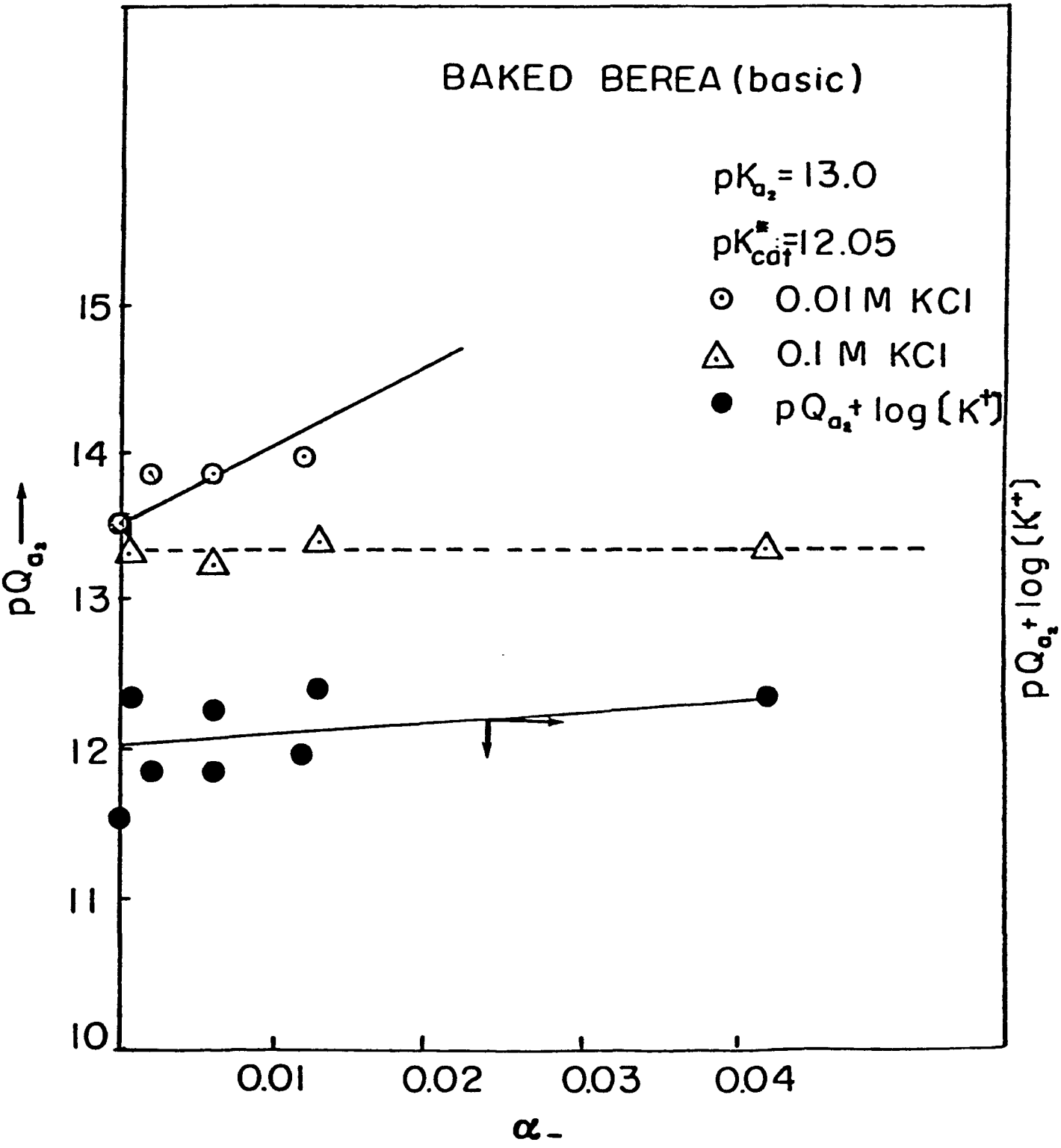

Fig. 3-10b - Plots similar to Fig 3- 8b for the baked Berea sample.

TABLE 3.2a

A Comparison of the pK values of the Detrital Grains of Our Samples with the pK values obtained by Davis et al.(9) for Pure Oxide Surfaces

	pKa_1^{int}	pKa_2^{int}	pK^*_{cat}	pK^*_{an}	ΔpKa	$\Delta pK_{complex}$
Sand	3.1	11.6	9.4	5.5	8.5	3.9
Unbaked Berea	3.1	11.7	9.8	5.4	8.6	4.4
Baked Berea	4.4	13.0	12.0	6.9	8.6	5.1
SiO_2/KCl^*	n.a.	7.2	6.7	n.a.	$\sim$8.4	$\sim$7.4
$\gamma Al_2O_3/NaCl^*$	5.7	11.5	9.2	7.9	5.8	1.3

* from Davis et al. (9).

TABLE 3.2b

Equilibrium Constants of Adsorption for the Three Samples Investigated

	K_1^{cat}	K_1^{an}	K_{11}^{cat}	K_{11}^{an}
Sand	1.26×10^{3}	2.51×10^{2}	3.98×10^{-10}	3.16×10^{-6}
Unbaked Berea	1.26×10^{3}	1.99×10^{2}	1.58×10^{-10}	3.98×10^{-6}
Baked Berea	2.51×10^{4}	10.0	1.0×10^{-12}	1.3×10^{-7}

Model Calculations for Surface Charges and Potentials

The parameters chosen as knowns for the model are K_i, K_j, K_{il}, K_{jk}, C_1, C_2 and N_S. As has been pointed out earlier the set of Equations 17 to 29 can now be solved self consistently for σ_0, σ_β, σ_d, ψ_0, ψ_β, ψ_d and the concentration of the various surface species.

It is noted that the equations are a set of simultaneous non-linear algebraic equations which cannot be solved by Gaussian elimination. Linearization is possible by guessing at initial values of σ_0 and ψ_d and then recalculating these values from the equations and iterating until convergence is achieved A computer program was written using such an algorithm. The initial guesses for σ_0 and ψ_d can be made quite accurately since they can be experimentally measured.

The zeta potential of the detrital grains is difficult to measure since they are large and much denser than water. Attempts were made using a Zeta Reader but proved unsuccessful as the settling rates are so high that no measurements could be made. However, the surface charge is available from the potentiometric titrations.

For our case of a single pair of potential determining ions and a single pair of indifferent electrolyte ions, $i = j = k = l = 1$, and the Equations 17 to 29 reduce to a set of 11 equations with 11 unknowns. This system of equations is then solved for the charges and potentials. A typical plot is shown in Fig. 3.11 at a typical pH value.
The thicknesses of the inner and outer Stern layers β and γ are calculated using the relations

$$\beta = \frac{\epsilon_0 \epsilon_\beta}{C_1}$$

and

$$\gamma = \frac{\epsilon_0 \epsilon_\gamma}{C_2}$$

An Illustration of the Surface Potential Variation of Ottawa Sand

$C_1 = 1.4\ F/m^2$; pH = 4.0

$C_2 = 0.2\ F/m^2$; $C_{KCl} = 0.1\ M$

Specific surface area = $5\ m^2/g$

σ_o = 0.4 C/g (from Fig. 4)

= $0.08\ C/m^2$

$\sigma_\beta = -0.065\ C/m^2$ $\beta = 0.44\ ^oA$

$\sigma_d = -0.015\ C/m^2$ $\gamma = 8.9\ ^oA$

ψ_o = 150.6 mV

ψ_β = 93.5 mV

ψ_d = 20 mV

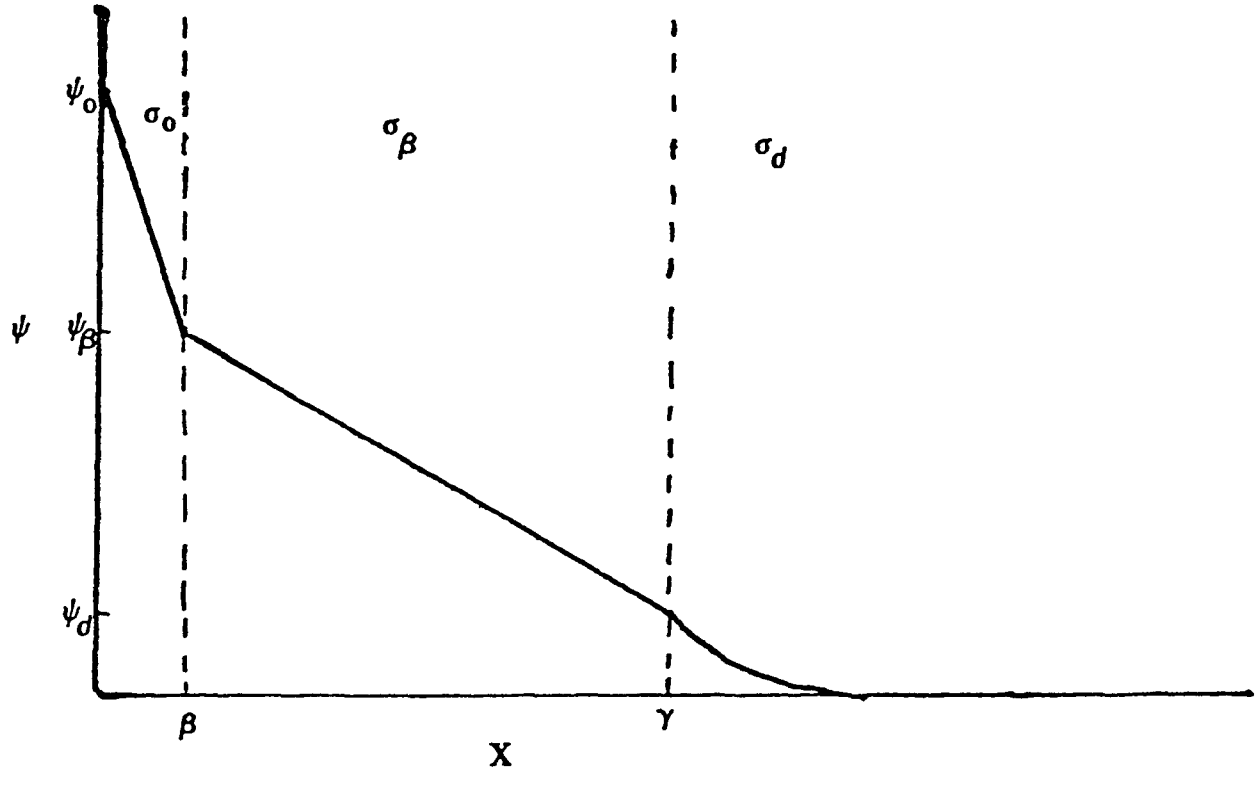

Fig. 3.11 - A typical surface potential distribution into the solution for the Ottawa sand sample at a typical pH value

where ε_o is the permittivity of vaccuum and ε_β and ε_γ are the dielectric constants of the inner and outer Stern layers respectively. The dielectric constant of the bulk water is 78.5 at 25°C. This value changes in the presence of an electric field and there are many models postulated to predict this dependence. (26,27,28,29). At very high electric field strengths ($\sim 10^9$ V m^{-1}) the dielectric constant reaches a limiting value of 6. In computing the Stern layer thicknesses, ε_β and ε_γ are taken equal to 7.0 and 20.0 respectively. More rigorous analyses may be carried out by using the exact dependence of ε_β and ε_γ on distance, but is considered unnecessary here.

Estimation of Surface Charges Using the Statistical Mechanical Approach

An independent estimate of surface charge can be made using Equation 31. The effects of surface complexation are not taken into account. Also the estimation of surface charge leaves us with the problem of estimating the surface potential distribution. An appropriate double layer model would have to be used to achieve this. This model however provides us with a quick independent check on whether or not the K_i^{cat} and K_j^{an} values are reasonable.

A typical calculation using Equation 31 and previously calculated values of K_i^{cat} and K_j^{an} for Ottawa Sand is shown in Fig. 3.12. Ideality is assumed ($\gamma_i = 1$) and N_{si} and N_{sj} are taken to be equal for H^+ and OH^- ions. The point of zero charge and the σ_o-pH curves are matched quite accurately, demonstrating that K_i^{cat} and K_j^{an} are reasonably accurate.

Discussion of Results

The method of sample preparation can be a determining factor in the above experimental results. It must be ascertained that no clays are present

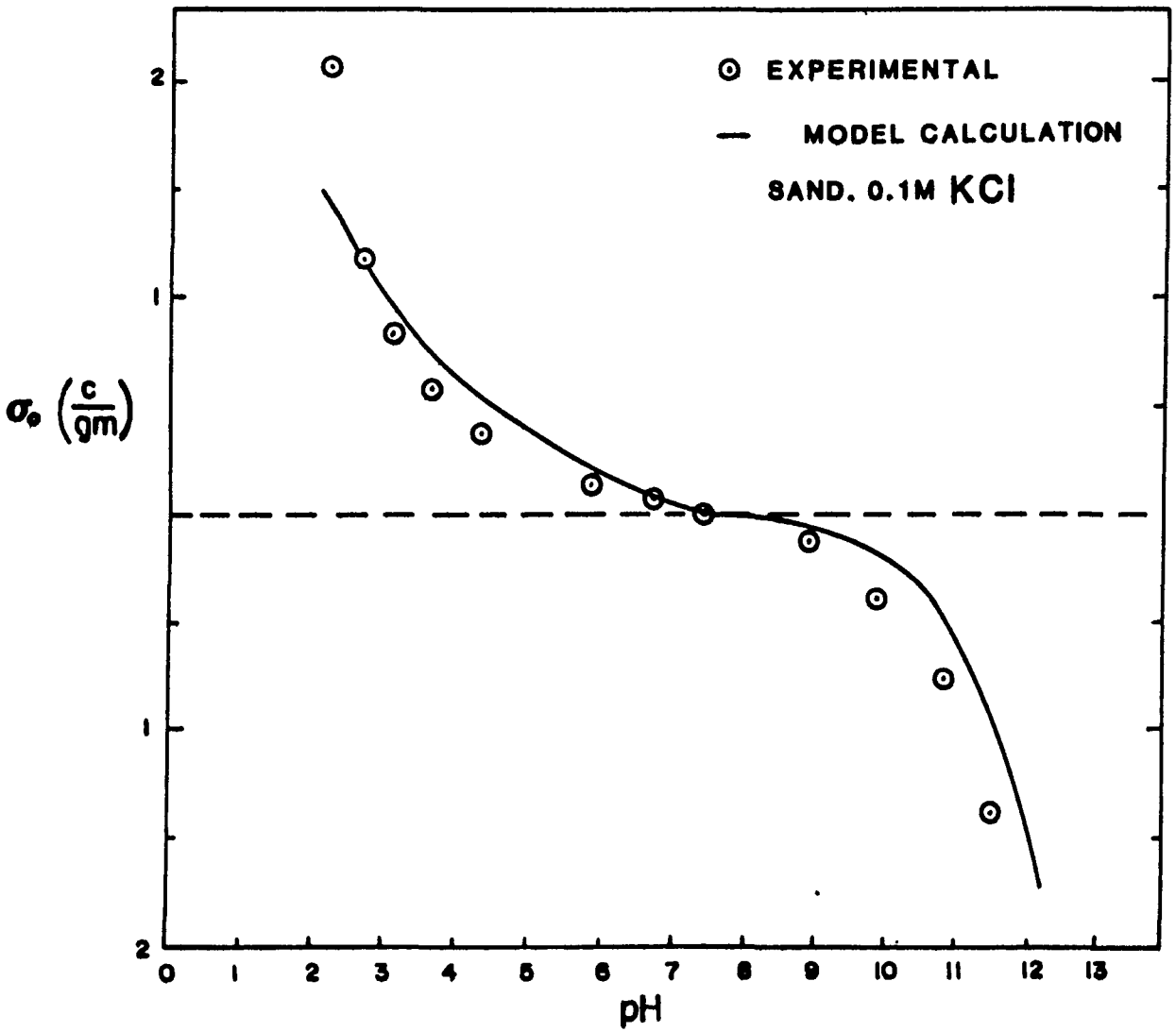

Fig. 3.12 - Model calculations done for surface charge using the statistical mechanical approach, match the experimental points quite closely.

in the system before the titrations are carried out. The samples were prepared all at the same time and potentiometric titrations were done after washing the samples repeatedly until no more clays were recoverable and no change was observed in the potentiometric titration readings. No peptizing agents were used for fear that they may irreversibly alter the surface properties of the grains. The SEM pictures however still show some traces of clays stuck to the oxide surfaces. The Ottawa Sand appears to be the cleanest sample, having very little clay in the first place.

The pzc value for the unbaked sandstone surface indicates that at pH values higher than 7.8 the surface becomes negatively charged and should electrostatically repell clay platelets. This phenomenon has been experimentally observed in clay release and dispersion studies on Berea Sandstone samples (19, 20). Clay particles in core pore spaces were significantly disturbed and thus made mobile in contact with pH 8 fluid. The effect was more noticeable when contacted with a pH 10 fluid. No disturbance was noted when the sample was contacted with a pH 4 fluid (19,21). In Berea sandstones, such pH effects reduced the permeability to 1% of its original value. These effects can be easily explained on the basis of the σ_0 -pH plot for the oxide surfaces presented here.

On the other hand the Baked Berea Sandstone is often used in conducting experiments where the effects of clay migration are to be minimized. It is commonly believed that baking the sandstone immobilizes the clays. The reason why this happens is evident from the σ_0-pH plot for the Baked sandstone sample. At commonly used pH values (pH $<$ 9.8) the oxide surfaces are positively charged and there is consequently a strong electrostatic attraction between the detrital grain and the clay platelets. This is why the clays remain immobilized in baked sandstone samples even at high pH values.

There is also a common misconception that high temperature baking of a sandstone sample alters only the clays in the sample. This is shown to be untrue by both the SEM pictures (Figs. 3.1, 3.2 & 3.3) and the σ_0-pH curves (Figs. 3.4, 3.5 & 3.6). The oxide surfaces of the detrital grains also seem to be altered and the surface charge properties are quite different for the two samples. The precise mechanism by which baking alters the surface is difficult to postulate. Probably the heating of the sandstone results in the breaking down of the smooth crystalline faces of the grains which are almost purely silica, into rough uneven pitted surfaces exposing other minerals with higher pzcs. This could explain both the higher pzc and the higher percentage of uneven surfaces in the baked sample.

A comparison of the values for the equilibrium constants K_i, K_j, K_{il}, K_{jk} with those reported earlier by Davis, James et al (9) for pure oxide surfaces show that although the K values are in the same range, no correlation with composition may even be attempted. Indeed the mixtures of oxides are quite complex from a surface chemical viewpoint, even though they may be simple, geologically. It is remarkable therefore that such a complex mixture of oxides can be described by a model that has in the past been used to describe carefully prepared pure oxide surfaces. Such a complete description will prove to be very useful in describing not only detrital grain-clay interactions, but also to predict the adsorption behavior of sandstone formations.

As has been noted by Yates et al. (8) non-porous quartz or pyrogenic silica surfaces have lower charge and differential capacities as compared to other oxides. This was attributed to large $\Delta pK_a = pKa_2 - pKa_1$ values. Our data show that the Ottawa sand sample, having the largest proportion of non-porous quartz surfaces has the least charge and the smallest ΔpKa value. Also, the adsorption of the indifferent electrolyte on the charged surface sites

seems to be strongest in the case of Ottawa Sand, as indicated by a small ΔpK complex value. A detailed mechanistic interpretation of the pK values is provided by Yates (8).

Of all the parameters estimated the values of β and γ are the least reliable. The choice of C_1 and C_2 and ε_β and ε_γ is made rather crudely and it is these parameters that affect β and γ. C_1 and C_2 the capacitances of the inner and outer Stern layers were based on typical values for pure oxides (8,9) and were chosen on the basis of matching experimental results of σ_0 and zeta potential simultaneously. ε_β and ε_γ were chosen as some average values for each layer but in reality will vary with the surface charge itself. The β and γ thus calculated are at best only approximate estimates and could vary substantially from the values shown in Figure 11. As Yates et al. (8) have pointed out, assigning a low value of 6-9 to ε_β implies that the inner Stern layer has a highly structured water layer adsorbed on it, with very few ionic species breaking this lattice. This ion exclusion is however unlikely. Yates et al (8) argue that the low value of C_2 needed to match the zeta potential measurements with ψ_d, is possibly due to one of the following reasons: (a) The shear plane may be further away from the surface than the outer Helmholtz plane, hence the value of C_2 would be larger than that based on identifying ψ_d with the zeta potential (b) the presence of a porous hydrated oxide layer at the interface which is penetrable by the supporting electrolyte ions. If this is the case a wider separation between the inner Helmholtz plane and the diffuse layer becomes plausible. In any case the values of β and γ should be regarded with caution.

The ability of hydrolysable metal ions to reverse the charge of anionic substrates has been reported by a few authors (22, 23). Certain metallic ions may act as potential determining ions and cause charge reversal. However the charge reversal discussed by James and Healy (23) for silica

surfaces is caused by surface precipitation of metal hydroxides. This is quite different from the phenomena discussed in this paper. The precipitation of the metal hydroxide results in a partial coating over the substrate surface. As a result the charge properties measured are no longer that of the original substrate but a combination of the exposed substrate and the coating. Such precipitation effects have not been taken into account in this paper.

However, if the metal ions act as pdi's instead of acting as indifferent electrolyte ions, and cause shifts in the pzc, then this can be accounted for by using the generalized equations presented in this paper. Breewsma and Lyklema (24) observed shifts in the pzc of haematite at high concentrations of $LiNO_3$ and LiCl (1.0 M), indicating that the Li^+ ion being comparable in size to H^+ and OH^- was being specifically adsorbed on the surface. This specific adsorption must be accounted for in the model in two ways. Firstly Li^+ must be treated as a pdi and potentiometric titrations done to estimate its K_i and K_j. Secondly the inner layer capacitance may be expected to decrease slightly and this change must be accounted for.

The statistical mechanical model which provides the simplest model for a surface acquiring charge by specific adsorption of ions is a quick independent check that demonstrates that the K values obtained are reasonable, and do indeed describe the charging mechanism adequately. The model is simplistic and although it can be generalized to include surface complexation it is difficult to evaluate the nonideality parameters (γ_i). Also it provides us with only the surface charge and from then on an appropriate double layer model will still have to be used to estimate the surface potentials.

3.5 Literature Cited

1. Levine, . and Smith, A.L., Disc. Faraday Soc., 52, 290 (1971).

2. Berube, Y.G. and deBruyn, P.L., J. Colloid Int. Sci., 27, 305 (1968).

3. Lyklema, J., J. Electrochem. Interfacial Electrochem., 18, 341, (1968).

4. Wright, H.J.L., Hunter, R.J., Austral. J. Chem., 26, 1183, 1191 (1973).

5. Smit, W., Holten, C.L.M., et al, J. Colloid Int. Sci., 63, 120 (1978).

6. Deryaguin, B.V., and Dukhin, S.S., Research in Surface Forces, Vol. 3, pg. 269, edited by B.V. Deryagin Consultants Bureau, New York-London (1971).

7. Churaev, N.V. and Deryagin, B.V., Ibid,. pg. 261.

8. Yates, D.E., Levine, S., and Healy, T.W., J. Chem. Soc. Faraday, Trans. I 70, 1807 (1974).

9. Davis, J.A., James, R.O., and Leckie, J.O., J. Colloid Int. Sci., 63, 480 (1978).

10. James, R.O., Davis, J.A., and Leckie, J.O., J. Colloid Int. Sci., 65, 331 (1978).

11. Davis, J.A., and Leckie, J.O., J. Colloid Int. Sci., 67, 90 (1978).

12. Sharma, M.M., and Yen, T.F., under preparation.

13. Sharma, M.M. et al., Enhanced Oil Recovery, Vol. 1, ed. E. C. Donaldson, G. V. Chilingar and T. F. Yen, Petroleum Science Series, Elsevier Pub. (1983).

14. Huang, C.P., Adsorption of Inorganics at Solid - Liquid Interfaces, Chap.5, Ed. M.A. Anderson and A.J. Rubin, Ann Arbor Science, Michigan (1981).

15. Feldman, I., Anal. Chem., 28, No. 12, 1859 (1956).

16. Fowler, R.H., and Guggenheim, E., Statistical Thermodynamics, Cambridge University Press, p. 426. (1965).

17. Wnek, W.J., "The Role of Surface Phenomena and Colloid Chemistry in Deep Bed Liquid Filtration", Ph.D. Thesis, Illinois Institute of Technology. (1973).

18. Devanathan., M.A.V. et al. Chemical Reviews, 65, 635 (1965).

19. Gray, D.H., Rex, R.W., Fourteenth National Conference on Clays and Clay Minerals, p. 355. (1966).

20. Simon, D.E. et al., Society of Petroleum Eng. Paper 6010. (1976).

21. Allen, T.O., Roberts, A.P., Production Operations, Vol II, Oil and Gas Consultants Int. Inc., p. 102 (1981).

22. Matijevic, E. et al., J. Phys. Chem. 65, 1724 (1961).

23. James, R.O., and Healy, T.W., J. Colloid. Int. Sci., 40, 42 (1972).

24. Breewsma, A., and Lyklema, J., Discuss. Faraday Soc., 52, 324 (1971).

25. Hohl, H., and Stumm, W., J. Colloid Int. Sci., 55, 281 (1976).

26. Hunter, R.J., J. Colloid Int. Sci., 22, 231 (1966).

27. Grahame, D.C., J. Chem. Phys., 18, 903 (1950).

28. Grahame, D.C., J. Chem. Phys., 21, 1054 (1953).

29. Booth, F., J. Chem. Phys., 19, 1615 (1951).

4. Effects of Sodium Pyrophosphate Additive on the "Huff and Puff"/Nutrient Flooding MEOR Process

4.1 Abstract

Techniques for using microorganisms in enhanced oil recovery involve deliberate introduction of bacteria into injection wells, and the encouragement of their growth in the oil reservoir formation. Bacterial transport in the reservoir links to the success of a MEOR process. In this chapter, effects of sodium pyrophosphate, a chemical additive, on the bacterial transport ability through the porous media were investigated. Two different microorganisms, B. subtilis and C. acetobutylicum were used in the experiments. Sandpack column, Berea sandstone, and low permeability Kansas limestone core were used as the porous media. It was found that the addition of pyrophosphate can induce higher oil recovery efficiency and C. acetobutylicum is more favorable in the MEOR process. 33% oil recovery efficiency was obtained in the Kansas core of permeability 15 mD.

4.2 Introduction

Due to the decreasing rate of discovery of new oil fields and the continuous rise in global demand, a number of enhanced oil recovery techniques have been employed by the petroleum industry during the last decade. These current enhanced recovery methods involve thermal flooding, polymer flooding, caustic flooding, and carbon dioxide flooding, etc. Recently, a new enhanced oil recovery technique, which employs microorganisms has been studied by the world's petroleum and genetic engineers. Techniques for using microorganisms in enhanced oil recovery involve the deliberate introduction of bacteria into injection wells, and the encouragement of their growth in the oil reservoir formation. However, the immediate problem is that bacterial cells are very easily absorbed in the area near the injection wells, and therefore a plugging problem is caused. The plugging effects caused by bacterial cells in the oil reservoir are due to: (1) the strong absorption tendency of bacteria on the surface of porous rock, (2) the very fast growth rate of bacterial cells in the injection wells or in the reservoir itself, (3) the products of bacterial metabolism (Moses and Springham, 1982). With the reduction of permeability in the rock, there is a negative influence on the whole oil recovery efficiency.

4.3 Effects of Sodium Pyrophosphate on the bacterial transport ability through the porous media:

According to the DLVO theory (Derjaguin-Laudau-Verney-Overback, 1948), once a particle has been brought into close proximity to a second particle, particle-particle interactions determine whether or not the particle is captured. Any suspended particles, whether of an inorganic or biological nature, are subject to van der Waals' force of attraction. If, in addition, the particles have superficially located inorganic groups and the suspending fluid contains polar, ionizing substances, they will be subject to the forces arising from the interaction of the charged electric double layers around them as well as from other interactive electrostatic forces. Therefore, the total interaction energy, V_T (equation 1), of two smooth particles is determined solely by the sum of the van der Waals' attractive energy, V_A (equation 2), and the repulsive electrostatic energy, V_R (equation 3) (Hogg, 1966).

$$V_T = V_A + V_R \qquad \text{(eq. 1)}$$

$$V_A = -\frac{A_{132}}{6KT}\left\{\frac{2a(h+a)}{h(h+2a)} - \ln\frac{h+2a}{h}\right\} \qquad \text{(eq. 2)}$$

$$V_R = \frac{a\varepsilon}{4KT} \{ (\psi_1^2 + \psi_2^2) \ln \frac{\exp(2\kappa h) - 1}{\exp(2\kappa h)} + 2\psi_1\psi_2 \ln \frac{\exp(\kappa h) + 1}{\exp(\kappa h) - 1} \} \qquad \text{(eq. 3)}$$

where: a is the particle's radius

ε is the dielectric constant of the suspending medium.

K is the Boltzmann constant

T is the absolute temperature

h is the separation distance between two approaching surfaces

κ is the Debye-Huckel parameter (reciprocal double layer thickness)

ψ_1, ψ_2 are the potentials of the two surfaces

A_{132} is the Hamaker constant between two surfaces in the suspending medium

When the computed total interaction energy, V_T, is plotted against the distance, h, separating them, a curve of the general type shown in Fig. 4-1 is obtained. Two characteristic values of h at which a net attraction occurs are relevant. These are referred to as the primary minimum (h very small) and the secondary minimum (h = 5-10 nm). They are separated by a repulsive maximum. This

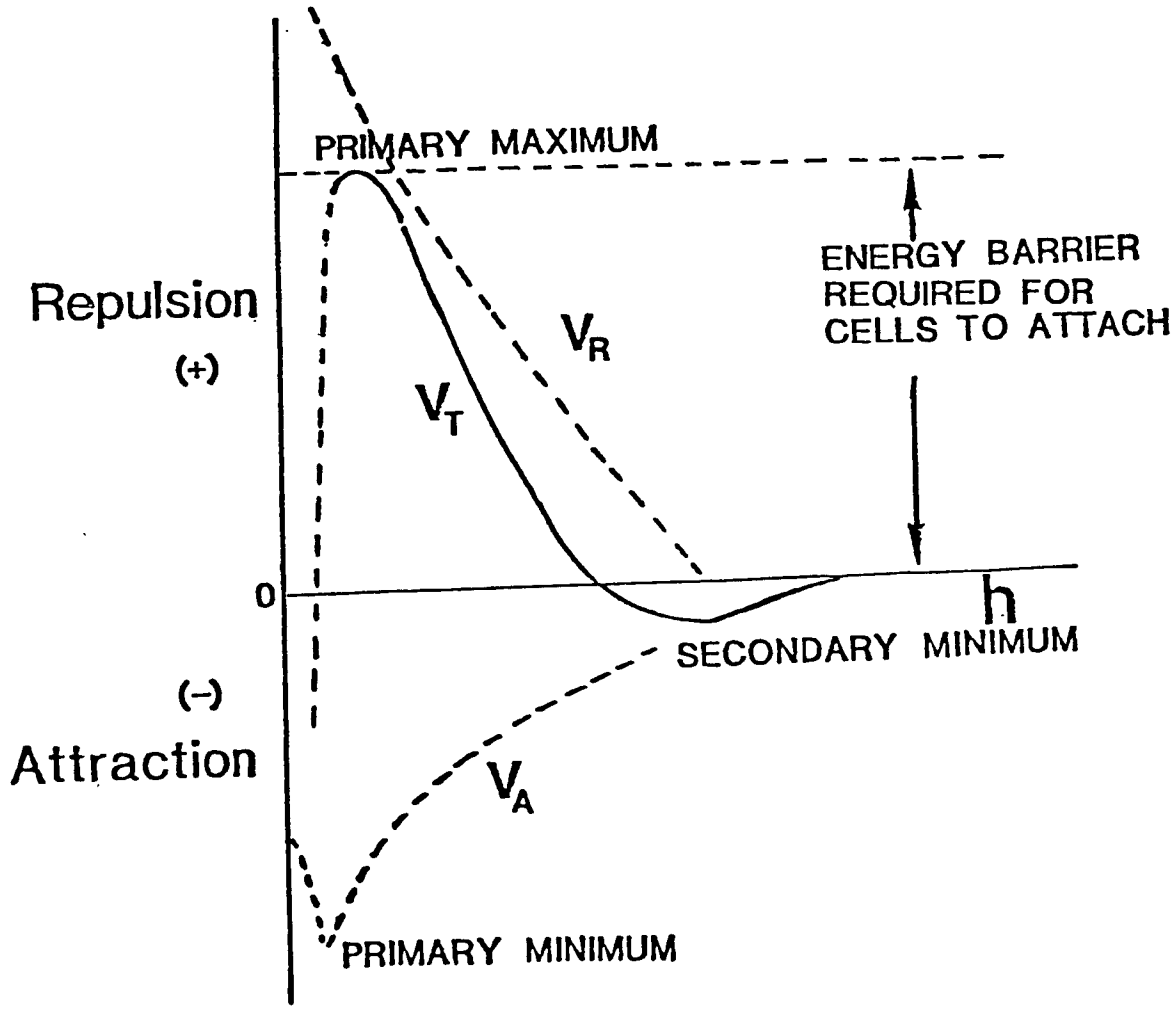

Fig. 4-1 Diagram to show the variation of the total interaction energy with the sepapration distance between a spherical cell and a substratum plate.

indicates that with decreasing distance a weak attraction between the two surfaces is found at first, until the secondary minimum is reached. For distances between the secondary minimum and the primary maximum, work must be performed in bringing the two surfaces together, and accordingly, a repulsive force is active between the two surfaces. For distances smaller than the primary maximum, again, we once more find attraction.

In order to reduce the probability of reversible or irreversible attachment of bacterial cells on the rock surfaces, based on the above analysis, chemical additives which can help the bacterial cells be transported through porous media should have the following characteristics: (a) they should have the ability of increasing the height of the primary maximum in the total interaction energy curve, (b) they should be able to form a complex ionic layer, either around the cell surface or substratum surface, which keeps the cells outside the secondary minimum. Also, the selection of a specific chemical additive should be based upon the type of chemical bonding between it and the surface, which would be enhanced by operating conditions such as pH and ionic strength.

From the results of previous experiments, it was found that a sodium pyrophosphate solution of suitable

concentration can help the bacterial cells be transported through the sandpack column (Chang, Y.I., 1984). Hence, in the following microbial enhanced oil recovery (MEOR) experiments, the method of introducing the sodium pyrophosphate additive in the sweeping slug, in order to improve the transport ability of bacterial cells in the porous media, was conducted.

4.4 Effect of Bacillus subtilis and pyrophophate additive on the oil recovery efficiency from sandpack column

As mentioned earlier, the biosurfactant generated by bacteria grown in-situ in the MEOR process can serve to improve the mobility of oil in the reservoir. B. subtilis is one of the bacterial species generally believed to be able to generate the biosurfactant, surfactin (Cooper, et al., 1981), which can lower the viscosity of the oil. In addition to the ability to generate biosurfactant, the B. subtilis species is one the few genera of bacteria that can produce endospore, which was reported to facilitate transport through the porous media (Yen, et al., 1983). Because of all these considerations, the B. subtilis was chosen as the first bacterial species in the following experiments.

An experimental procedure of repeating the cycle of huff-and-puff followed by nutrient broth flooding was conducted (Jang, L. K., et al., 1984). The crude oil from Range Zone, Long Beach, California with API=17^{o} was used in the experiment. An oil-containing sandpack column (11 in. long X 1 in. diameter) with permeability of 4000 md was prepared. The dry weight of residual oil left after secondary waterflooding was found to be about 10 grams. The growth media contained 0.8% nutrient broth and 0.5% glucose. At the end of secondary waterflooding, about 4 pore volumes of sterilized nutrient broth solution were injected into the sandpack columns. About 0.1 pore volume of B. subtilis was then inoculated into one column (Column 1). Another column (Column 2), which was not inoculated, served for the control run. The columns were kept at 32^{o}C during the experiments.

The accumulated oil recovery from both columns is shown in Fig. 4-2. The horizontal sections in Fig. 4-2 represent the incubation periods during which bacteria multiply and migrate in the sandpack column. During those periods, no production of oil occurred because both ends of the column were sealed. The step change at the end of each incubation period represents the amount of oil pushed out due to the "power" produced by B. subtilis

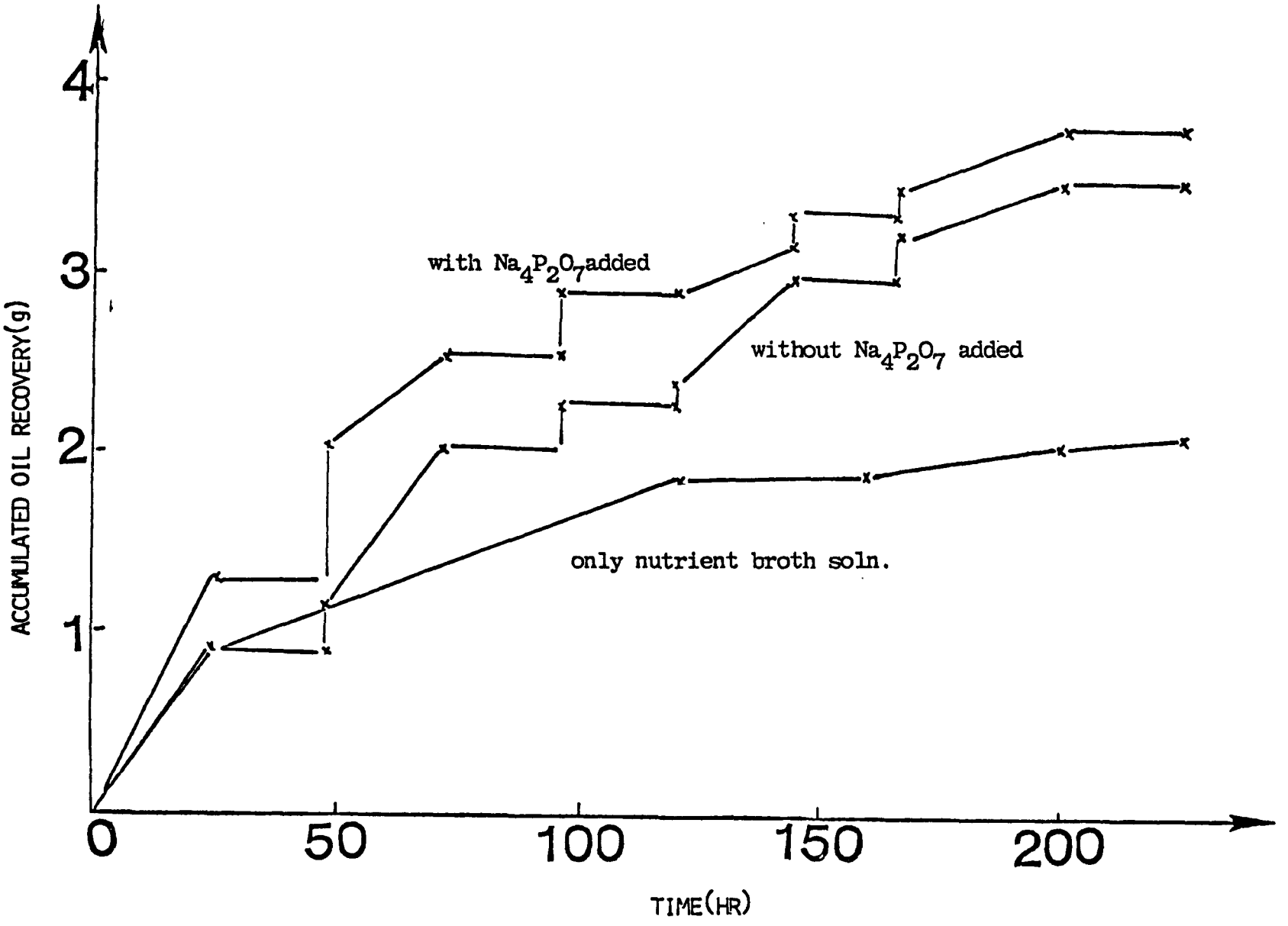

Fig. 4-2 Comparison the oil recovery efficiency from an oil-containing sandpack column, at which 0.1 p.v. B. subtilis was inoculated.

during the incubation periods. The oil viscosity was reduced by the biosurfactant produced from B. subtilis, and the pressure head was increased by the biogas generated during in-situ incubation. These are believed to be the two major mechanisms to push oil out. The slope of the inclined section represents the average production rate of oil during the periods of nutrient broth flooding. During the flooding period, the new nutrient broth medium displaces the metabolic wastes which were produced in the former incubation period. Those metabolic wastes might hinder the activity of bacteria, therefore, it is necessary to supply a new energy source for bacteria. This will enhance further its ability to push oil out. It was observed that there was nutrient solution accompanying the oil going out from the sandpack column both during the production period, and during the flooding period. Inspection of the output samples showed that instead of formation of an oil-water emulsion, the oil was floating on the top of nutrient-water solution in the collection container. The output sample at each period was treated by shaking with toluene in a separation funnel in order to obtain a pure oil sample. The final net weight of the output samples was obtained after they were dried in a hood overnight.

Because the oil was not sterilized, the recovery of oil from column 2 can reveal the influence of those bacteria indigenous to the residual oil. In Fig. 4-2 it may be seen that the overall oil recovery efficiency obtained from above experiment and the control run are 35%, and 21% respectively. It was apparent that B. subtilis was more active than the indigenous bacteria present in the control run in the latter stage of the experiment (time > 2 days). Since the transport ability of bacteria through the porous media is a critical factor in the whole MEOR process, and it was already proved that sodium pyrophosphate solution at the proper concentration can help the bacterial cells transport through the sandpack column. Therefore, under the same operational conditions and the same procedures as those described above, another experiment with nutrient broth-pyrophosphate mixture as a sweeping slug was conducted. The mixture contained 0.1% sodium pyrophosphate, 0.8% nutrient broth and 0.5% glucose. The result is also shown in the Fig. 4-2. It indicates that with pyrophosphate added, the oil recovery efficiency of 38% is better than the previous work where no pyrophosphate was added. Also, compared to the run without pyrophosphate additive, it was found that the average output concentration of B. subtilis was increased

from 10^6/ml to 10^8/ml when the pyrophosphate was added. The following hypotheses are offered to explain these positive results:

(1) As the pyrophosphate solution was introduced, the adsorption of $P_2O_7^{-4}$ anions on either bacterial surface or sand particle surface induced higher repulsion forces. Because of the higher repulsion forces, more bacterial cells can transport or migrate deep inside the sandpack column at nutrient flooding and incubation periods. As a consequence, a higher oil recovery efficiency is obtained compared to the experiment with no pyrophosphate present. This suggests that the transport ability of bacterial cells has a positive influence on the whole MEOR process.

(2) The pyrophosphate anions can serve as surface-active electrolytes which lower the interfacial tension between oil and nutrient broth solution. Due to the different solubility of the $P_2O_7^{-4}$ anions and the Na^+ cations in the oil phase and in the nutrient medium phase, (usually the anions will be somewhat more oil soluble than the cations), the addition of sodium pyrophosphate will induce an interfacial potential difference (Adamson, 1982).

4.5 Effect of *Clostridium acetobutylicum* and pyrophosphate additive on the oil recovery efficiency from sandpack column

In the previous oil recovery experiments, the aerobic bacterial species *B. subtilis* was injected into the oil-containing sandpacks filled with nutrient broth. It was found that biogas and biosurfactant generated in-situ displaced 30-40% of the residual oil from the sandpack columns. In the following experiment, the efficiency of residual oil recovery by use of an anaerobic bacterial species, *C. acetobutylicum*, was investigated. In order to improve the economics of the recovery process, a molasses medium was chosen as the nutrient source in this experiment. The growth media contained 4% molasses and 0.5% ammonium diphosphate, which was supplied as the nitrogen source for the growth of *C. acetobutylicum*. The permeability of the sandpack column was 4,000 md. The dried weight of residual oil left after secondary waterflooding was about 10 grams. Hence, under the same operational conditions as the experiment with *B. subtilis*, the procedure involving the cycle of huff-and-puff followed by molasses flooding was conducted.

The accumulated oil recovery from Column 1 (inoculant C. acetobutylicum) and Column 2 (control run) are shown in Figure 4 - 3. Comparing the two curves in Fig.4-3, it was found that C. acetobutylicum was more effective in enhancing oil recovery than indigenous bacteria. About 50% of the oil was recovered from Column 1, while less than 30% was recovered from Column 2. It is also demonstrated that the step changes from Column 1 are higher than those from Column 2, which indicates C. acetobutylicum generates much more biogas (believed to be CO_2 and CH_4) than indigeneous bacteria.

Although the anaerobe C. acetobutylicum grows more slowly than the aerobe B. subtilis, it is found that there are several advantages in using C. acetobutylicum. Because of the anaerobic condition in the oil reservoir, and the difficulty in supplying oxygen for the requirements of aerobes, anaerobes can be better candidates for MEOR processes. Also, the experiments show that the oil recovery efficiency of C. acetobutylicum is higher than that of B. subtilis (50% vs. 35%). Finally, C. acetobutylicum is a much stronger gas producer than B. subtilis; the strength of eruption at the end of the incubation periods was observed to be stronger for C. acetobutylicum. Therefore, C. acetobutylicum would be a more effective bacterial species in repressuring the oil

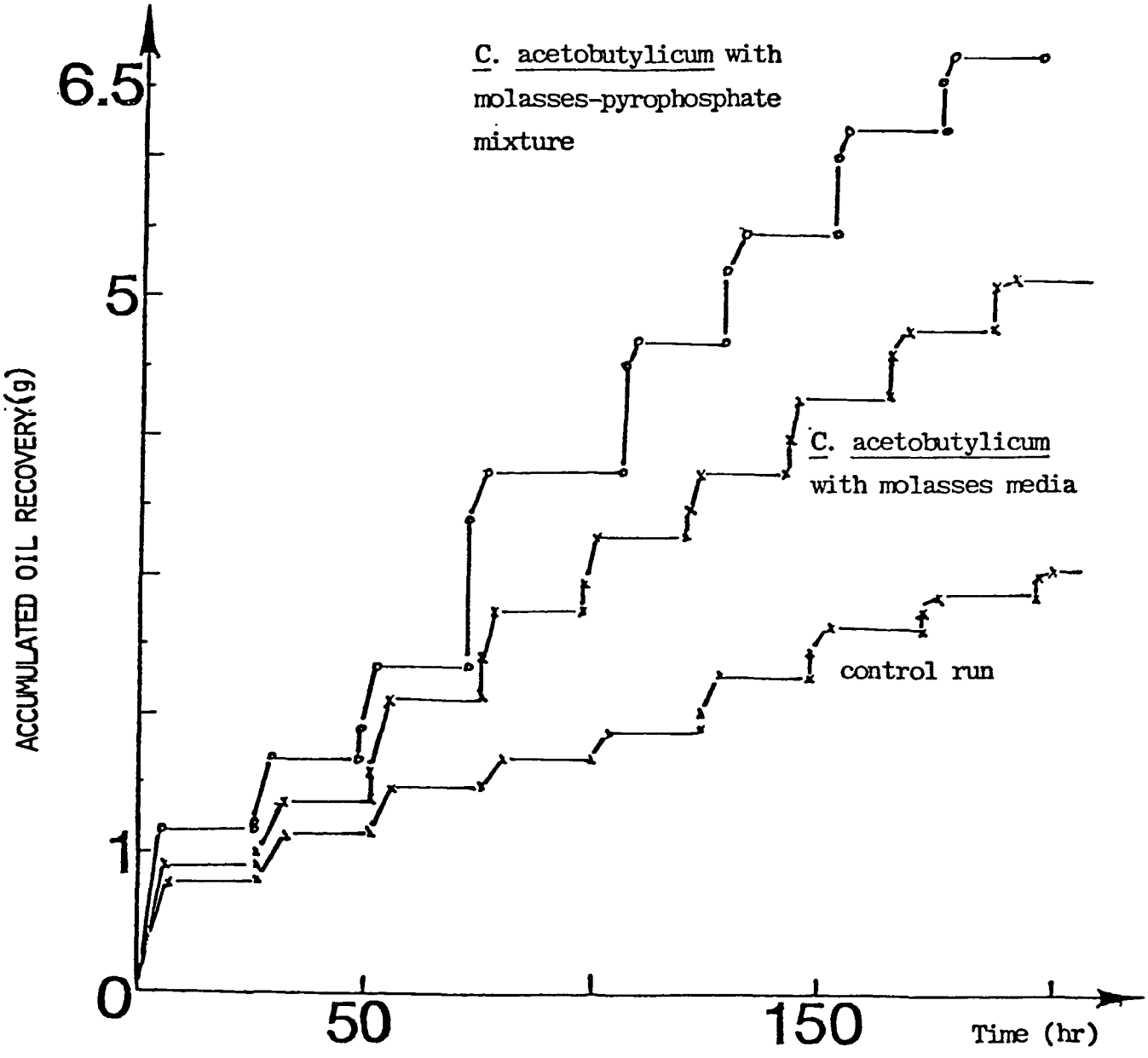

Fig. 4-3 Comparision the oil recovery efficiency from an oil-containing sandpack column, at which 0.1 p.v. C. acetobutylicm was inoculated.

reservoir. In addition to the above advantages, from the experience obtained in the experiments with B. subtilis and C. acetobutylicum, it should be noted here that molasses medium is a more powerful nutrient source for bacterial growth than nutrient broth.

Since it was proved in the previous work that pyrophosphate can enhance bacterial cell transport through a sandpack column, and was able to increase the oil recovery efficiency in the experiment using B. subtilis, an experiment using molasses-pyrophosphate as the sweeping slug for the oil recovered by C. acetobutylicum was also attempted. The growth medium contained 4% molasses, 0.5% ammonium diphosphate, and sodium pyrophosphate at a concentration of 1.5×10^{-3}M. Under the same experimental conditions and procedures as described earlier, the result of this experiment is shown in Fig. 4-3. It is very interesting to find that there is about 66% oil recovery efficiency obtained with the use of the molasses-pyrophosphate mixture. In addition to the two hypotheses given earlier in the discussion of the results of the B. subtilis experiment, the higher mobility ratio induced by molasses, over that induced by nutrient broth is another probable reason to explain this high oil recovery

efficiency. Because C. acetobutylicum is a high biogas production species, it is suggested that the oil recovery process with C. acetobutylicum is a gas driven process.

4.6 Effect of Clostridium acetobutylicum and pyrophosphate additive on the oil recovery efficiency from Berea sandstone core

From the above experiments, it was found that C. acetobutylicum and a molasses-pyrophosphate mixture can increase the oil recovery efficiency from a sandpack column tremendously. Due to the high porosity, and the inability to take into account the clay displacement problem in the sandpack experiments, the results obtained previously might be too unrealistic to give a practical view of the true MEOR process. Therefore, for the purpose of simulating a real oil reservoir, a Berea sandstone core was used in the following experiment.

The Berea core (1 inch in diameter and 10 inches in length) was from the Northern part of Ohio. The permeability of the core was found to be 310 md, and the porosity 19%. The core was first mounted in plastic tubing to prevent liquid by-passing, and then it was placed into a Lucite column with two caps on each side. A strong adhesives (cat. No. A-611 supplied by the Armstrong Epoxy company, Warsaw, Indiana), was injected

into the gap between the core and the Lucite tubing in order to fix the core at the central position in the tubing. Two pressure valves were connected right next to the inlet and outlet ends to provide a way of measuring the pressure drop when the experiment was conducted. The oil-containing core was prepared by vacuum-saturating the core with 1,000 ppm NaCl Brine, and then by the Long Beach oil (same oil used in the above experiments). The residual oil left after secondary waterflooding was found to be about 9 grams.

When C. acetobutylicum and the molasses-pyrophosphate mixture were applied, the accumulated oil recovery from this Berea sandstone core is shown in Fig. 4-4. It was found that there is a 40% oil recovery efficiency obtained in this experiment. Compared with the oil recovery efficiency from the sandpack column (66%), the lower recovery efficiency (40%) from Berea sandstone is due to the lower permeability of the core, which makes bacterial cell transport more difficult. Fig. 4-5 shows the pressure drop history when the experiment was conducted. The pressure drop difference between the preinjection period (30 psi) and the mixture flooding period (45 psi) was caused by the bacteria themselves, and the metabolites generated during the incubation periods. Because the kaolinite clay in the

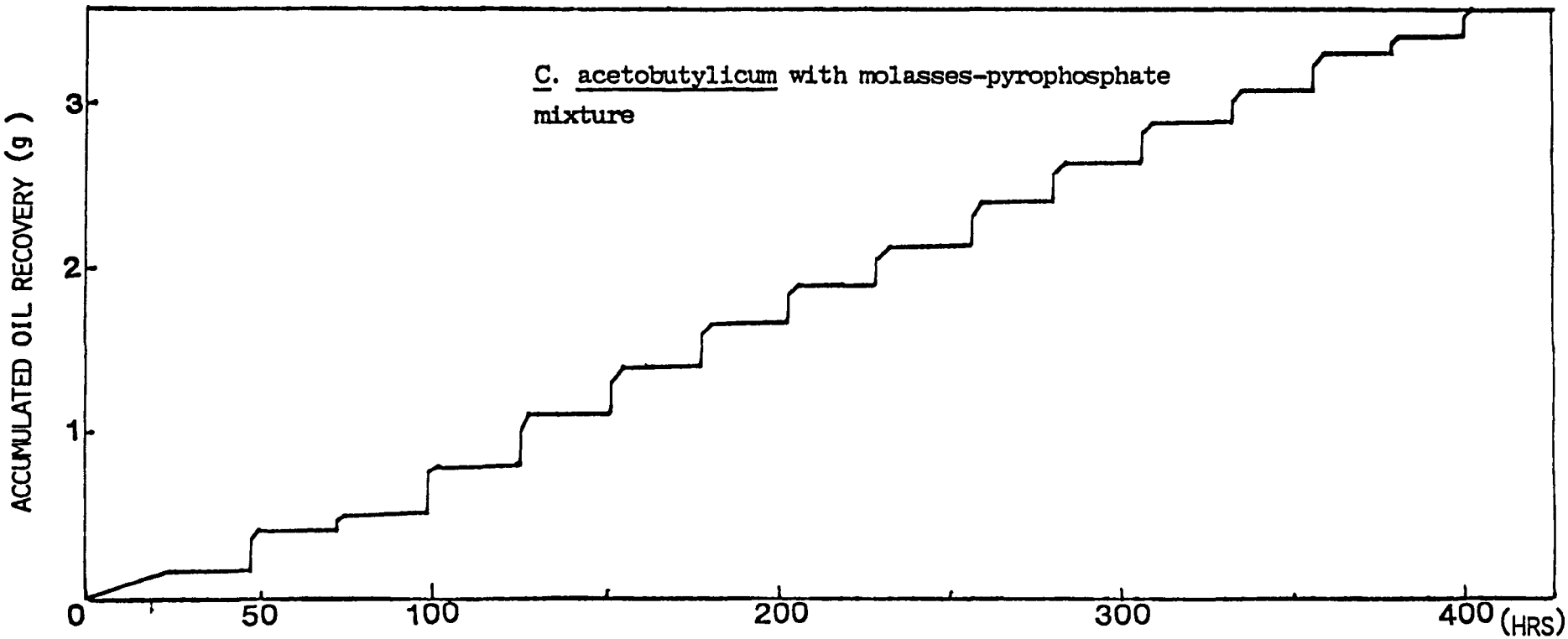

Fig. 4-4 The accumulated oil recovery from a Berea sandstone with permeability 300 md, which was inoculated by 0.1 p.v. C. acetobutylicum and was flooded by the molasses-pyrophosphate mixture.

Berea sandstone is not water sensitive, the plugging effects caused by clay were not observed in this experiment.

4.7 Effects of Clostridium acetobutylicum and pyrophosphate additive on the oil recovery efficiency from Kansas limestone core

Bubela (1978) reported that for oil reservoirs with tight formations having a permeability below 100 md, the transport ability of bacteria was limited to the well bore region. It has already been found that sodium pyrophosphate can help the bacterial cell transport through the porous media, and can increase the oil recovery efficiency. Therefore, it is intended to test sodium pyrophosphate in MEOR experiments conducted with a core which has a permeability below 100 md.

The core (2 inches in diameter and 3 inches in length) was from an Eastern Kansas oil field (Osawatomie, Kansas). It was a waterflooded limestone with final oil saturation of 25%. The permeability of the core was found to be as low as 15 md. The API value for the oil in this core was found to be 30^{o}. The concentration of NaCl in the brine was estimated to be about 10,000 ppm, which is an unsuitable concentration for bacteria to grow.

After the core was fixed in a Lucite column in a similar manner to the Berea sandstone core, it was saturated with the brine containing 10,000 ppm of NaCl. Which was similar with the real situation in the Kansas oil field. It was observed that there was no oil coming out from the core during the period of brine flooding. The procedure of repeating the cycle of huff-and-puff, followed by flooding with the molasses-pyrophosphate mixture, as was described above, was then conducted. C. acetobutylicum was still used in this experiment.

The accumulated oil recovery from this Kansas core is shown in the Fig. 4-6. It was found that C. acetobutylicum can still grow and produce a strong biogas pressure under such a high concentration of NaCl (10,000 ppm). Fig. 4-7 shows a pressure drop as high as 65 psi caused by the low permeability of the core. In spite of these unfavorable conditions, when C. acetobutylicum culture was introduced and incubated, it was observed that there still was a 33% oil recovery efficiency obtained in the experiment. During each period of molasses-pyrophosphate mixture flooding, it was observed that there were a lot of clay particles accompanying the oil-molasses solution coming out from the core. This was probably due to the sodium pyrophosphate (1.5×10^{-3}M) being able to stabilize the clay particles in solution; once the clay particles are detached from the rock

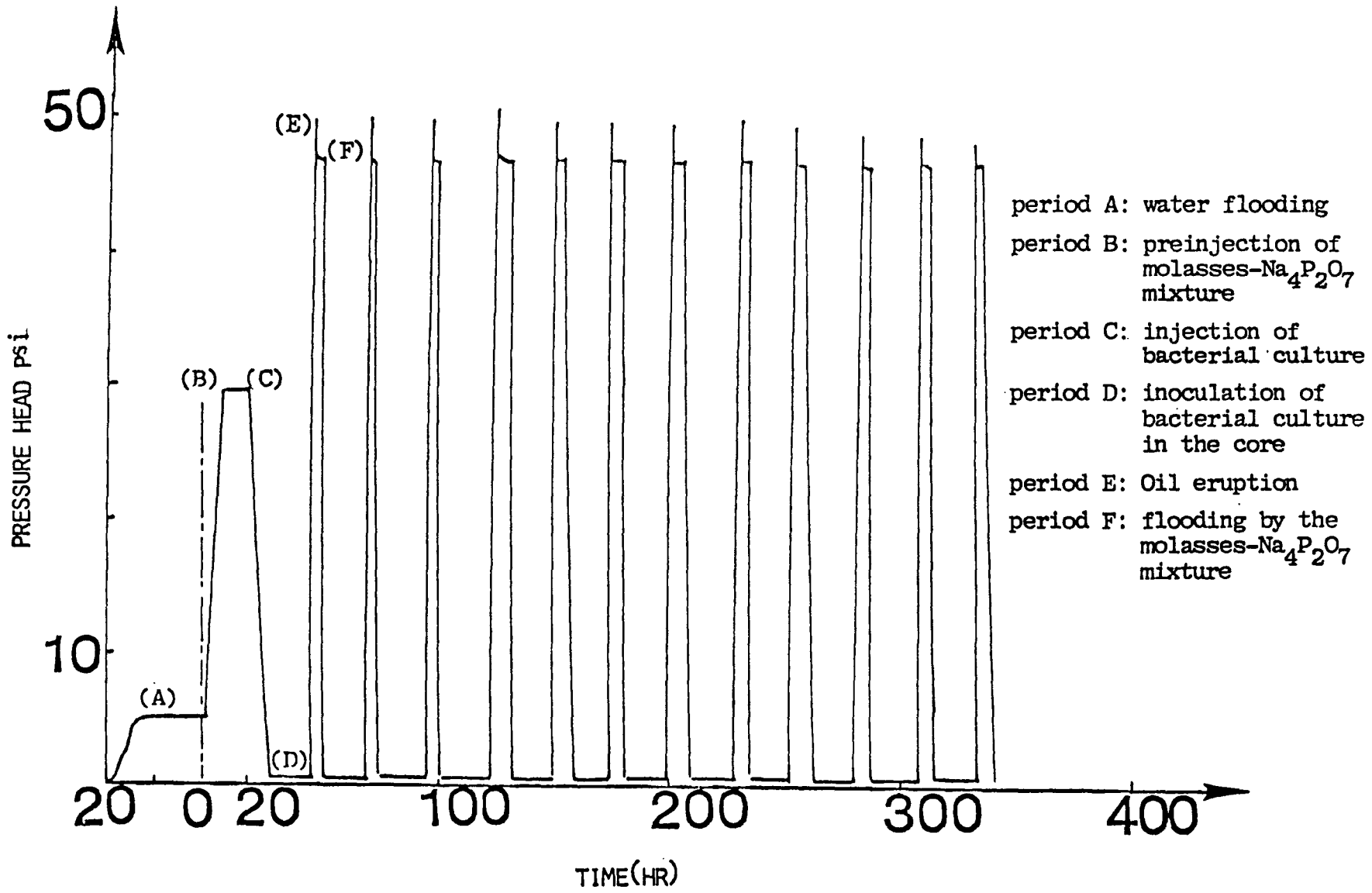

Fig. 4-5 The pressure drop history from the Berea sandstone core which was inoculated by 0.1 p.v. C. acetobutylicum and was flooded by the molasses-pyrophosphate mixture.

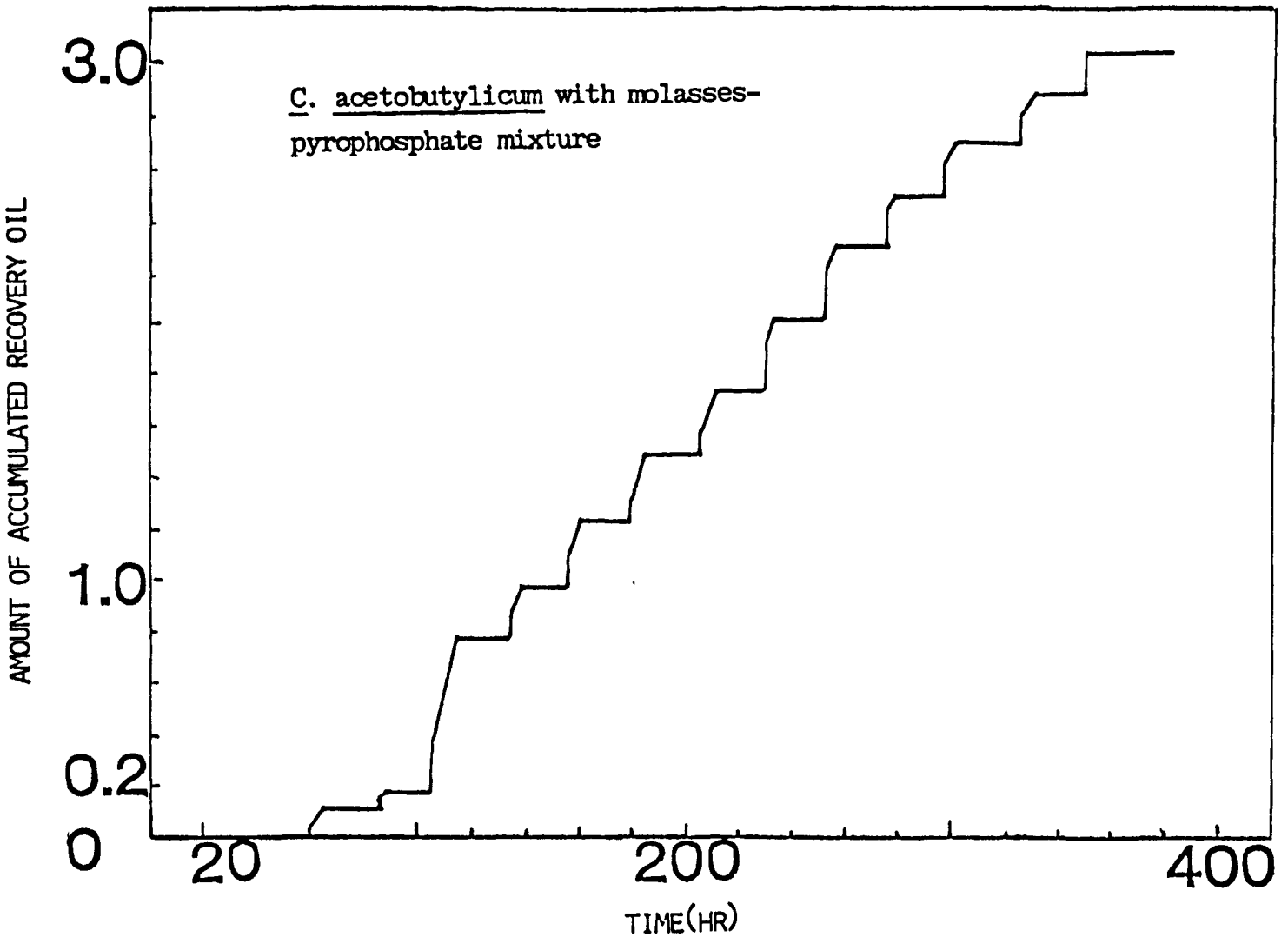

Fig. 4-6 The accumulated oil recovery from a Kansas core with permeability 15 md, which was inoculated by 0.1 p.v. C. acetobutylicum and was flooded the molasses-pyrophosphate mixture.

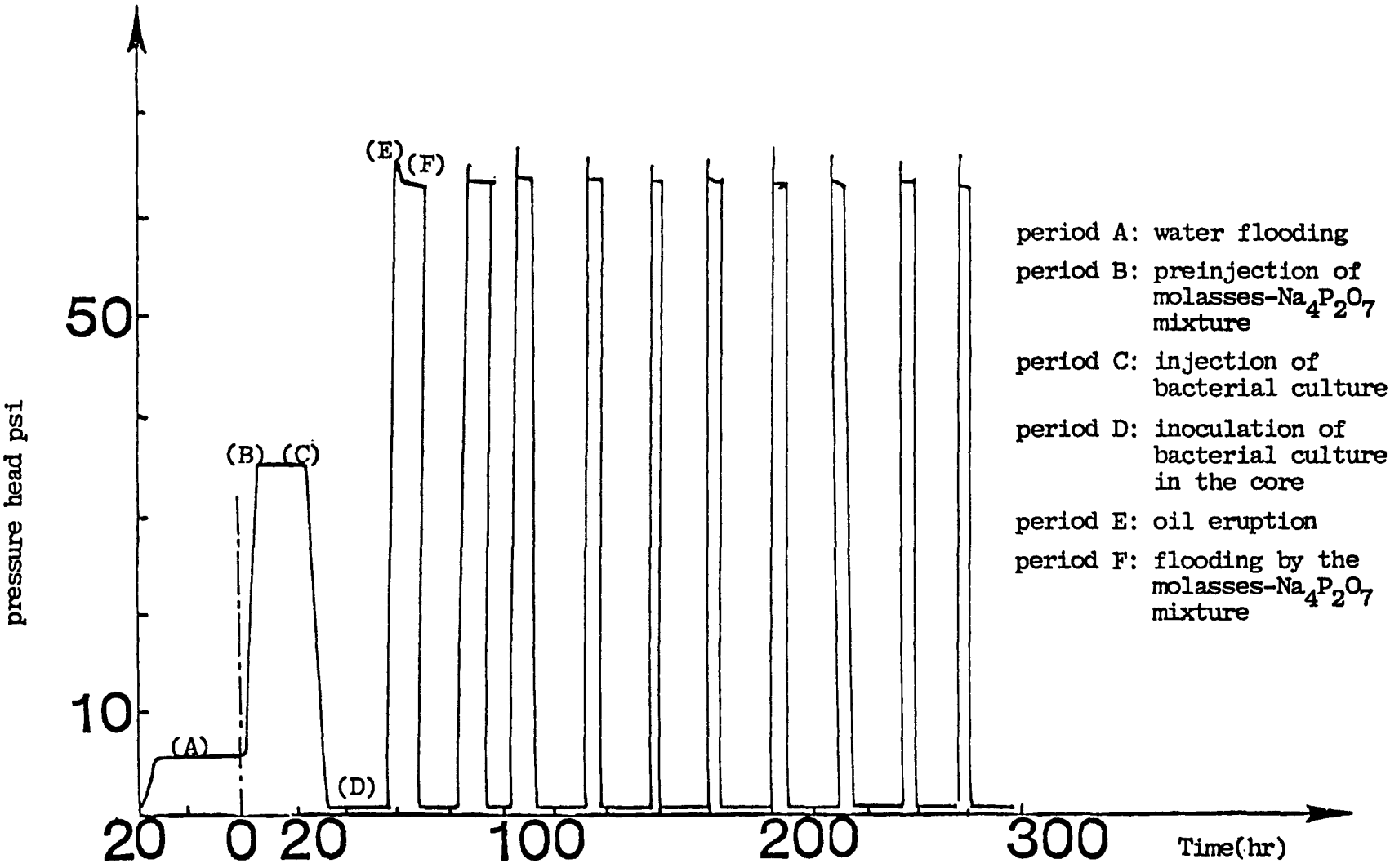

Fig. 4-7 The pressure drop history from the Kansas core which was inoculated by 0.1 p.v. C. acetobutylicum and was flooded by the molasses-pyrophosphate mixture.

surface, they will not redeposit on the rock surface or reflocculate with other clay particles. Therefore, no plugging effects caused by these displaced clay particles were observed when the experiment was conducted. Because of the high pressure drop obtained in the experiment with the Kansas core, it is suggested that oil might also be pushed out by that high pressure head during the production periods.

An experiment to analyze the major organic acids, and sugars composition in the molasses medium, before and after the incubation period, was also conducted. The sample was analyzed by the method of ion chromatography (Dionex, 2000i instrument) with a high capacity anionic column (Dionex, As6) and a Pulsed Amperometric detector. The mixture of molasses-pyrophosphate without any bacterial species being inoculated is taken as the inital sample for analysis. The sample collected after the initial molasses flooding from the core (about two days) is taken as the sample being digested by C. acetobutylicum. The results are summarized in the Table 4-1. For the organic acid portion, it was shown that C. acetobutylicum digests most of the organic acids, which are decomposed into carbonate, and detected in the final sample. Comparing the data on phosphate concentration indicates that a great amount of phosphate is retained in

the core, which allows the bacterial cells to migrate or transport more easily through the core. For the sugar portion results show that C. acetobutylicum consumes a large amount of sucrose, which is then decomposed into glucose, fructose, maltose and finally carbon dioxide during the periods of incubation. Also, C. acetobutylicum consumes the major part of the sorbital content in the molasses medium.

4.8 Conclusions

From the above experiments, five conclusions can be drawn:

1. C. acetobutylicum is more efficient than B. subtilis in the MEOR process. Due to the anaerobic condition in the oil reservoir, C. acetobutylicum would be a better candidate for the future MEOR work.

2. When Sodium pyrophosphate can, not only induce a higher oil recovery efficiency, but it can also overcome the plugging problems caused by bacterial cells and clay displacement.

3. A comparison of the molasses medium with the nutrient broth indicates that due to the cheaper prices of molasses, and ability of alternating mobility ratio with oil, molasses will serve as a better bacterial growth

medium for use in future work.

4. Comparing the experimental results of the sandpack column with the Berea sandstone core, it is concluded that the permeability of the medium has an influence on the oil recovery efficiency in the MEOR process.

5. Even though the permeability of the Kansas core is as low as 15 md, it still allows an oil recovery efficiency of 33% as shown in the experiment conducted above. It is probably due to the fact that the Kansas crude has a high API value of 30^{o}, which makes it easier to be recovered by either the surfactant or by the biogas generated from the bacterial species.

6. The results of the molasses composition analysis indicate that, if C. acetobutylicum is to be chosen for future work, it will be valuable to increase the concentration of sucrose, which consequently will promote the biological functions of bacterial cells in the whole MEOR process.

4.9 Literature cited

1. Verney, E. J. W. and Overbeek, J. Th. G., Theory of the Stability of Lyophobic Colloids, Elsevier Pub. Inc., Amsterdam, (1948).
2. Hogg, R., Healy, T. W., and Fuerstenau, D. W., Mutual Coagulation of Colloidal Dispersion. Trans. Faraday

medium for use in future work.

4. Comparing the experimental results of the sandpack column with the Berea sandstone core, it is concluded that the permeability of the medium has an influence on the oil recovery efficiency in the MEOR process.

5. Even though the permeability of the Kansas core is as low as 15 md, it still allows an oil recovery efficiency of 33% as shown in the experiment conducted above. It is probably due to the fact that the Kansas crude has a high API value of 30^{o}, which makes it easier to be recovered by either the surfactant or by the biogas generated from the bacterial species.

6. The results of the molasses composition analysis indicate that, if C. acetobutylicum is to be chosen for future work, it will be valuable to increase the concentration of sucrose, which consequently will promote the biological functions of bacterial cells in the whole MEOR process.

4.9 Literature cited

1. Verney, E. J. W. and Overbeek, J. Th. G., Theory of the Stability of Lyophobic Colloids, Elsevier Pub. Inc., Amsterdam, (1948).
2. Hogg, R., Healy, T. W., and Fuerstenau, D. W., Mutual Coagulation of Colloidal Dispersion. Trans. Faraday

Soc. 62, 1638 (1966).

3. Chang, Y. I., Effects of chemical additives on the Bacterial Transport ability through the Porous Media and its application on the Microbial Enhanced Oil Recovery Process, ph.D. Dissertation, Universtiy of Southern California, in Progress.
4. Jang, L. K., Chang, P. W., Findley, J. E., and Yen, T. F., Selection of Bacteria with Favorable Transport Properties through Porous Rock for the Application of Microbial Enhanced Oil Recovery, Applied and Environmental Microbiology, p. 1066-1072, Nov., (1983).
5. Jang, L. K., Sharma, M. M., and Yen T. F., The Transport of Bacteria in Porous Media and its Significance in Microbial Enhanced Oil Recovery 1984 California Regional Meeting in Long Beach, CA., Society of Petroleum Engineers of AIME, SPE 12770.
6. Adamson, A. W., Physical Chemistry of Surfaces, 4th Ed., John Wiley and Sons, New York, (1982).

5. THE INTERACTION OF *Escherichia coli* B, B/4, and, BACTERIOPHAGE T4D WITH BEREA SANDSTONE ROCK IN RELATION TO ENHANCED OIL RECOVERY

5.1 Abstract

Much research and development is needed in order to recover oil reserves presently unattainable. Microbiological Enhanced Oil Recovery (MEOR) are technologies that may be used for that purpose. To address the problem of bacterial contamination in an oil field injection well region, we connected each end of a teflon sleeved Berea Sandstone rock to a flask containing nutrient medium. By inoculating one flask with *Escherichia coli* B, we could observe bacterial growth in the uninoculated flask resulting from the transport and establishment of cells across the rock. Differences in bacterial populations occurred depending on whether or not bacteriophage T4D was first adsorbed to the rock. The results of these experiments indicate that the inhibition of bacterial establishment within a rock matrix is possible via lytic interaction. Some nonlytic effects are also implied by experiments with B/4 cells which are T4D resistant mutants of *E. coli* B. A 10 - 40% retention of T4 by the rock occurs when loaded with 10^5 - 10^6 plaque forming units. We also describe a lysogenic system for possible use in MEOR.

5.2 Introduction

Microbiological enhanced oil recovery (MEOR) is in the basic development state. To date, the processes have not been successfully commercialized on a significant scale due to technological and other difficulties. However, since an estimated 2/3 of the world's oil or some 2 trillion barrels of petroleum reserves are not recoverable by present means, research and development into recovery processes is well motivated particularly if applications to other industrial systems can be offered.

Currently research in MEOR is being conducted in various laboratories to assess bacterial capabilities for production of suitable biosurfactants which can better miscify oil-water substrates, biopolymers to thicken push waters in oil bearing strata, or, to assess their production of carbon dioxide or methane gas *in situ* to raise the underground pressure. Research into the biomodification of high viscosity fractions of oil is also ongoing. Our laboratories have been studying the selection of bacteria with favorable transport properties through porous rock for the application of MEOR (10,11,22). Reviews of the MEOR projects are available (4,6,15,23). Ideally, a nonpathogenic microorganism capable of utilizing or modifying expendable or undesirable oil fractions *in situ* with concurrent oil recovery metabolic by-products (surfactants, polymers or gas) can be developed which, in addition, is low in cost, available in commercial quantity, amenable to the process technique and useful in reasonably low cell densities. Unfortunately unchecked bacterial growth in contaminated oil recovery systems can result in biomass clogging of wellbore rock matrices, pipe lining corrosion, and, degradation of lighter valuable oil portions (2) which are

problems existing today. Thus in any MEOR process, a means for mitigating bacterial proliferation via chemical or biological agents must also be developed.

Prior to this report, no studies into the use of lytic or lysogenic bacteriophage in a petroleum recovery situation have been done, and, to our knowledge, experiments exploring the lytic ability of phage adsorbed to porous rock have not been done either. Much literature does exist on the adsorption of phage to clays, minerals, soils (1,7,8,9,17-21) and activated carbon (5), and also the adsorption of animal virus to various minerals and soils (7,8,9,13,14,17,18). Those studies were largely for municipal and industrial sewage and sludge treatment applications. However, such information could complement the research to be described here.

We investigated the extent of bacterial lysis possible within a porous Berea Sandstone rock such as that found in an oil field injection well by using *Escherichia coli* B, B/4 and bacteriophage T4D as a model bacteria and phage system. In this paper, data on the inhibition of bacterial establishment and growth across the permeable rock matrix containing adsorbed phage is presented in the context of MEOR. Factors governing the interaction of the model bacteria and phage within the rock will be discussed and a simple apparatus which can be used to study a variety of MEOR problems is described. The possibility of using lysogenic phage in MEOR is also raised.

5.3 Materials and Methods

Bacteria: Coliform bacteria, *Escherichia coli* B, obtained from Dr. Myron F. Goodman (Molecular Biology Department, Univ. of So. Calif.) was maintained on two 2.3% nutrient agar (Difco) slants at 4°C. To maintain strain clarity, only one designated slant was used for loop inoculating a series of experi-

ments , while the other slant was kept in reserve and opened only to generate two fresh "use" and "reserve" slants every six weeks. The slants were initially incubated 12-18 h at 37°C (GCA/Precision Scientific Model 6M incubator) before transfer to 4°C for storage.

B/4 bacteria are variants of *E. coli* B that are resistant to infection by bacteriophage T4. B/4 cells were obtained from confluently lysed plates of *E. coli* B, and streak isolated on 2.3% nutrient agar. Isolates were passaged and identified as B/4 cells according to resistance to the T4D stock. B/4 preparations were similarly maintained at 4°C using the slant method described above.

Coliphage: Phage T4D which infects *E. coli* B was obtained through Dr. W. B. Wood (Caltech phage collection). Our working stocks of T4D were generated by isolating a plaque via a sterile applicator stick into 2 ml Tryptone broth (Difco) saturated with chloroform. After 3-4 h, 1 ml of this solution farthest from the chloroform was added to a 250 ml flask containing 50 ml stationary phase *E. coli* B in M9 medium (3). This was maintained at 37°C, 150 rpm in a Controlled Environment Incubator Shaker (New Brunswick Co.) before chloroform was added to saturation after 12 h of incubation and the flask brought to 4°C for another 12 h. Following centrifugation at 4°C, 3000 x g for 10 min in 50 ml polypropylene tubes to remove debris, the resultant supernatant was stored in screw cap bottles at 4°C. This process yielded a phage stock titer of 5×10^{11} pfu/ml and storage under the described conditions has shown no appreciable drop in titer.

Berea Sandstone Rock: Two Berea sandstone rock columns (Cleveland Quarry Co.) 1" in both length and diameter with a 400 mD permeability and specific

internal surface area of 1 m^2/gm were each sleeved in thermal shrinkage teflon (Penn Dixon Co.). Each rock had a 0.5 - 1 ml residual pore volume and weighed 28 g. Rock 1 was used in 2-4 sets of experiments whereas Rock 2 was used in only 1 set of experiments.

Double Flask Apparatus: The double flask apparatus (Fig. 5-1) was constructed by attaching a 1" i.d. glass sleeve to each of two 250 ml round Erlenmeyer flasks centered at their widest diameter. Cotton-gauze-foil plugs were fitted to the original necks of each flask. Vacuum hosing connected the ends of the rock column to each flask sleeve. Band clamps ensured no leakage.

Bacterial Titration: Viable bacterial populations in the double flask apparatus were determined by taking samples from the flasks and serially diluting in 0-4°C M9 medium. Samples were loaded onto the center of standard Falcon sterile disposable 15 mm x 100 mm petri dishes (VWR Scientific Co.), and 13-15 ml of 2.3% molten nutrient agar at 47°C (GCA/ Precision Scientific Waterbath Model 80) was added. Each plate was mixed by hand rotational and linear agitation. The plates were inverted and incubated unstacked at least 12 h at 37°C before colonies were counted. Triplicate samples per dilution were done and only counts between 30-300 colonies/plate were considered significant.

Phage Titration: Phage titration during the experiment was accomplished by the following standard double layer agar plaque assay. Dilutions of samples in M9 medium over ice were transferred in 0.1 ml aliquots to 13 mm x 100 mm test tubes containing 2.5 ml Tryptone Top agar (0.7% Agar, 1% Tryptone, 0.5% NaCl) at 47°C (Thermolyne Dry Bath). Iced stationary phase *E. coli* B (0.1 ml in M9 medium was then added as an indicator. The phage and bacteria containing tubes were poured onto standard petri plates containing 40 ml, Tryptone bottom agar (1% Agar, 1% Tryptone, 0.5% NaCl) within 3-8 min and

swirled to allow uniform bottom agar plate coverage. Plates were inverted and incubated unstacked, 12-18 h. at 37°C before plaques were counted. All phage titrations were performed in duplicate.

Sterilization: M9 medium components, i.e., M9 salts, M9 glucose and M9 Casamino Acids - were autoclaved 15-20 min. at 130°C separately then aseptically mixed prior to use. The nutrient and Tryptone agars were also autoclaved 15-20 min. at 130°C.

The Berea Sandstone rock after each experiment was reverse flushed (uninoculated to inoculated side) then forward flushed with 750 ml deionized water which had been through a Type HA 0.45 μm cellulose acetate-nitrate (Millipore) filter, then autoclaved 25 min at 130°C. This procedure for rock sterilization was found to be effective in a test where the rock was submerged in nutrient media with no detectable growth after one week incubation.

All glassware was washed with Micro detergent (International Products Corp., N.J.) rinsed in industrial water and deionized water, dried, then sterilized by autoclaving.

Experimental Procedures: In control tests without phage, the double flask apparatus was fully assembled then autoclaved. Following sterilization the apparatus was placed in a 37°C incubator overnight. Roughly 750 ml, 37°C, M9 medium was aseptically filtered through a Millipore 0.45 μm filter apparatus.

Then, 250 ml M9 medium was aseptically loaded into the flask of the apparatus to be inoculated accompanied by brief vacuum at the opposite flask to remove entrapped air. An equivalent volume of M9 medium was then loaded into the opposite flask. The fluid level and temperature were allowed to stabilize in a 37°C incubator for at least 45 min before loop inoculation

of one flask. Equal volume samples from each flask for bacterial density determinations were taken at time zero (immediately following inoculation), and at 45 min intervals thereafter until the third hour and finally at the sixth hour.

The sampling routine for experiments with phage was the same as in phageless control tests although slightly larger volumes were sampled to facilitate both bacteria and phage titrations. To observe the effects of phage in the rock on the transport of the bacteria, care was taken to eliminate non-rock associated phage. It was, therefore, necessary to attach the rock column to a separate flask when loading the phage into the rock. This was easily accomplished via vacuum hosing and a 50 ml sidearm flask.

For all experiments involving phage, the phage loading apparatus was sterilized and equilibrated to 37°C. 5 ml of appropriately diluted phage stock at 37°C was then passed through the loading unit by a 50 mm Hg vacuum applied at the sidearm flask wnd by a Doerr-Gast 1/6 hp. Type 1 Vacuum Pump (VWR Scientific). The volume of the collected phage containing solution was determined and phage titrations of this and the prepassaged solution were performed. A 20 ml rinse with 37°C, M9 medium at 50 mm Hg followed using the same emptied sidearm flask. Care was taken to stop vacuum when the rinse fluid level reached the rock face to avoid drawing air into the rock. Phage contained in the rock was calculated by the difference in total plaque forming units between the solution loaded in, the loaded solution collected, and the rinse medium. The rock was then aseptically attached to the original double flask components and the filtered M9 medium added without vacuum.

5.4 Results

Two identical rock samples were used in these experiments. Figure 5-2 are the average *E. coli* B, B/4 and T4 population densities in the

inoculated and uninoculated flasks as they varied with time during 2-4 separate experiments with Rock 1. Variations in the inoculated and hence the uninoculated flasks due to the loop inoculation procedure are expressed by bars representing the high and low values obtained from particular experiments.

Fig. 5-2a depicts the growth profiles of *E. coli* B where no T4 is added to the rock. An inoculum of 10^6 cells/ml resulted in an increase to 10^8 cells/ml by 6 hours. Concurrently the uninoculated flask population rose to 10^6 cells/ml. Fig. 5-2b reveals at least a 10 fold lower uninoculated flask *E. coli* B population when compared to phageless tests in Fig. 5-2a despite comparable inoculum levels. The rock initially contained T4 from 0.3×10^5 to 1.3×10^5 plaque forming units (pfu). The larger variations in the 3/4 and 1.5 hour samples are because of difficulties in obtaining statistically significant viable colonies at the lowest (1.0 ml, 0.1 ml) dilutions in some experiments. By the final hour, although very turbid, the inoculated flask viable cell density dropped below 10^6 cell/ml. The phage levels in both flasks increased greatly due to lysis within the rock followed by further lysis and seepage (of progeny phage) from the rock. By the sixth hour, phage levels in the inoculated and uninoculated flasks were 10^{10} and $10^{5.5}$ pfu/ml respectively.

Fig. 5-2c shows the growth of B/4 cells using an initial inoculum averaging 10^5 cell/ml. A 2.5 order of magnitude increase in viable cells occurred after 6 hours.

The slopes of the corresponding curves in both Fig. 5-2a & 5-2c are verv similar to each other. Fig. 5-2d demonstrate the average B/4 growth curves with 10^4 - 10^5 pfu T4 contained in the rock. A 5-fold less uninoculated flask profile is seen relative to the phageless B/4 curve shown in the previous figure if the inoculum curves are matched. Despite the large variation in inoculums used, the average curves are still very similar to previous trends. The majority of high and low values from the inoculated curve correspond to those values on the uninoculated curve in Fig. 5-2d. No phage could be detected at the 1 $\log_{10}$ unit level throughout. Since B/4 cells are biologically insensitive to T4 the results described in Fig. 5-2c & 5-2d indicate that some nonlytic mechanism contributes to the decrease in the uninoculated *E. coli* B concentrations when the rock contained T4.

Supporting results were found using Rock 2. In Figure 5-3 , experiments identical to those described for Figure 5-2 were done except each figure represents only one experimental trial. Fig. 5-3a & 5-3c are phageless *E. coli* B and B/4 growth tests respectively. The resultant curves are no different from each other and very similar to Fig. 5-2c (B/4 experiments) with respect to average differences between inoculated and uninoculated flask values.

The results of the *E. coli* B + T4 test shown in Fig. 5-3b imply uninoculated flask bacteria population densities are 1.5 orders of magnitude lower than the phageless controls (Figs. 5-3a & 5-3c) and, the other population densities are very similar to the previous experiments. 1.6 x 10^5 pfu T4 was initially contained within this rock sample. The reduction in uninoculated flask *E. coli* B due to phage loaded rock - Fig 3b vs. 3.a - is similar to the average reduction using the first rock sample - Fig. 2b vs. 2a Inoculated flask *E. coli* B levels were found to have dropped to 10^4 cells/ml by 6 hours. B/4 densities using a rock loading of 2 x 10^5 pfu T4 shown in Fig. 5-3d indicates a 5-fold nonlytic interaction contributes to the previously

observed decreases in *E. coli* B + T4 tests. This correlates well with the first set of B/4 + T4 data.

Tables 5-1 & 5-2list the differences between the $\log_{10}C_i$ (inoculated flask cell counts), and $\log_{10}C_u$ (uninoculated flask cell counts), in each experiment comprising Figs. 5-2 & 5-3. The tables represent a normalization of the inoculated flask curves. Due to the unstirred inoculum procedure, the first inoculated flask sample shows greater variation than subsequent samples where the cells became more homogeneously distributed. These tables also list the total plaque forming units in the original solution loaded to the rock samples and the amount retained by the rock after rinsing with M9 medium. The percent adsorbed is calculated to be 10-40% of the original solution.

5.5 Discussion

Early experiments by Sproul (20) indicated that T4 does adsorb to various silicas of which Berea sandstone is comprised of. Now it is the general consensus that retention of virus by clays and soils is primarily by adsorption. Related work by Schaub and Sagik (17) revealed that the inactivation of enterovirus EMC does not occur while adsorbed to clays or organic colloids. Findings by Moore *et al.* (12) indicate that bacteriophages T2 and T7 and also poliovirus type I (Mahoney strain) are not inactivated by adsorption to bentonite however coliphage f2 is. Thus it is difficult to generalize on the effects on viral activity due to adsorption to surfaces. The focus of our attention was on the detection of noticeable changes in bacterial establishment due to lysis by phage adsorbed to porous rock such as that found in a well bore region where bacterial establishment is known

to occur . The rather short length of rock and experimental run time is to represent a small slice of a well bore region whose results may be extrapolated to longer lengths. Thus a reduction in uninoculated flask cell levels due to lysis may correspond to a significant mitigation of bacterial growth in a well rock region. The results of these experiments indicate that a lytic interaction impeding host bacterial growth is possible within a rock matrix. However, as implied above, care must be excercised in translating results to MEOR situations.

Some interesting possibilities applicable to MEOR arise when the data from the two rock samples are compared. Upon superimposing the growth curves from each rock, the separation between inoculated and uninoculated flask population should be constant for the same experiments using identical rocks. This is not the case with the *E. coli.* B and *E. coli.* B + T4 set of curves from Rock sample 1 which appear too low. One explanation for the variation is that the rock had a low permeability when the *E. coli.* B and *E. coli.* B + T4 tests were conducted due to accumulated debris which may have been flushed out prior to the B/4 control experiments. Although not evident from these data, a lower permeability rock found in some oil fields may allow for greater lytic effect due to longer bacterial contact time with the rock and phage.

Alternatively, the difference in the physicochemical properties of the *E. coli.* B and B/4 surfaces could effect the transport of the cells through the rock. According to Puck (16), the agglutination curves of virus resistant mutants of *E. coli.* B including B/4 indicate they are lower in negative surface charge than wildtype cells. Thus, the higher average B/4 curves from the first rock sample may result from varied electrostatic attachment, relative to wildtype cells on the negatively charged rock. Factors affecting the physicochemical properties of the rock and cell surfaces during oil recovery must

be considered.

A less likely reason is that the B/4 cells could establish themselves in greater numbers in the Rock 1 uninoculated flask because it's original inoculum was 10 - fold lower than the other tests. Conceivably, bacterial plugging could impede the transport of cells through the rock under static conditions. Plugging phenomenon have been observed by Jang et al. in cultures pumped through sandpack columns (10). Thus, even though the B/4 inoculated flask levels are lower, the resultant uninoculated flask concentrations are relatively high. We assume throughout that the inoculated flask growth curves are superimposable in the concentration range used.

Lacking electron micrographs of rock cross sections following phage loading, the distribution of the 10^5 plaque forming units within the rocks was unknown. The phage may have formed a physical plug which could account for an uninoculated flask bacterial population reduction The experiments using B/4 and T4 indicate that this is a possibility, although, methodological artifact arising from the loading procedure itself cannot be ruled out. In either case, nonlytic interaction only partially accounts for the decreases in *E. coli* B levels where T4 is contained in the rock. The degree of viral damage and deactivation following passage through the rock is a question that has not been addressed but may change the retention data stated in Tables 5-1 & 2. Electron microscopy of the initial rock rinse liquid used to remove the unattached phage may be an approach to this problem although quantitative information may be difficult to obtain.

From the standpoint of applying these results to enhanced oil recovery many unresolved details remain. Additional experiments testing the lytic phenomenon under a range of temperature, pressure, dissolved oxygen levels and medias need to be done. Our experiments were conducted using optimal conditions for T4 lysis of *E. coli*. B. The bacteria genera which

tend to establish themselves in an oil well bore region are a mixture of *Desulfovibrio* and *Pseudomonads* (2) among others, the former being a strict anaerobe of which no phage has been found. In any case, a multi-species population will be dealt with, and a mixed phage population lytic for such hosts must be found. Goyal and Gerba (8) have indicated that generalizations concerning adsorptive behavior of viruses to soils cannot be based on any one phage and soil system. Their result may be applicable in this lytic system also. Other considerations are the mutation ability of a multispecies to resist phage and the stability of the phage with time in such an environment. Schaub and Sorber (18) observed tracer phage survival in groundwater at horizontal distances up to 183 meters from a wastewater application site, however, the survival of phage may be at least as sensitive as animal virus which Hurst *et al.* have found to be highly dependent on the temperature and the adsorptive capacities of the environment (9). Perhaps the use of rapid lysis phage will be more suitable in these applications. In the remaining paragraphs, the double flask apparatus applications will be mentioned and a lysogenic model for enhanced oil recovery will be described.

It is our opinion that the simple double flask apparatus can be used for a number of experiments where a porous matrix complementary to packed sand columns is desired. For example, the use of bacteria injected underground to recover oil requires that the cells can be transported through a porous medium. A screening application using this apparatus can be done to determine which bacterial species can be most easily passaged through rock by simply plate counting the populations that appear across the rock. The loading of the rock with residual oil and the modification of such environmental factors as temperature, pressure, or, media is forseeable as is switching rock types to investigate the effect of per-

meability or anion or cation exchange capacities on bacterial interactions. Quantitative results to model bacterial transport through porous media or the interaction of bacteria and phage using this apparatus is possible - application of such data to water treatment fields is evident.

Lastly, the possibility of using a lysogenic strain of bacteria in an oil recovery situation exists. The injection of oil recovery microbes will invariably require a growth control mechanism to prevent over degradation or excessive reservoir plugging. It may be possible to use bacteria carrying inducible latent phage - potentially triggered by reduction of a specific substrate level, presence of a certain cell density, concentration of bioproduct, or, application of some subsequent oil recovery agent. The technology involved in virus research and biological enhanced oil recovery must be developed further before this lysogenic plan can become reality.

In summary, our results indicate that lysis of bacteria via bacteriophage contained within a porous rock occurs and may have potential in biological enhanced oil recovery. Similar research could also be applied to other disciplines.

5.6 Literature Cited

1. Burge, W.D., and N.K. Enkiri. 1978. Adsorption kinetics of bacteriophage. J. Environ. Qual. 7(4):536-541.
2. Carlson, V., E.O. Bennett and J.A. Rowe, Jr. June 1961. Microbial flora in a number of oilfield water injection systems. Society of Petroleum Engineering:71-80.
3. Clowes, R.L., W. Hayes, ed. 1968. Experiments in Microbial Genetics, Appendix A-media, p.178. Blackwell Scientific Publications, Oxford and Edinburgh.
4. Conference Proceedings, "The role of microorganisms in the recovery of oil". Proceedings 1976, Engineering Foundation Conference. Easton, Maryland, November 9-14, 1975. NSF/RA-770210 (Available from U.S. Government Printing Office, Washington, D.C. 20402).
5. Cookson Jr., J.T. and W.J. North. 1967. Adsorption of viruses on activated carbon-equilibria and kinetics of the attachment of *Escherichia coli*. bacteriophage T4 on activated carbon. Environ. Sci. Tech. 1(1):46-52.
6. Davis, J.B. 1967. Petroleum Microbiology. Elsevier Publishing Co., New Jersey.
7. Duboise, S.M., B.E. Moore, L.A. Sorber and B. P. Sagik. 1979. Viruses in soil systems. Crit. Rev. Microbiol. 7(3):245-301.
8. Goyal, S.M. and C. P. Gerba. 1979. Comparitive adsorption of human enteroviruses, simian rotavirus and selected bacteriophages to soils. Appl. Environ. Microbiol. 38(2):241-247.
9. Hurst, C.J., C.P. Gerba and I. Cech. 1980. Effects of environmental variables and soil characteristics on virus survival in soil. Appl. Environ. Microbiol. 40(6):1067-1079.

10. Jang, L.K., P.L. Chang, J.E. Findley and T.F. Yen. 1983. Selection of bacteria with favorable transport properties through porous rock for the application of Microbial Enhanced Oil Recovery. Appl. Environ. Microbiol. 46(5): 1066-1072

11. Jang, L.K. and T.F. Yen. 1983. An experimental investigation on the role of bacterial growth and bacterial transport in MEOR process. American Chemical Society, Division of Petroleum Chemistry Preprint, 28(2):789-799.

12. Moore, B.E., B.P. Sagik and J.F. Malina Jr. 1975. Viral association with suspended solids. Water Res. 9(1):807-820.

13. Moore, R.S., D.H. Taylor, M.M.M. Reddy and L.S. Sturman. 1982. Adsorption of reovirus by minerals and soils. Appl. Environ. Microbiol. 44(4):852-859.

14. Moore, R.S., D.H. Taylor, L.S. Sturman, M.M. Reddy and G.W. Fuhs. 1981. Poliovirus adsorption by 34 minerals and soils. Appl. Environ. Microbiol. 42(6):963-975.

15. Moses, V. and D.G. Springham. 1982. Bacteria and the enhancement of oil recovery. Applied Science Publishers, Inc., New Jersey.

16. Puck, T.T. 1953. The first steps of virus invasion, p. 149. *In* Cold-Spring Harbor Symposia on Quantitative Biology, vol. 18.

17. Schaub, S.A. and B.P. Sagik. 1975. Association of enteroviruses with naturally and artificially introduced colloidal solids-associated virions. Appl. Environ. Microbiol. 30(2):212-222.

18. Schaub, S.A. and C.A. Sorber. 1977. Virus and bacteria removal from wastewater by rapid infiltration through soil. Appl. Environ. Microbiol. 33(3):609-619.

19. Schiffenbauer, M. and G. Stotzky. 1982. Adsorption of coliphages T1 and T7 to clay minerals. Appl. Environ. Microbiol. 43(3):590-596.

20. Sproul, O.J. 1969. Adsorption of viruses on mineral surfaces. Water Res. Cat. U.S. Dept. of Int. Washington D.C.

21. Vilkner, V.L. and W.D. Burge. 1980. Adsorption mass transfer model for virus transport in soils. Water Res. 14(7):783-790.

22. Yen. T.F., L.K. Jang, M.M. Sharma, J.E. Findley and P.L. Chang. 1982. An investigation of the transport of bacteria through porous media. 1982 International Symposium on Microbial Enhanced Oil Recovery Proceedings, pp. 60-70.

23. Zajic, J.E., D.C. Cooper, T.R. Jack and N. Kosaric. 1983. Microbial Enhanced Oil Recovery. Pennwell Publishing Company, Oklahoma.

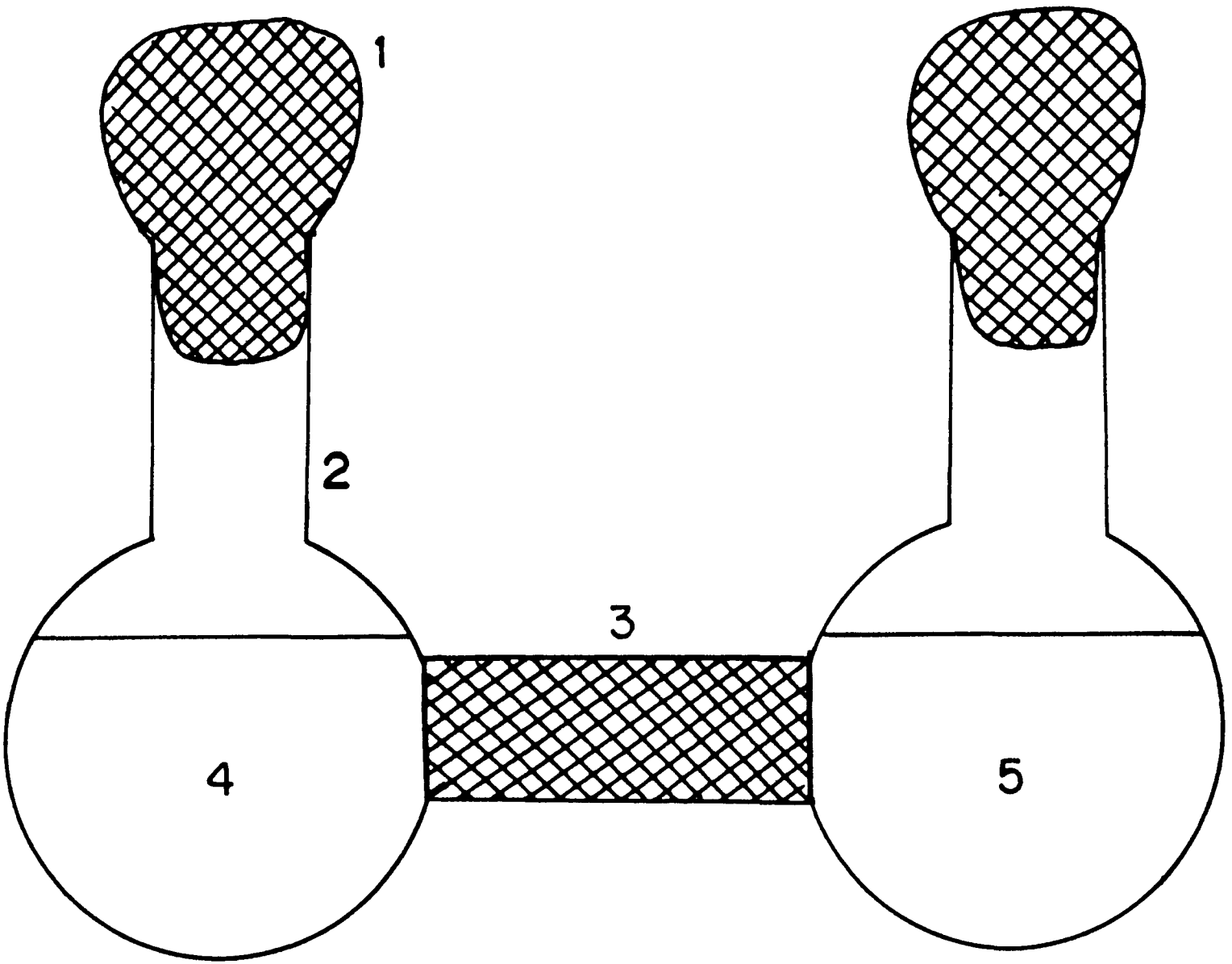

Fig. 5-1 - Double-flask apparatus. 1,Cotton foil gauze plug; 2,250ml flask; 3,Bera sandstone column sleeved in Teflon; 4,E. coli B or B/4 loop-inoculated flask; 5,uninoculated flask.

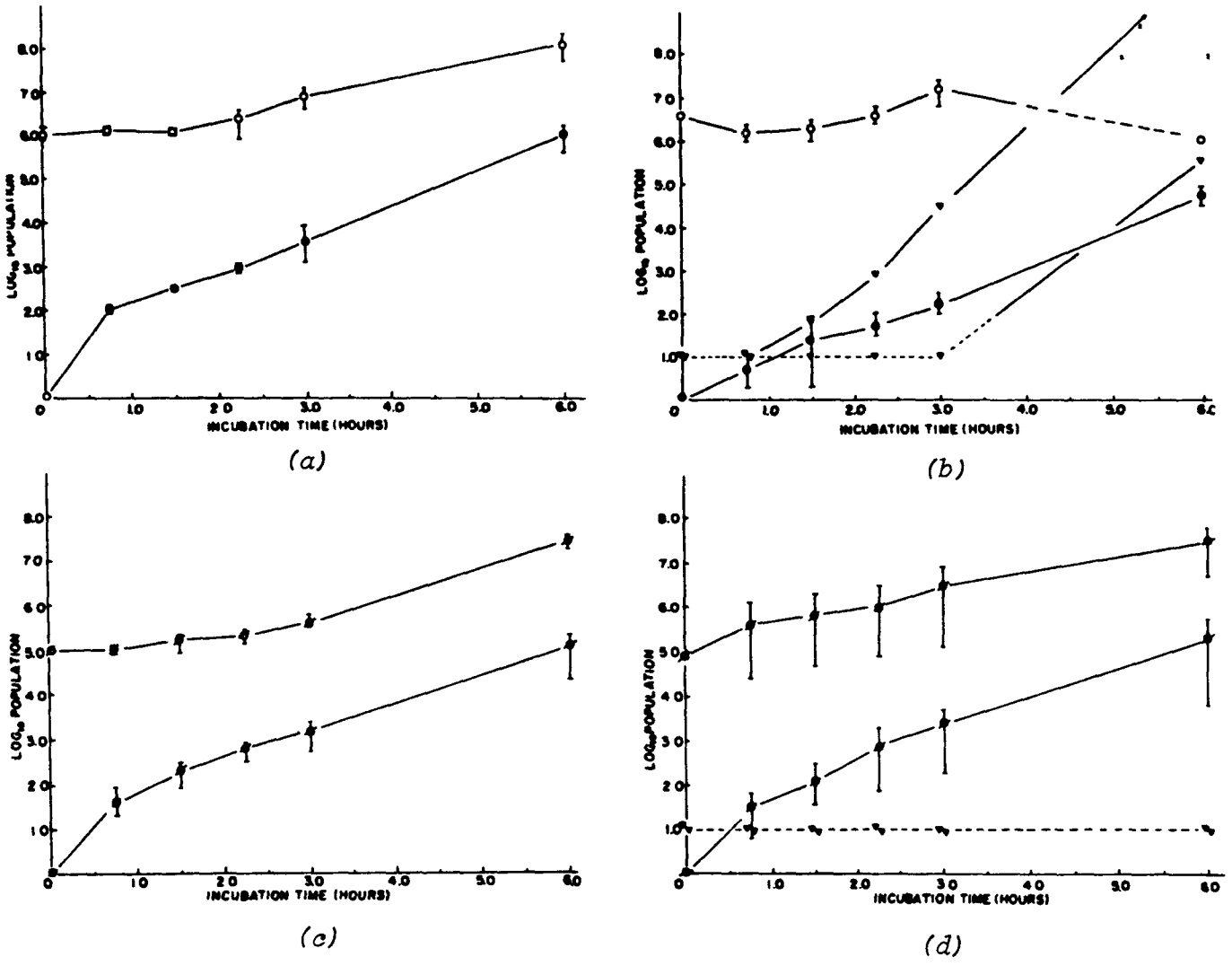

Figure 5-2 *Average E. coli B and B/4 populations in the inoculated (o,ø) and uninoculated (●,ø) flasks from 2-4 experiments using rock sample 1 as determined by plate counting. Vertical bars indicate observed variation between experiments; a) Phageless E. coli B control, uninoculated flask population represents transport and growth of cells across the rock from the inoculated side, b) reduction of E. coli B populations is observed when the rock contains 0.3-1.5 x 10^5 plaque forming units T4. Uninoculated and inoculated flask progeny phage (▼,▽) titers are indicated, c) phageless B/4 control and d) nonlytic cell transport inhibition is implied by B/4 reductions in the presence of 0.4-1.0 x 10^5 pfu T4 although less pronounced compared to tests where T4 sensitive cells are used.*

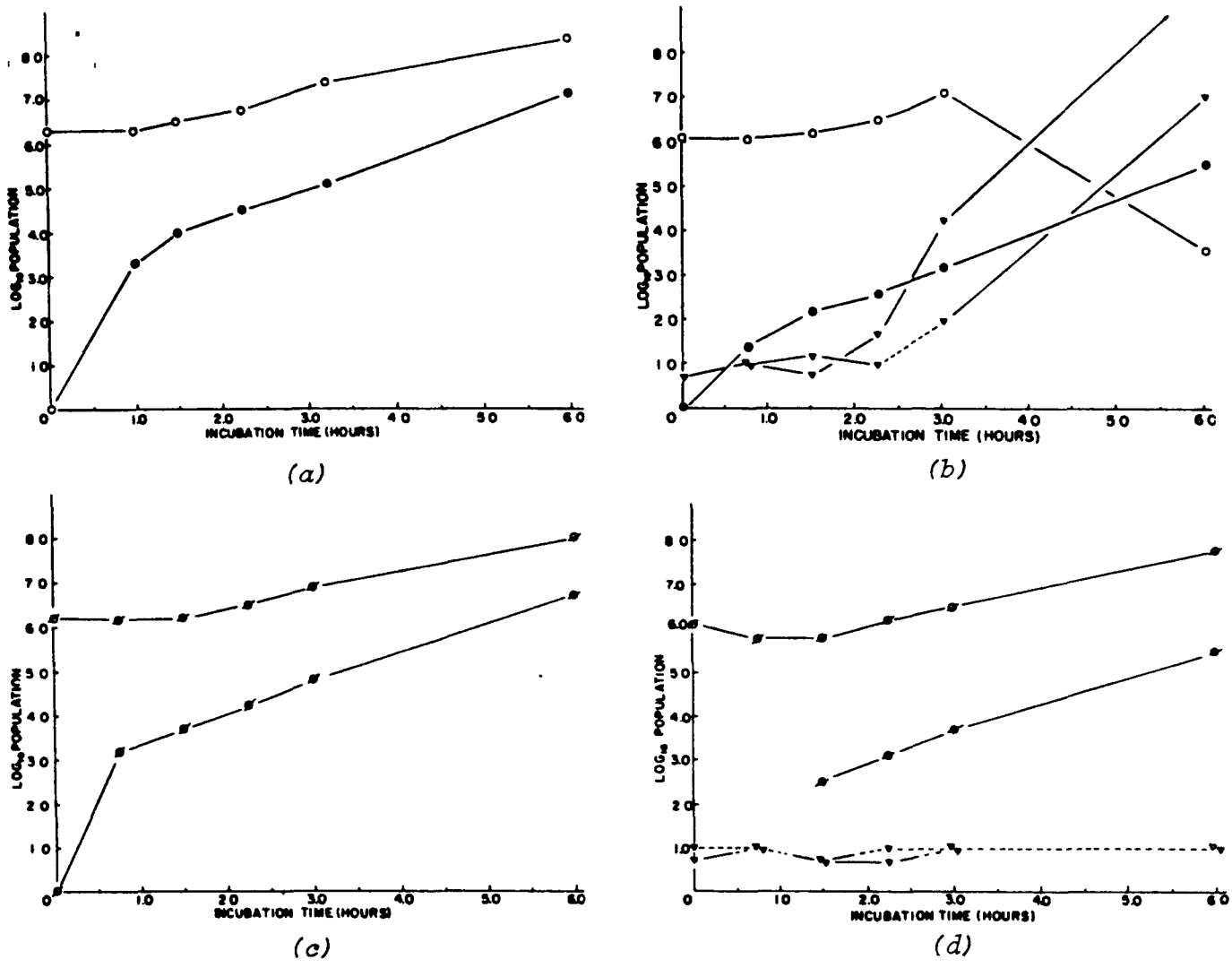

Figure 5-3 *E. coli B(o), B/4(ϕ) and T4 (∇) populations in a single experimental set using a rock identical to rock sample 1. Darkened points are uninoculated flask samples. a) Phageless E. coli B control, b) significant E. coli B population reductions occur with 5 x 10^4 pfu T4 initially contained in the rock, c)phageless B/4 control is identical to the E. coli B control, d) using B/4 and 1.6 x 10^5 pfu T4, nonlytic interaction appears to partially account for the previously observed inhibition of uninoculated flask growth in the presence of phage.*

Table 5-1

Comparisons of cell populations and phage adsorption data in experiments with Rock sample 1.

Experiment	Population Differences ($\log_{10}C_i - \log_{10}C_u$) @time (hr)[0]						Total Phage Titered (expressed in 10^5 pfu)		
	0	3/4	3/2	2½	3	6	Phage Loaded	Phage Retained	% Phage Adsorbed
B[1]	5.9	4.0	3.6	3.6	3.2	2.1	-	-	-
B	6.2	4.1	3.5	3.0	3.5	2.1	-	-	-
B + T4	~6.6	>6.5	>6.2	5.0	5.2	<1.5	4.4	1.3	30%
B + T4	>6.4[2]	>5.5[2]	4.5	4.2	4.3	<1.1	4.2	1.2	30%
B + T4	>6.6	~6.3	>6.4	>5.6	>6.1	ND	2.8	0.3	10%
B/4	5.0	3.7	4.6	3.2	3.0	3.0	-	-	-
B/4	ND	3.7	2.7	2.5	3.5	2.2	-	-	-
B/4	5.1	3.0	2.4	2.3	2.0	ND	-	-	-
B/4 + T4	>4.2	~4.3	3.5	3.2	2.9	2.0	3.2	0.9	28%
B/4 + T4	>5.0	5.2	3.3	3.0	2.6	2.5	3.9	0.4	10%
B/4 + T4	ND	4.4	3.8	3.2	3.6	2.1	2.9	0.5	18%
B/4 + T4	3.9	2.6	2.6	2.3	ND	ND	3.2	1.0	31%

[0] $C_{i,u}$ are viable cells in the inoculated and uninoculated flasks

[1] B denotes *E. coli* B.

[2] Temperature not maintained @ 37° C

Table 5-2

Comparisons of cell population and phage adsorption data in experiments with Rock sample 2.

Experiment	Population Differences ($\log_{10}C_i - \log_{10}C_u$) @time (hr)[o]						Total Phage Titered (expressed in 10^5pfu)		
	0	3/4	3/2	2¼	3	6	Phage Loaded	Phage Retained	% Phage Adsorbed
B[1]	6.3	3.0	2.5	2.3	2.3	1.3	-	-	-
B + T4	6.1	4.7	4.0	4.1	2.9	-2.4	4.0	1.6	40%
B/4	6.2	3.0	2.5	2.6	2.1	1.2	-	-	-
B/4 + T4	6.1	ND	3.3	3.1	2.8	2.3	1.9	0.5	26%

[o] $C_{i,u}$ are viable cells in the inoculated and uninoculated flasks respectively.

[1] B denotes *E. coli B*.

6. THE TRANSPORT OF BACTERIA IN POROUS MEDIA AND ITS SIGNIFICANCE IN MICROBIAL ENHANCED OIL RECOVERY

6.1 Abstract

MEOR is a tertiary recovery process which has only recently been accepted as a technically feasible alternative to other EOR processes in certain shallow, highly permeable reservoirs. The transport of injected bacteria in the porous media is among the problems which need to be resolved before a MEOR process can be successfully applied in a candidate reservoir. In order to contact trapped oil with active metabolites generated in situ, potential strains of bacteria must be transported deep into the reservoir. The problem of transport of bacteria is linked closely with the success or failure of an MEOR process.

This chapter presents a bench-scale investigation of bacterial transport in sandpack columns and sandstone cores and its relationship with oil recovery efficiency. Various oil recovery processes utilizing *Bacillus subtilis* (a bio-surfactant producer) have been attempted: (a) Continuous flooding with bacterial culture, (b) inoculation of bacteria followed by injection of nutrient, (c) inoculation followed by repeated cycles of static incubation, pressure release and nutrient (or water) drive. Experiments revealed that the above processes recovered 30%-40% of the heavy oil (Ranger Zone, Long Beach, CA) in the sandpack column remaining after secondary waterflooding. It was found that bacteria are able to migrate 1 ft/day through the sandpack column saturated with nutrient broth.

The transport of bacteria (or spores) in process (c), which is tentatively thought to be the most feasible among the three processes, is achieved through injection with nutrient followed by a period of static incubation during which cells mutiply and migrate. Separate experiments simulating the two stages of bacterial transport revealed that bacterial spores of B. subtilis and C. acetobutylicum are most easily pushed through the sandstone core while B. subtilis cells migrate through the core faster than Pseudomonas putida during static incubation. This suggests that the procedure developed in this work provides a criterion of selecting bacterial cells with favorable transport properties in porous media.

6.2 Introduction

Although its development has not yet resulted in economically feasible processes and some of its technical difficulties remained to be resolved, the utilization of microorganisms to recover residual oil from low-producing fields has been successfully demonstrated (1 -4a,5). Except for the proposed use of microbial cells and extracellular slimes to selectively plug the high permeable zones, microbial enhanced oil recovery (MEOR) methods mainly utilize the metabolites (biosurfactant, biopolymer, organic acid, and biogas) generated in-situ or ex-situ by bacteria to improve the oil-phase mobility. A well-known example of ex-situ MEOR process is to inject Xanthan gum separated from the growth culture of Xanthomonas to thicken the waterflood.

This chapter mainly deals with the factors influencing the efficiencies of oil recovery by in-situ microbial processes. Since in-situ MEOR is mainly targeted toward the residual oil left after the primary production or the secondary waterflooding, like most tertiary recovery processes, its success depends, among other factors, strongly on the penetration and the stability of recovering agents. In other words, in order to contact trapped oil with bacteria that have favorable oil displacement properties, the microbes must be transported from wellbore to locations deep within the reservoir. Early research indicated that the penetration of the selected bacterial species is rather poor (6-8) as the suspension is continuously injected into a clean porous rock. However, recent studies showed that the presence of oil in the sandstone core can facilitate bacterial penetration (6). Bacterial spores of **Bacillus subtilis** and **Clostridium acetobutylicum** were found to penetrate more easily than vegetative cells (7,9). Certain chemicals added to the suspending medium can also improve the penetration of bacteria (6,7).

Most of the work mentioned above defined bacterial "transport" by the extent of penetration as the suspension is continuously injected, a notion essentially derived from the injection of non-living chemicals in conventional waterflooding. In addition to passively flowing with suspending medium and gradually being retained by porous matrix, cells are able to propagate on the nutrient in suspending medium. Some microbial species can utilize the hydrocarbon in the reservoir

as the carbon source for growth. An increase in the population density can, therefore, result in the migration and further growth of cells toward the uninvaded zone even in the absence of pumping. Also, cells of motile bacterial species are able to swim by flagella propulsion. Recently, some progress has been made by use of a double flask apparatus to investigate exclusively the rate of migration of Pseudomonas putida and Bacillus subtilis through the stagnant nutrient broth that filled the Berea Sandstone core. It was found that B. subtilis migrated faster (1.5 inch/day) than P. putida (0.7 inch/day) (9).

In order to obtain further basic data on the relationship among bacterial growth, bacterial migration, rate of metabolite synthesis, and oil recovery efficiency, bench-scale experiments were conducted. It is felt that this type of work is essential in that a systematic study will yield a quantitative criterion which along with other considerations of reservoir conditions, may be used to predict the performance of a MEOR process.

This work utilized the aerobic, Gram-positive rod B. subtilis, a biosurfactant producer, to recover residual heavy crude from sandpack columns. Two continuous flooding process and a process of repeated cycles of "huff-and-puff" were attempted. The continuous flooding processess were primarily to investigate the efficiency of oil recovery by bio-surfactant and the effect of in-situ growth. The discussion will be focused on the so-called "huff-and-puff" process which made use of a combination of several recovery mechanisms such as in-situ generation of metabolites, solution gas drive, and biosurfactant

flooding. It also demonstrates the bacterial transport at various stages of operation, i.e., initial distribution of cells during inoculation, migration during static incubation, cells being pushed toward exit by solution gas drive, and the growth and migration during make-up nutrient flooding. Details will be presented in the following section. Extension of this method will be discussed.

6.3 Material and Method

Crude Oil

Heavy crude from Ranger Zone, Long Beach, California, was used. It has an API gravity of 17%.

Microbial Species - Bacillus stubilis

Growth Medium

The medium contained 0.8% nutrient broth (0.5% peptone, 0.3% yeast extract) and 0.5% glucose. The medium and the culture were aerated by agitating with a magnetic stirrer bar. Fig. 6-1 shows the schematic diagram of the experimental apparatus.

Porous Media

The oil-containing sandpack column (11 in. long x 1 in. diameter) was prepared by vacuum saturating the column with 1,000 ppm NaCl brine followed sequentially by several pv (pore volumes) of 75% alcohol flood, sterile brine flood, 4 pv of crude oil flood, and 20 pv of sterile brine flood. The pumping rate was kept at 10 ml/hr, or equivalent to 4 pv/day. The porosity of the clean sandpack column was 39%. The residual

oil saturation was about 20% of one pv after secondary brine flooding.

Processes

(i) Continuous Flooding Processes

(a) Old Culture Flooding

An old chemostat culture operating at a dilution rate of 0.03 hr^{-1} was injected into an oil-containing column without interruption. In the control run, nutrient medium was injected for 16 pv followed by flooding the column with 4 pv of *B. subtilis* culture. Nutrient flood was continued afterwards.

(b) Old Culture Flooding/Nutrient Flooding

In the modified run, the inlet was switched to the fresh nutrient medium after the column had been flooded with 28 pv of an old chemostat culture (dilution rate 0.007 hr^{-1}).

(ii) Process of Repeated Cycles of "Huff-and-Puff"

About one-tenth pv of *B. subtilis* culture was inoculated through the inlet end after the oil-containing column had been flooded with 4 pv of fresh nutrient medium. The inlet end and the outlet end were then sealed off. The outlet end was opened after the column was incubated at 32 ^{o}C for one day. The oil being pushed out by the pressure of biogas was treated and weighted. The cycle of sealing and opening was repeated arbitrarily a few times with each for a period of about one day. When the strength of fluid eruption diminished, a few pv of fresh medium were fed in. Both ends were again sealed off. Several cycles of incubation, fluid eruption, and fresh medium flooding followed.

The first control run was operated in a similar

manner except that no B. subtilis culture was inoculated. The puppose was to investigate if the bacteria indigeneous to the crude oil can be revived and grow in the nutrient medium. In the second control run, 1/10 pv of culture was inoculated into the column which contained no oil. The purpose was to monitor the effluent bacterial count, and by doing so, some information regarding the migration and the growth of B. subtilis in this process can be obtained.

Calculation of Recovery Efficiency

The oil in each sample and the final residual oil remained in the column was separated by adding and shaking with toluene. The hydrocarbon layer was removed, predried in the hood, and was further dried at 10 psi vacuum overnight. The percentage of oil recovery was calculated as the ratio of the accumulated dry weight of oil recovered (A) to the dry weight of the initial residual oil after secondary brine flooding (A+B, where B is the dry weight of the final residual oil after flooding with bacterial culture and/or with nutrient medium).

6.4 Results

(i) Continuous Flooding Processes

(a) Old Culture Flooding and Its Control Run

The history of the accumulated oil recovery during the first four days of the experiment is shown in Fig.6-2. The old chemostat culture recovered about 35% of the initial residual oil, while in the control run only about 12% recovery was obtained. It clearly demonstrated that the chemostat

culture containing metabolites and cells are more effective in releasing residual oil than the fresh medium. Since the in-situ bacterial activity in this process was presumably fairly low, we can consider it as an application of B. subtilis culture grown ex-situ in the tertiary recovery operation.

The history of the accumulated oil recovery beyond the fourth day is shown in Fig. 6-3. An increase in production rate was observed in the control run after 4 pv of B. subtilis culture was injected. The dashed line is the long-term prediction of the production history if the column in the control run was not flooded with bacterial culture. The difference between the solid and the dashed lines in the control run might reveal the effect of in-situ growth on the oil production. The supposition of in-situ growth was supported by the bacterial count in the effluent. Before inoculation, the effluent bacterial count in the control run was about 10^4/ml. It increased to 10^6-10^7/ml as the inlet end was switched to fresh medium following inoculation.

The overall oil recovery from this process and its control run was 50% and 44%, respectively.

(b) Culture Flooding/Nutrient Flooding

The history of the accumulated oil recovery and the pressure drop across the column is shown in Fig. 6-4. The recovery in the first four days was lower than the oil produced in the previous case probably because the activity of the influent cells in this process was lower. Also, the content and the composition of metabolites in the culture were different in the two processes.

A significant increase in oil production rate was observed after the inlet end was switched to the fresh medium. The pressure drop decreased slightly and then increased very quickly. Meanwhile, gaseous bubbles were found to appear in the effluent tubing. In the sandpack column, it was observed that some pore spaces were occupied by the biogas. We may explain the fast increase in pressure drop by the following reasons: 1) the vigorous in-situ growth resulting in an increase in the density of bacteria, 2) the emergence of biogas occupying some pore spaces and, therefore, the relative permeability to liquid was decreased, and 3) the possible formation of an oil bank. The overall recovery was about 42%.

(ii) Process of Repeated Cycles of "Huff-and-Puff"

The history of accumulated oil recovery is shown in Fig. 6-5. The horizontal sections represent the incubation period during which both the inlet and the exit were sealed off. The slope of each inclined section represents the average oil production rate during each period of nutrient medium flooding. The height of each step change was the amount of oil pushed out each time the exit was opened after incubation.

The oil recovered at the first time the exit was opened (at the 48th hr.) was about 20% of the overall recovery, while in the first control run only a small amount was obtained (Fig. 6-6). It was apparent that *B. subtilis* was more active than the indigeneous bacteria especially in the early stage of the experiment. The oil production in the first control run gradually increased in the latter half of the experiment probably resulting from the revival of the indigeneous

bacteria. The oil recovered during nutrient medium flooding was presumably due to the biosurfactant secreted from the cells grown in-situ.

In the third control run, bacterial concentrations in the effluent were around 10^6/ml. It is worth noticing that the bacterial count in the erupted sample reached 2 x 10^5/ml only one day after inoculation through the inlet end. The column was initially sterile. Thus, it is apparent that *B. subtilis* cells are able to migrate through the sandpack column saturated with nutrient medium.

6.5 Discussion

Although the continuous flooding with an old chemostat culture can recover an appreciable amount of oil, it is not recommended for application. First, the metabolites are generated ex-situ and the activity of cells injected into the porous media is fairly low. Therefore, many pore volumes of bacterial culture are required to bring about the desired result. Second, continuous injection of bacterial suspension at a density of 10^9-10^{10} cells/ml can have a potential danger of plugging the inlet surface (9) of the wellbore around which the permeability is usually much lower than that of the sandpack column.

The process of repeated cycle of "huff-and-puff" developed in this work has shown several advantages. Although only a small amount (1/10 pv) of bacterial culture is inoculated and the initial distribution of cells is limited within the inlet

region, the further penetration of cells into the column was achieved by growth and migration during static incubation. It was also known that B. subtilis is a motile species capable of swimming in the medium by the propulsion of flagella surrounding the bacterial surface (peritrichous arrangement). During incubation, cells migrate through the column and nutrients are gradually converted into metabolites.

Since both ends were sealed off, the CO_2 generated in this period increased the system pressure and is believed to be readily dissolved in water. Once the pressure was suddenly released by opening the exit, the dissolved gas not only pushed out some residual oil but also flushed cells toward the exit. This would definitely improve greatly the penetration of cells. The following make-up nutrient flooding served to displace the oil released by biosurfactants during static incubation and the oil pushed out from dead ends by solution CO_2 drive. Additionaly, nutrient flooding displaced metabolic wastes in the column and revived the activity of the cells. Therefore, the cells will grow and migrate even deeper into the porous media. Thus, several cycles of "huff-and-puff" followed by nutrient flooding can be repeated to recover more residual oil.

To the best of our knowledge, this work is among the first attempts to investigate systematically the use of bacteria to recover residual oil in a bench scale. It does not, however, imply that the processes developed here including the selection of bacterial species and nutrient medium can be directly applied to a candidate reservoir. Many factors must be seriously assessed. First, it is impossible to sterilize the reservoir

before injecting the selected species. Although the bacteria indigenous to the Long Beach crude did not seem to hinder the activity of B. subtilis in the "huff-and-puff" process developed in this work, such might not be the case in the real situation. Therefore, a careful study on the geomicrobiology is necessary to ensure that the selected species (or a group of several species) is the dominant one under the reservoir condition and the nutrient supplied. Second, considering the anaerobic condition in the reservoir and the difficulty in supplying oxygen, it should be more feasible to inject anaerobic species such as Clostridium acetobutylicum instead of aerobic species such as the one used in the present work. Third, the nutrient medium used in this work is a high-priced, rich proteinaceous nutrient broth (0.5% peptone and 0.3% yeast extract) commonly used by microbiologists to cultivate a wide spectrum of aerobic bacteria. In practice, one might want to choose an inexpensive, less concentrated nutrient source such as dilute molasses solution. Of course, the growth rate, metabolic products and the recovery mechanisms can be different from those presented in this work. However, some of the methods and the sequences of flooding developed in this work can be extended and modified.

The B. subtilis cells injected into the sandpack column in this work grew on the nutrient broth supplied in the suspending medium. It has been proposed that since many bacterial species are able to grow using hydrocarbon in the reservoir as the sole carbon source, only minerals (such as nitrogen source and phosphates) are needed to be added to the suspending medium (4b) if those bacteria are introduced. Bacteria of this group can

grow and migrate in the reservoir as long as the hydrocarbon is sufficient. However, it has been pointed out that this group of bacteria are mostly aerobic and, therefore, the in-situ approach of recovering oil can encounter some problems. Additionally, those bacteria mainly utilize the light ends of the petroleum. Although the metabolic products (mainly biopolymer and biosurfactant) can improve the oil production, the quality of the oil can be seriously downgraded (4c). It has been reported that the metabolic products can also make the viscosity of oil higher.

There is no doubt that in non-biological recovery processes, a complete penetration of chemicals into the reservoir is needed. However, this is not the case in all the MEOR processes. In the production of surfactants in-situ by bacterial metabolisms of nutrients (or petroleum), a higher rate of migration is usually accompanied with a higher production rate of metabolites. However, it might be sufficient for bacteria to penetrate only part of the way into the reservoir, the surfactant produced being carried to the rest of the field by the waterflood. Other possible mechanisms such as the ejection of oil from blind capillaries by in-situ generation of gas, would require a very intimate and complete penetration by bacteria (4d).

6.6 Conclusion

1. *B. subtilis* can recover more than 40% of the Long Beach crude remained in the sandpack column after secondary

waterflooding by the processes developed in this work.

2. B. subtilis were able to grow and migrate in the oil-containing sandpack columns if oxygen supply and nutrient supply were ample. The oil production was improved by the vigorous in-situ growth.
3. The process of repeated cycle of "huff-and-puff" developed in this work made use of a combination of several recovery mechanisms such as release of oil by biosurfactants, solution CO_2 (in water) drive, revival of bacterial activity by make-up nutrient flooding, and the displacement of oil by biosurfactant generated in-situ and nutrient drive.
4. Limiting factors to the application of the above mentioned process should be carefully assessed. Reservoir conditions, indigeneous bacteria present, oil properties, selection of potential bacteria, penetration of bacteria, selection of a suitable nutrient medium, and economic factors have to be seriously considered.

6.7 Literature Cited

1. Bubela, B.: "Role of Geomicrobiology in Enhanced Recovery of Oil: Status Quo, "APEA Journal (1987) 161-166.
2. Karaskiewicz, J.: "Recovery of Crude Oil from Reservoirs by the Use of Bacteria," translated from Nafta (Polish) (1968), Vol. 24, NO. 7, p. 198.
3. ZoBell, C.E.: "Bacterial Release of Oil-Bearing Materials" (Part I) World Oil (Aug. 25, 1947), Vol. 126, No. 13,

35-47.

4. Moses, V. and Springham, D.G.: Bacteria and the Enhancement of Oil Recovery, Applied Science Publishers, London, England (1982), (a) 69-105, (b) 27-29, (c) 52-54, and (d) 60-61.

5. Yarbrough, H.F. and Coty, V.F.: "Microbially Enhanced Oil Recovery from the Upper Cretaceous Nacatoch Formation, Union County, Arkansas," in E.C. Donaldson and J.B. Clark (eds.), Proceedings, of 1982 International Conference on Micorbial Enhancement of Oil Recovery (May 16-21, 1982, Shangri-La, Afton, Oklahoma), published by the U.S. Department of Energy (Feb. 1983), 149-153 (Available through NTIS under CONF-8205140).

6. Jang, L.K., Sharma, M.M., Findley, J.E., Chang, P.W., and Yen, T.F.: "An Investigation of the Transport of Bacteria through Porous Media," ibid., 60-70.

7. Jang, L.K., Findley, J.E., and Yen, T.F.: "Preliminary Investigation on the Transport Problems of Microorganisms in Porous Media," in J.E. Zajic, D.G. Gooper, T.R. Jack, and N. Korsaric (eds.), Microbial Enhanced Oil Recovery, Penn Well Books, Tulsa, Oklahoma, (1983), 45-49.

8. Hart, R.T., Fekete, T., and Flock, D.L.: "The Plugging Effect of Bacteria in Sandstone System," Can. Mining and Metallurgical Bull., (July 1960), Vol. 53, 495-501.

9. Jang, L.K., Chang, P.W., Findley, J.E., and Yen, T.F.,: "Selection of Bacteria with Favorable Transport Properties through Porous Media for the Application of Microbial Enhanced Oil Recovery." Appl. Environ. Microbial. (Nov. 1983), Vol. 46, No.5, 1066-1072.

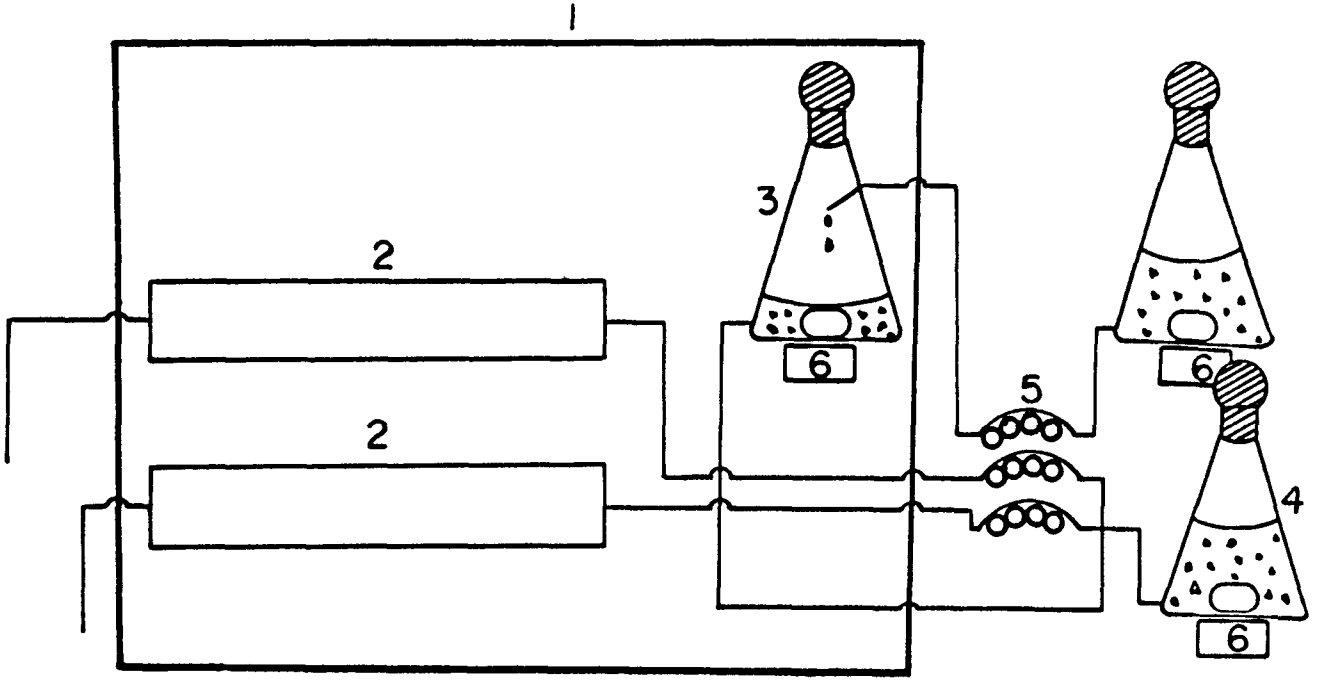

Fig. 6-1 Schematic diagram of the apparatus for recovering residual oil from the sandpack columns.

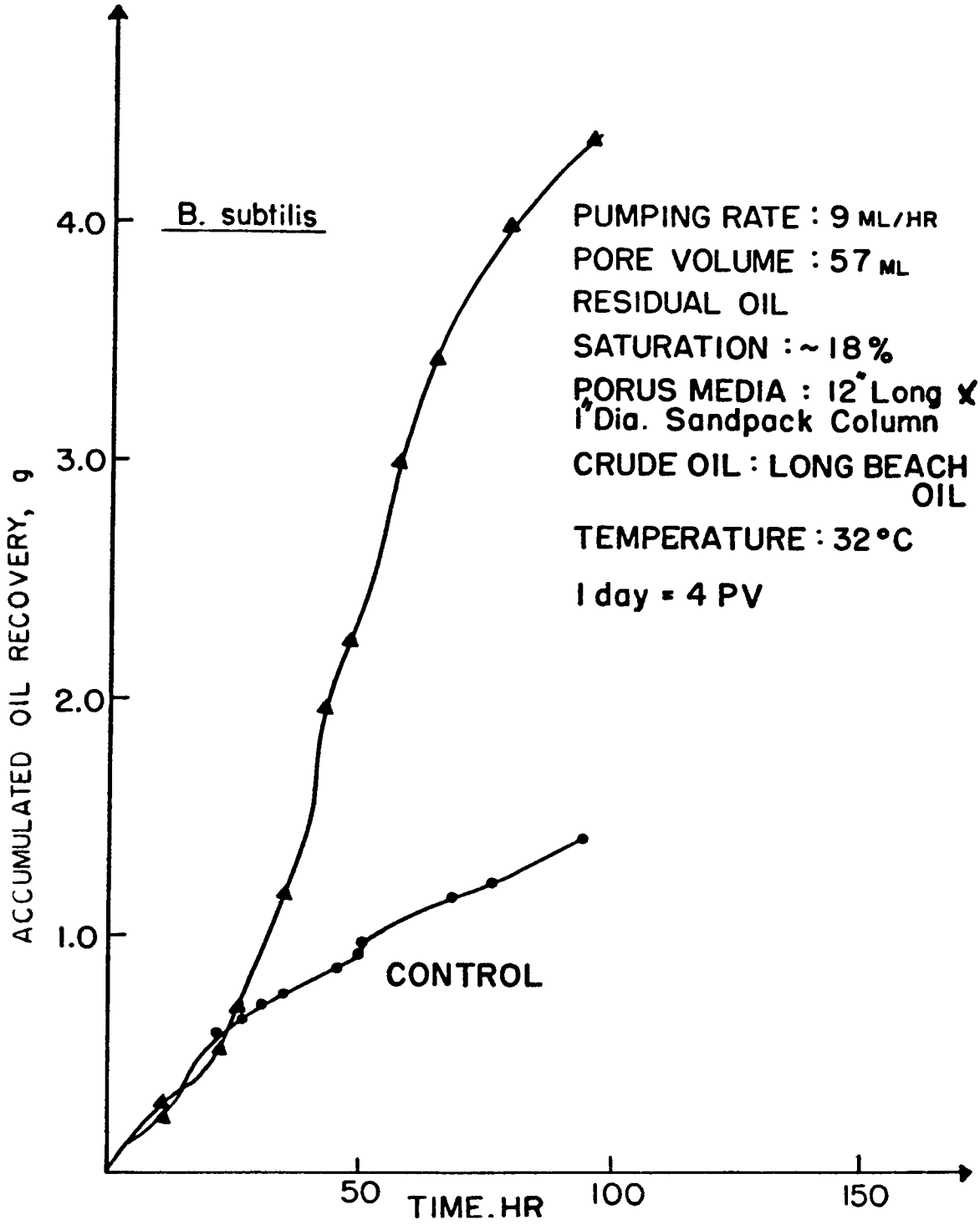

Fig. 6-2 The accumulated oil recovery from sandpack columns which were respectively flooded with *B. subtilis* culture and nutrient (control) for the first four days of experiment.

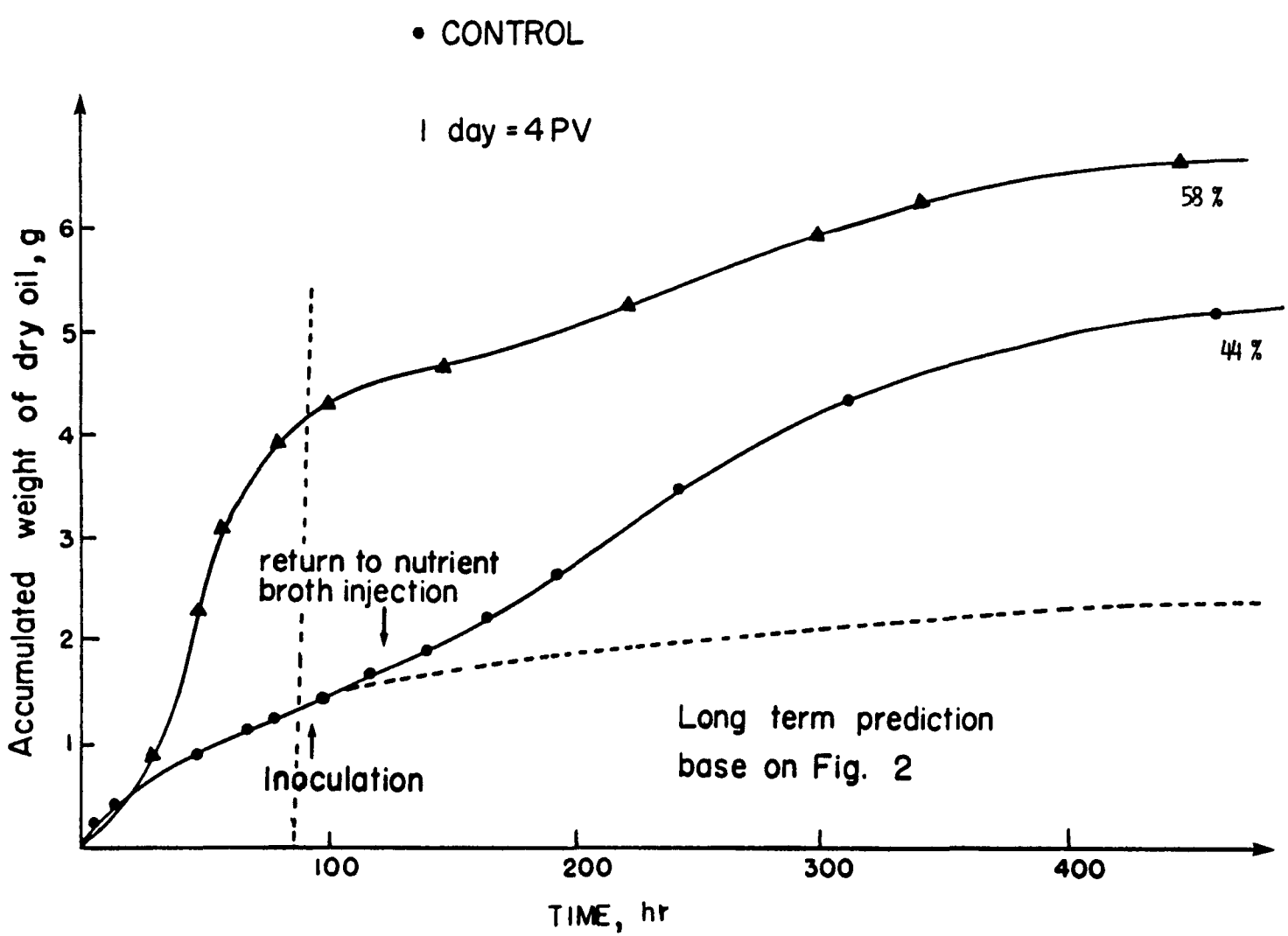

Fig. 6-3 Comparison of the oil recovery efficiencies between continuous culture flooding and its control beyond the 4th day of the experiment.

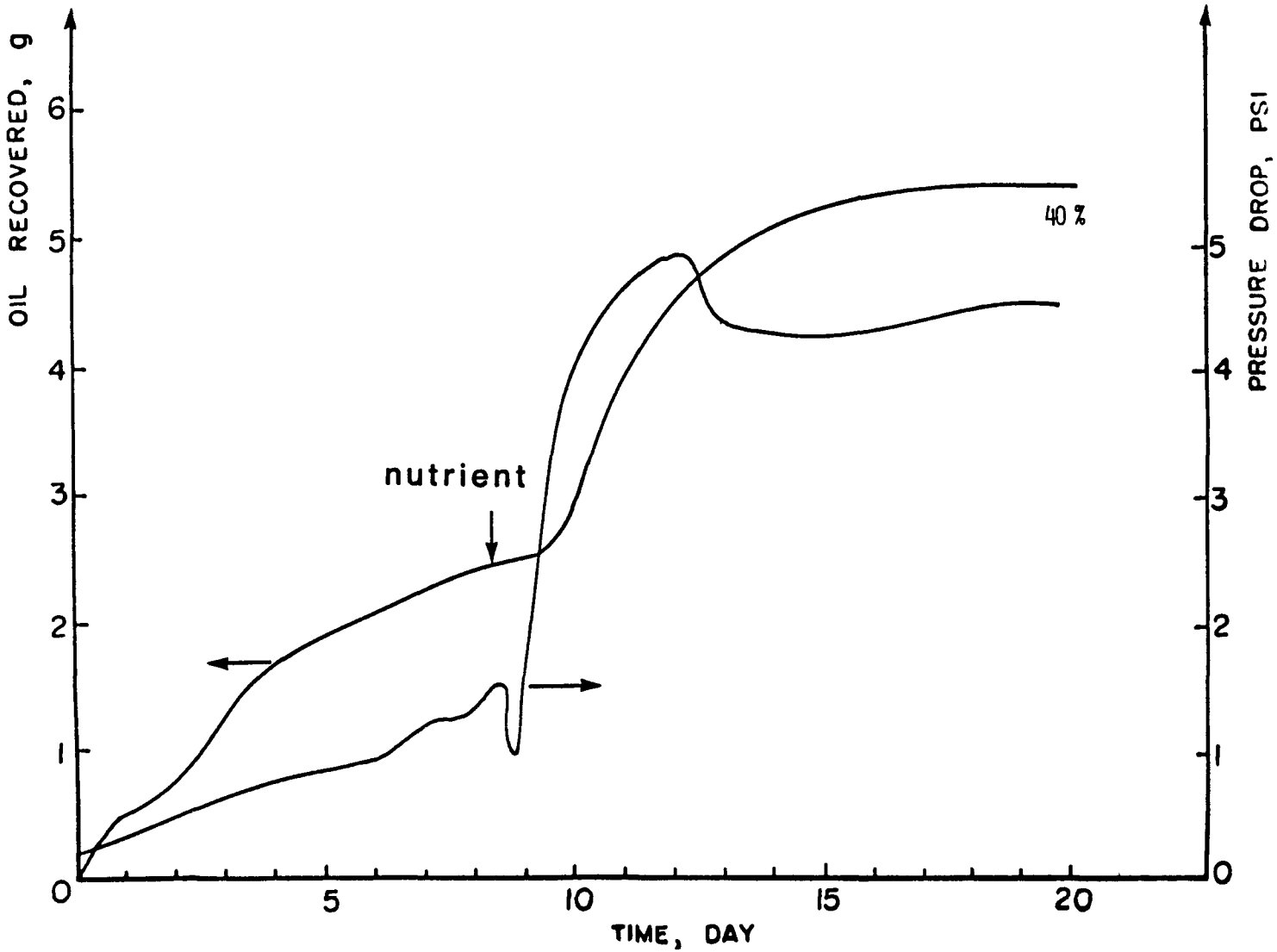

Fig. 6-4 The history of accumulated oil recovery and the pressure drop in the process of culture flooding/nutrient flooding.

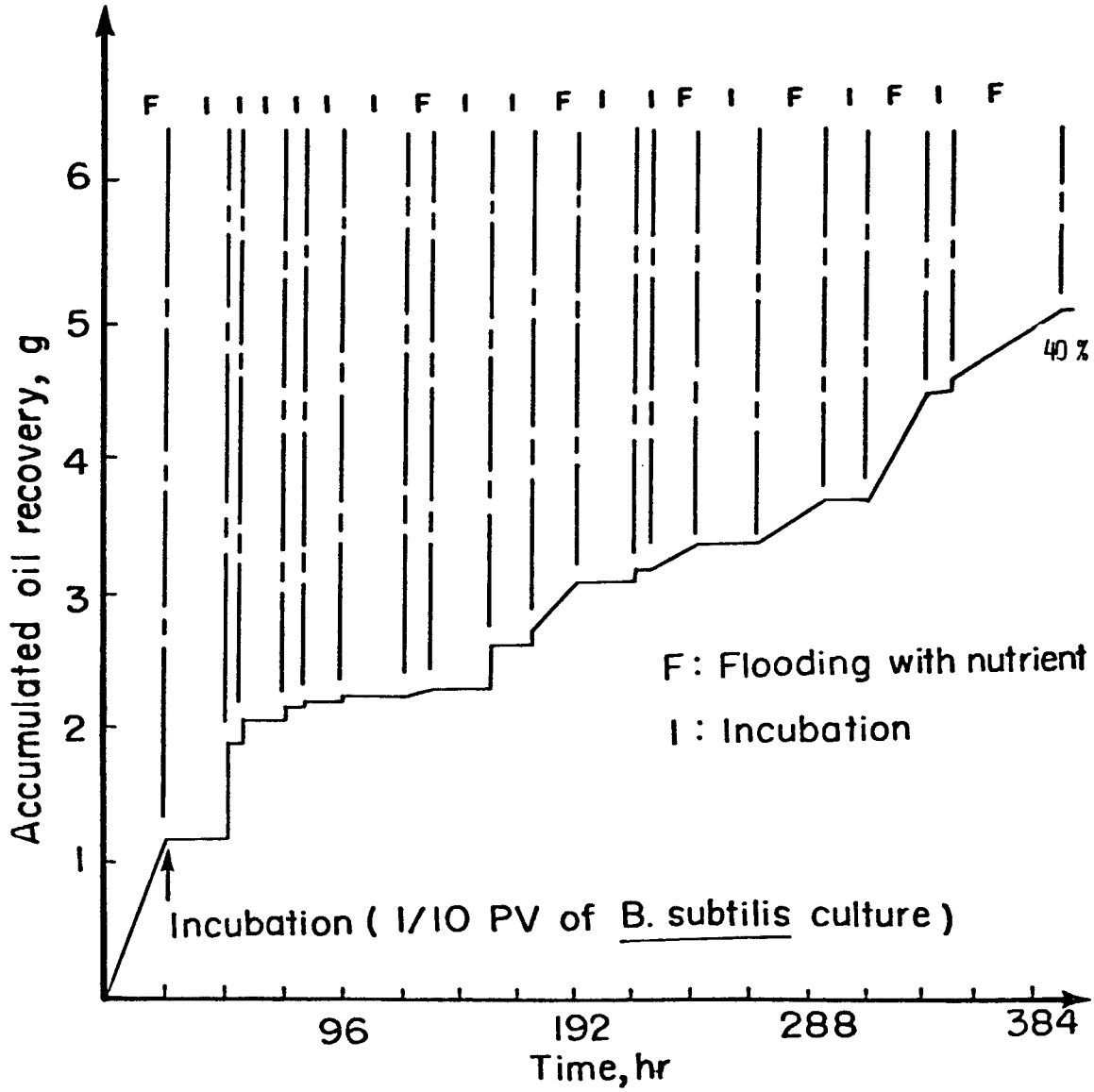

Fig. 6-5 The accumulated oil recovery in the process of repeated cycles of "huff-and-puff". F: nutrient flooding, I: incubation.

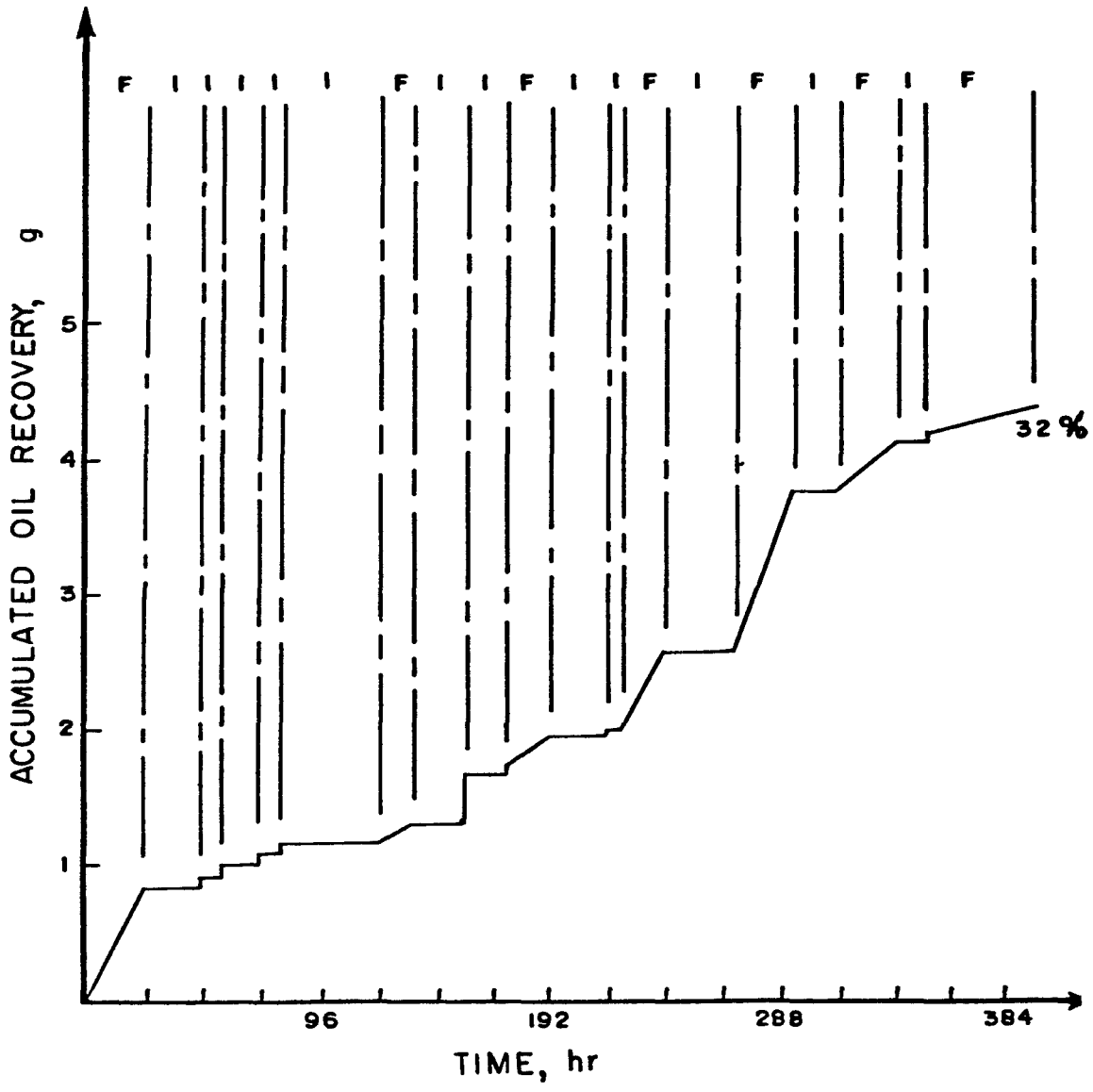

Fig. 6-6 The accumulated oil recovery in the first control run of the "huff-and'puff" process.

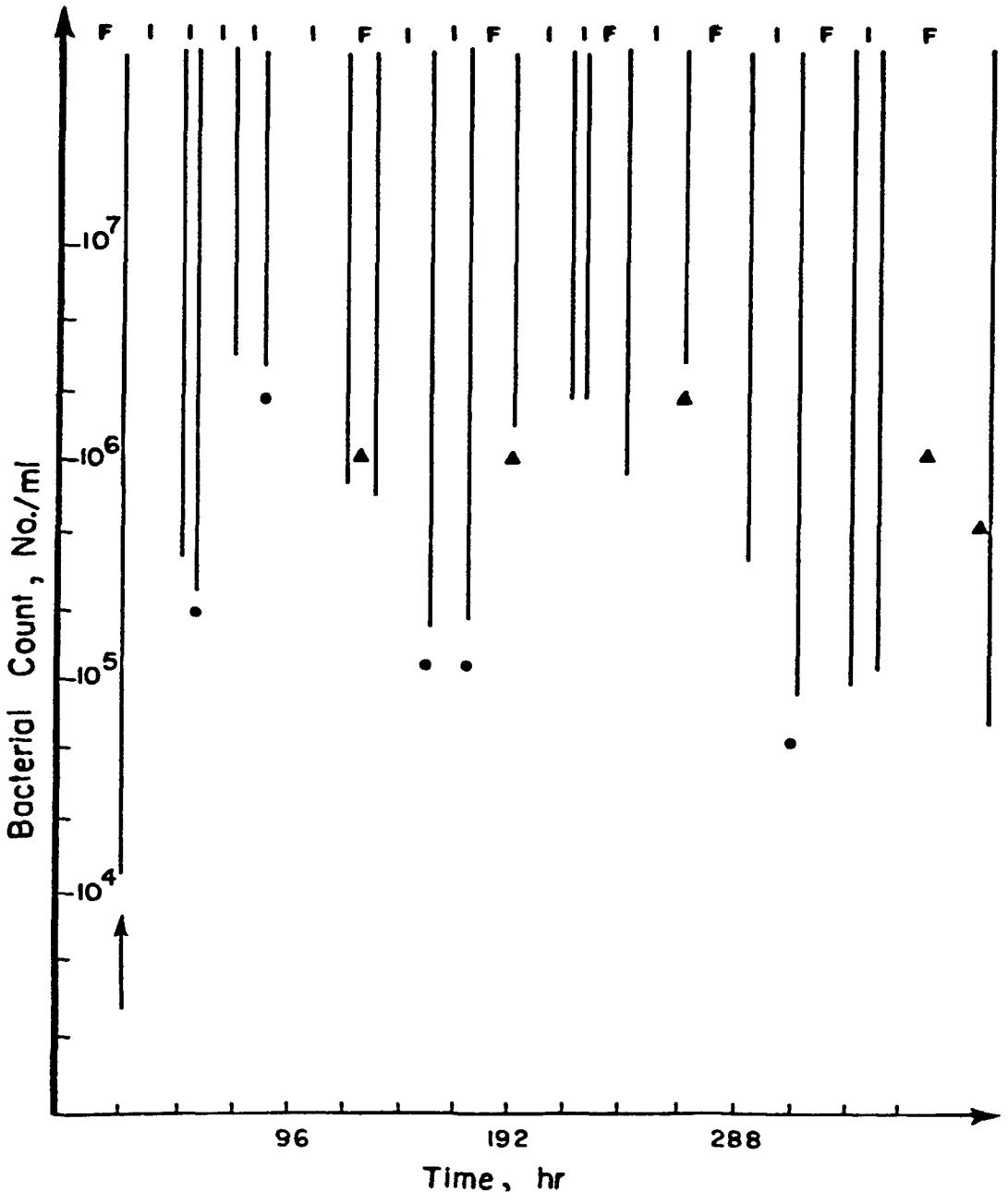

Fig. 6-7 The *B. subtilis* count in the effluent in the second control run of the "huff-and-puff" process. ●: the samples pushed out by biogas, ▲: the samples obtained during nutrient flooding.

Acknowledgement

This work is supported by the U.S. Department of Energy under contract DE-AS19-81BC10508. Appreciations of many discussion and technical input from Drs. John E. Findley, L.K. Jang, and M. Sharma are acknowledged. A special thanks is extended to the project officer, Dr. Keith Westhusing, of the Bartlesville Project Office for his support and quidance. Current Graduate students working on the projects, J.F. Kuo, D. Momeni, P. Chang, M. Sadeghi, and R. McDavid are also acknowledged.

*U.S. GOVERNMENT PRINTING OFFICE: 1986-0-659-031/40031